PNC TN9410 93-037

DYNAMIC BUCKLING ANALYSIS OF A HEMISPHERE SUBJECTED TO EXTERNAL FLUID PRESSURE

A Joint Benchmark Study between AGT-9B and PNC

December 1992

O-ARAI ENGINEERING CENTER

POWER REACTOR AND NUCLEAR FUEL DEVELOPMENT CORPORATION

動力炉・核燃料開発事業団（Power Reactor and Nuclear Fuel Development Corporation）

DYNAMIC BUCKLING ANALYSIS OF A HEMISPHERE SUBJECTED TO EXTERNAL FLUID PRESSURE

A Joint Benchmark Study
between
AGT-9B and PNC

December 1992

by :

M. Morishita

STRUCTURAL ENGINEERING SECTION
SYSTEMS AND COMPONENTS DEVELOPMENT DIVISION
O-ARAI ENGINEERING CENTER
POWER REACTOR AND NUCLEAR FUEL DEVELOPMENT CORPORATION

PNC TN9410 93-037
1993年 2月

流体外圧を受ける半球殻の動的座屈解析

森下 正樹

要 旨

動燃—欧州AGT9B 間の国際協力の枠組みの中で，構造健全性の分野における各種解析評価法に関するベンチマーク解析が計画，実行されている。その中で，流体による外圧を受ける薄肉半球殻の動的座屈の問題が欧州から提示された。本報告書はこの問題に関する解析の結果を取りまとめたのである。

同心の二重半球殻（外側が剛で内側が薄肉）のアニュラス部に水を満たしておき，この系を上下方向に正弦波加振する。流体に動圧が発生し，この圧力によって内側の薄肉半球殻が外圧座屈を生じる。この場合の加振振動数と座屈時の圧力が評価すべき量である。

実験結果に関する情報が得られていない段階で，いわゆる blind analysis を実施した。解析には FINAS を使用した。解析の結果得られた結論は以下のとおりである。

- 加振振動数は 27 Hz（半球殻の流体構造連成による固有振動数）
- 座屈圧力は 0.16 MPa （弾性座屈）
- 流体構造連成による固有振動モードは軸対称モードであり，座屈形状も同じく軸対称モードである。

なお，報告書では解析の結果のみを取りまとめており，実験結果との比較検討，並びにここで用いた解析手法の妥当性に関する検討等は，実験結果に関する情報が得られた段階で改めて行う予定である。

機器構造開発部 構造工学室

PNC TN9410 93-037
Feburary, 1993

DYNAMIC BUCKLING ANALYSIS OF A HEMISPHERE SUBJECTED TO EXTERNAL FLUID PRESSURE

M. MORISHITA*

Abstract

In the frame work of international cooperation between PNC and European AGT9B, benchmark studies were planned on the structural integrity analyses. Among these, a problem on the dynamic buckling of a hemisphere was supplied by the European side. A small annular gap between two concentric hemisphere is filled with water and the whole system is subjected to a vertical harmonic excitation so that the inner thin shell buckles by the dynamic fluid pressure. The problem is to infer the frequency of the excitation and the pressure at which the hemisphere buckles.

An intensive series of analyses were performed using a general purpose non-linear finite element code, FINAS. The analyses were a blind test since no information was available on the experimental results.

It is inferred as a result of the analyses that;

- The frequency of the excitation is 27 Hz.
- The critical buckling pressure is about 0.16 MPa.
- The fundamental vibration mode and the buckling mode are axi-symmetric, and the buckling occurs in the elastic range.

Discussion on the adequacy of the analyses will be made when the experimental result is available.

---

* Structural Engineering Section, Systems and Components division

agt9b\exec

CONTENTS

LIST OF TABLES

List of Figures

List of Figures (cont'd)

List of Figures (cont'd)

List of Figures (cont'd)

1. INTRODUCTION

At the first PNC/Europe AGT9B Specialists Meeting on the Structural Integrity of Fast Reactor Components, held at Saclay Laboratory of C.E.N., France, in January 1989, it was agreed to conduct a joint benchmark study in the field of the structural thermal/dynamic analysis. After a period of discussion between the correspondents of the both sides, three sets of experimental data were selected as the benchmark problems, which include;

- Thermal shock test on a straight pipe by FORTUNA
- Dynamic buckling of a hemisphere by external fluid pressure
- Thermal transient test on a nozzle model by STST

The data for the former two problems were supplied by the European side, while the last was by PNC.

This report describes the result of analysis on the problem 2, i.e., the dynamic buckling of a hemisphere by external fluid pressure. A very narrow annular gap between two coaxial hemispheres is filled with water. The inner sphere is very thin and flexible, while the outer one is relatively rigid. A vertical harmonic excitation is given to this system until the inner sphere buckles by the external fluid pressure. The problem is to identify the frequency of the excitation and the value of critical buckling pressure.

Since no information was available on the experimental results, this work was done as a fully blind analysis.

A general purpose non-linear finite element code, FINAS, was utilized throughout this study. First, a series of dynamic fluid-structure interaction analyses was performed to identify the fundamental frequency and the mode shape. The pressure distribution associated with the mode was also determined. Then using this pressure profile, static buckling analyses were performed. In the analyses, the material non-linearity and the measured thickness distribution were considered. From these analyses, the critical buckling pressure was identified. Both a 2-D axisymmetric model and a full 3-D model were used in the dynamic and the static analyses.

2. PROPOSED PROBLEM

2.1 PROBLEM DESCRIPTION

2.1.1 Summary

The system studied in the benchmark is composed of two concentric hemispheres. The outer hemisphere is thick and rigid, while the inner hemisphere is thin and flexible. The two shells are separated by a very thin water layer, and subjected to a harmonic excitation in the vertical direction at the fundamental frequency of the fluid-structure system composed of the shells and the annular fluid. A dynamic pressure field is formed by the excitation which acts on the inner thin shell to cause it buckle.

The main purpose of the benchmark is to determine the frequency of the harmonic excitation and the value of the non uniform pressure distribution at which the inner hemisphere buckles.

A series of dynamic fluid-structure interaction analyses was performed to identify the fundamental frequency and the pressure field profile. Then using the pressure distribution, static buckling analyses were carried out to identify the critical pressure at which the inner shell buckles.

2.1.2 Geometry, Material and Boundary Conditions

The basic information to define the test specimen is given as follows.

GEOMTRY : The geometry of the test specimen is defined by Fig. 2.1-1. The nominal dimension of the inner hemisphere is as follows ;

Radius	R = 0.455 m
Thickness	t = 8 x 10^{-4} m
Radial Gap	s = 4 x 10^{-3} m
Water Level	H = 0.5 x R

The actual thickness distribution along a meridional line is measured and given in

Table 2.1-1 and Fig. 2.1-2.

The Initial imperfection of the inner hemispherical shell is defined by the maximum initial deviation and its value is given as follows ;

$$\delta = 0.94 \times 10^{-3} \text{ m}$$

MATERIAL DATA : The material of the inner hemisphere is pure Aluminum whose property is given as follows;

Elastic Medullas	$E = 6.6 \times 10^{10}$ Pa
Poisson's Ratio	$\nu = 0.3$
Density	$\rho = 2700$ kg/m^3

The stress-strain relation is given in the form of numerical pair of stress and strain at several discrete points as listed in Table 2.1-2. Fig. 2.1-3 was drawn based on the table. Fig. 2.1-4 shows the work hardening coefficient as a function of inelastic strain, which is also calculated based on the stress-strain table.

BOUNDARY CONDITIONS : The hemispherical shell is clamped at its edge, which was interpreted that the rotational degree of freedom around the tangential axis is not fixed. The outer vessel is supported at its bottom.

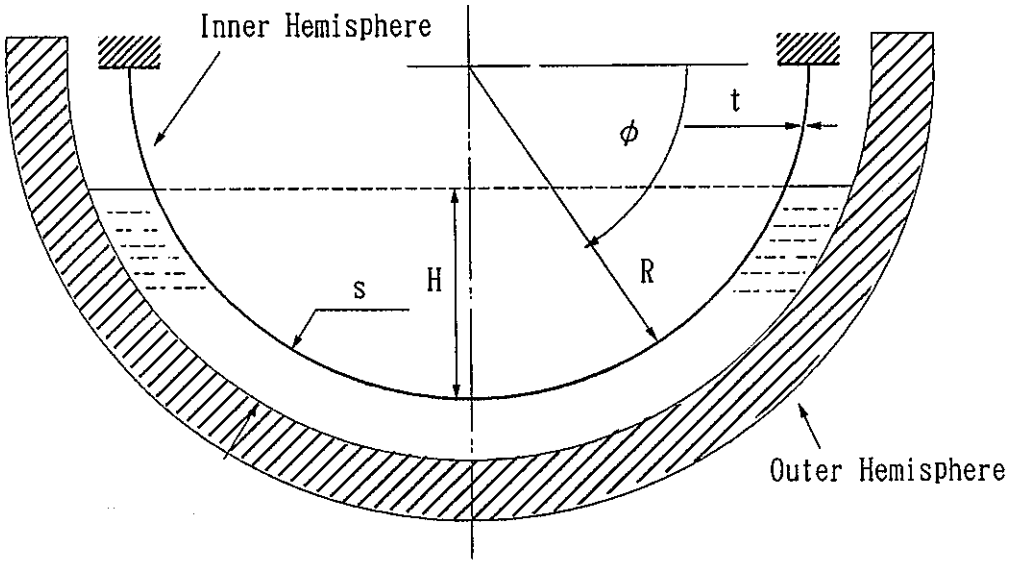

Radius	R = 0.455 m
Thickness	t = 8 x 10 $^{-4}$ m
Radial gap	s = 4 x 10 $^{-3}$ m
Water level	H = 0.5 R

Fig. 2.1-1 Schematic Representation of Test Model

agt9b\ch_2

Table 2.1-1

Measured Thickness Variation of Inner Hemisphere

ZONE	THICKNESS (mm)
$0.0 \leq \phi \leq 5.4$	7.1
$5.4 \leq \phi \leq 16.2$	8.1
$16.2 \leq \phi \leq 25.2$	7.7
$25.2 \leq \phi \leq 36.0$	8.3
$36.0 \leq \phi \leq 45.0$	7.6
$45.0 \leq \phi \leq 55.8$	6.8
$55.8 \leq \phi \leq 64.8$	6.9
$64.8 \leq \phi \leq 73.6$	6.4
$73.6 \leq \phi \leq 86.4$	7.2
$86.4 \leq \phi \leq 90.0$	6.8

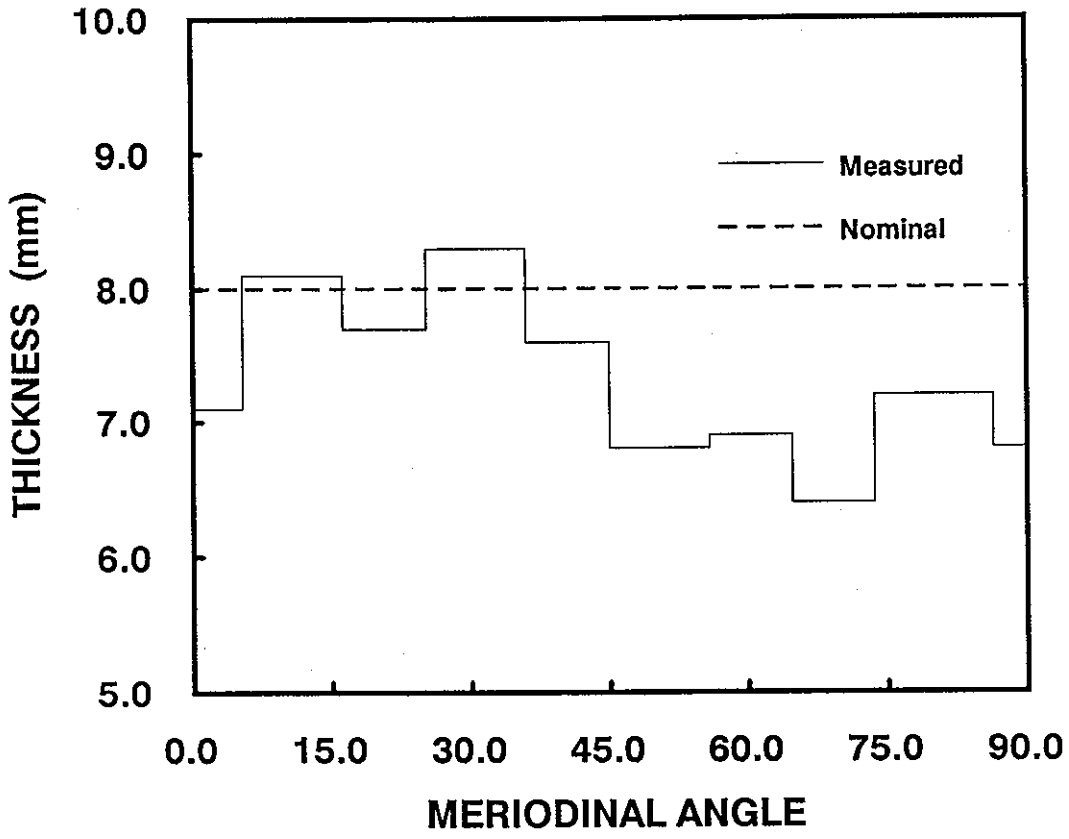

Fig. 2.1-2 Measured Thickness Distribution of Inner Hemisphere

agt9b\ch_2

Table 2.1-2

Stress-strain Relation of Inner Hemisphere Material (pure Al)

σ 10^7 Pa	ϵ 10^{-3}
5.00	0.750
6.23	0.960
6.77	1.125
7.09	1.292
7.45	1.625
7.68	2.208
7.75	3.100
7.84	4.125
8.00	2000.

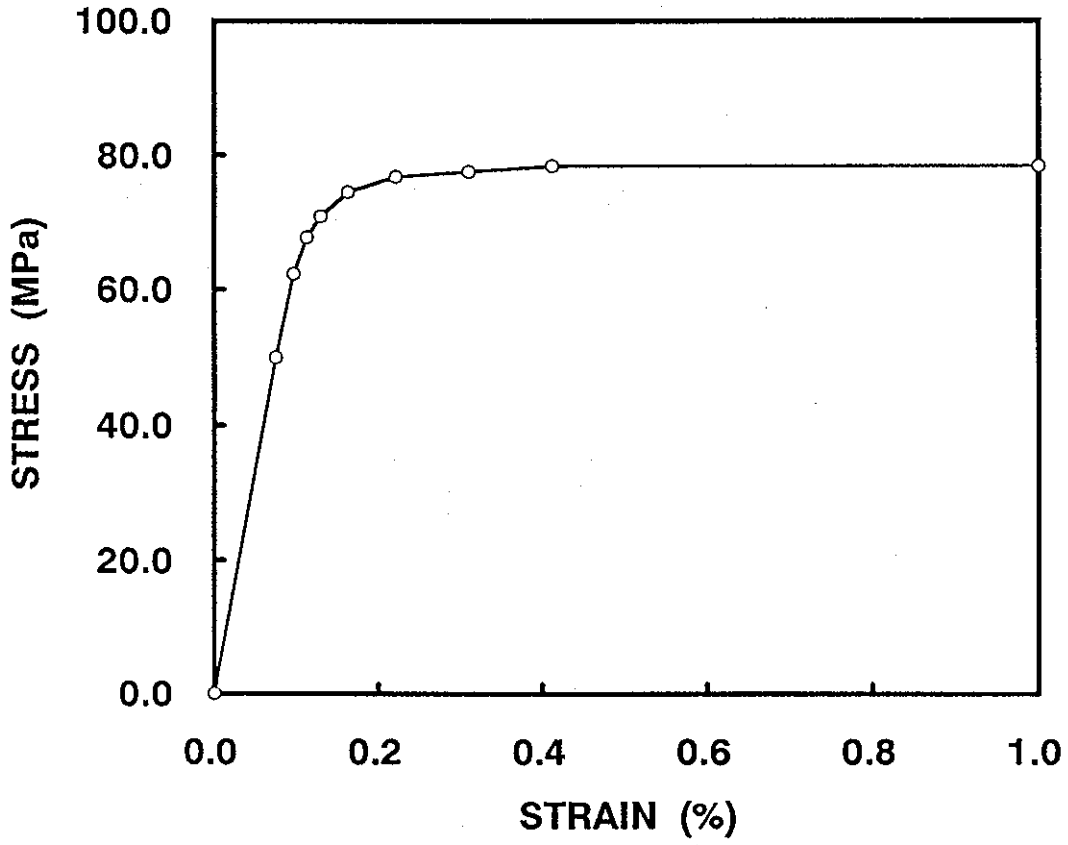

Fig. 2.1-3 Stress-strain Curve of Pure Aluminum

agt9b\ch_2

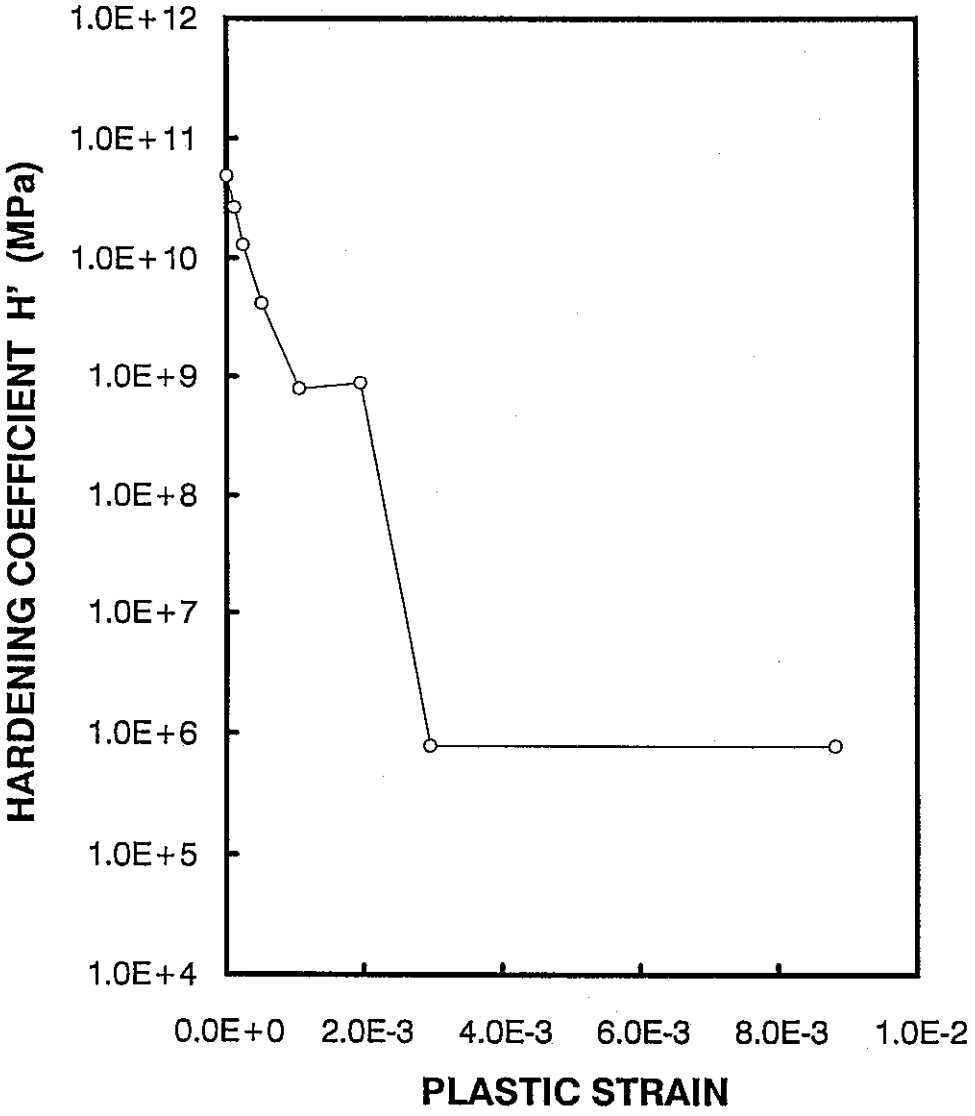

Fig. 2.1-4 Work Hardening Coefficient of Pure Aluminum

agt9b\ch_2

3. DYNAMIC EIGENVALUE ANALYSIS

With a purpose of defining the profile of pressure distribution on the inner hemisphere to be applied in the buckling analysis and the frequency of the harmonic motion creating the pressure, a series of dynamic eigenvalue analyses was performed with fluid-structure interaction taken into account.

First, a series of 2-D analyses was carried out to probe the fundamental vibration mode and its frequency, and the conclusion drawn by these analyses was confirmed by 3-D analyses.

3.1 METHOD OF ANALYSIS

3.1.1 2-D Axi-symmetric Analysis

ANALYSIS MODEL : Both outer and inner hemispheres and the water region in the annlus were all incorporated in the analysis model to take into account fluid-structure interaction effect. Fig. 3.1-1 Schematically shows the 2-D axisymetric model. The finite elements used are;

two node conical shell elements,	NCONC2
four node quadrilateral axi-symmetric fluid elements,	LNQAX4
two node axisymmetirc fluid-structure interface elements,	INLAX4
two node axisymmetric fluid free-surface elements,	SNLAX2

These elements are formulated with the harmonic series expansion technic and capable of dealing with non-axisymmetric deformation of axisymmetric bodies.

As shown in Fig. 3.1-1, the upper part of the spheres ($0° \leq \phi \leq 30°$) were divided at 5° pitch, while the lower part ($30° \leq \phi \leq 90°$) where the annulus is filled with water were divided at 1° pitch. The annulus water region was divided into two layers in the radial direction. The summary of overall analysis model is as follows;

number of nodes	195

total degree of freedom	715	
number of elements	374	(132 * NCONC2)
		(120 * LNQAX4)
		(120 * INLAX4)
		(2 * SNLAX2)

MATERIAL CONSTANTS : The material constants used in the analysis is as follows.

For inner hemisphere (pure Al) ;

wall thickness	8.00 E-04 m (uniform)
Young's modulus	6.60 E+10 Pa
Poisson's ratio	0.30
mass density	2.70 E+03 kg/m^3

For outer hemisphere (steel) ;

wall thickness	1.00 E-03 m
Young's modulus	1.96 E+10 Pa
Poisson's ratio	0.30
mass density	7.81 E+03 kg/m^3

For water and other constants ;

mass density	1.00 E+03 kg/m^3
gravitational acceleration	9.806 m/sec^2

BOUNDARY CONDITIONS : The boundary conditions adopted in the analysis are as follows. For the inner hemisphere, the upper edge is clamped, while the outer hemisphere was assumed to be rigid.

3.1.2 3-D Analysis

ANALYSIS MODEL : Fig. 3.1-2 shows the 3-D model. A quater section of the hemispheres were incorporated in the model based on the symmetry condition. The

finite elements used are;

four node qudrilateral shell elements,	NCONC2
eight node hexahdron fluid elements,	LNQAX4
four node quadrilateral fluid-structure interface elements,	INLAX4
four node quadrilateral fluid free-surface elements,	SNLAX2

As schematically shown in Fig. 3.1-3, the upper part of the spheres ($0° \leq \phi \leq 30°$) were divided at 5° pitch, while the lower part ($30° \leq \phi \leq 90°$) where the annulus is filled with water were divided at 3° pitch. The annulus water region was divided into two layers in the radial direction. The shells were divided by 3° pitch in the circumferential direction (θ). The summary of overall analysis model is as follows;

number of nodes	2325	
total degree of freedom	6520	
number of elements	4020	(1560 * NCONC2)
		(1200 * LNQAX4)
		(1200 * INLAX4)
		(60 * SNLAX2)

MATERIAL CONSTANTS : The material constants used in the analysis are the same as in the 2-D analysis.

BOUNDARY CONDITIONS : The boundary conditions adopted in the analysis are as follows.

inner hemisphere:	clamped at the upper edge.
outer hemisphere:	assumed to be rigid.
symmetr condition:	for the nodes on the meridional lines at θ=0° and 90°, translation in θ and rotation about R and ρ degree of freedom were fixed.

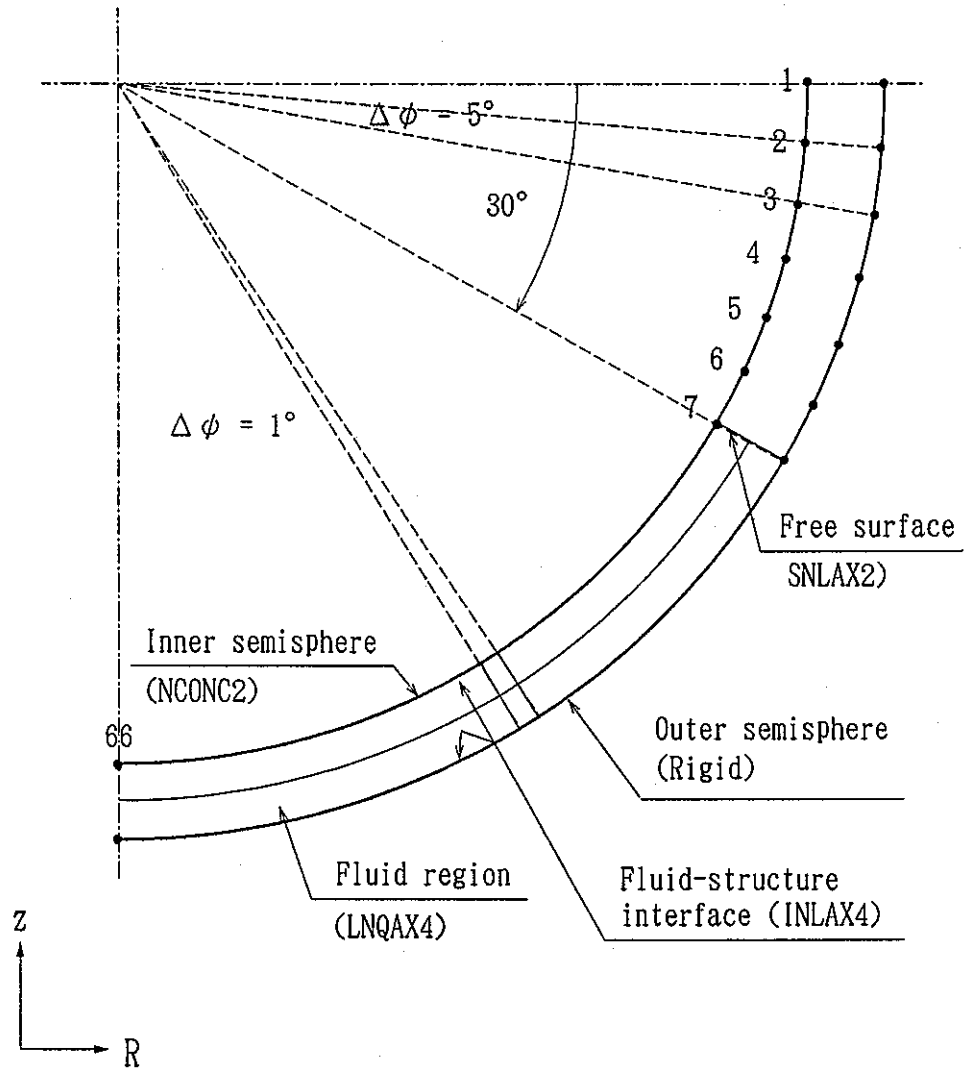

Fig. 3.1-1 Schematic of 2-D Axi-symmetric Analysis Model

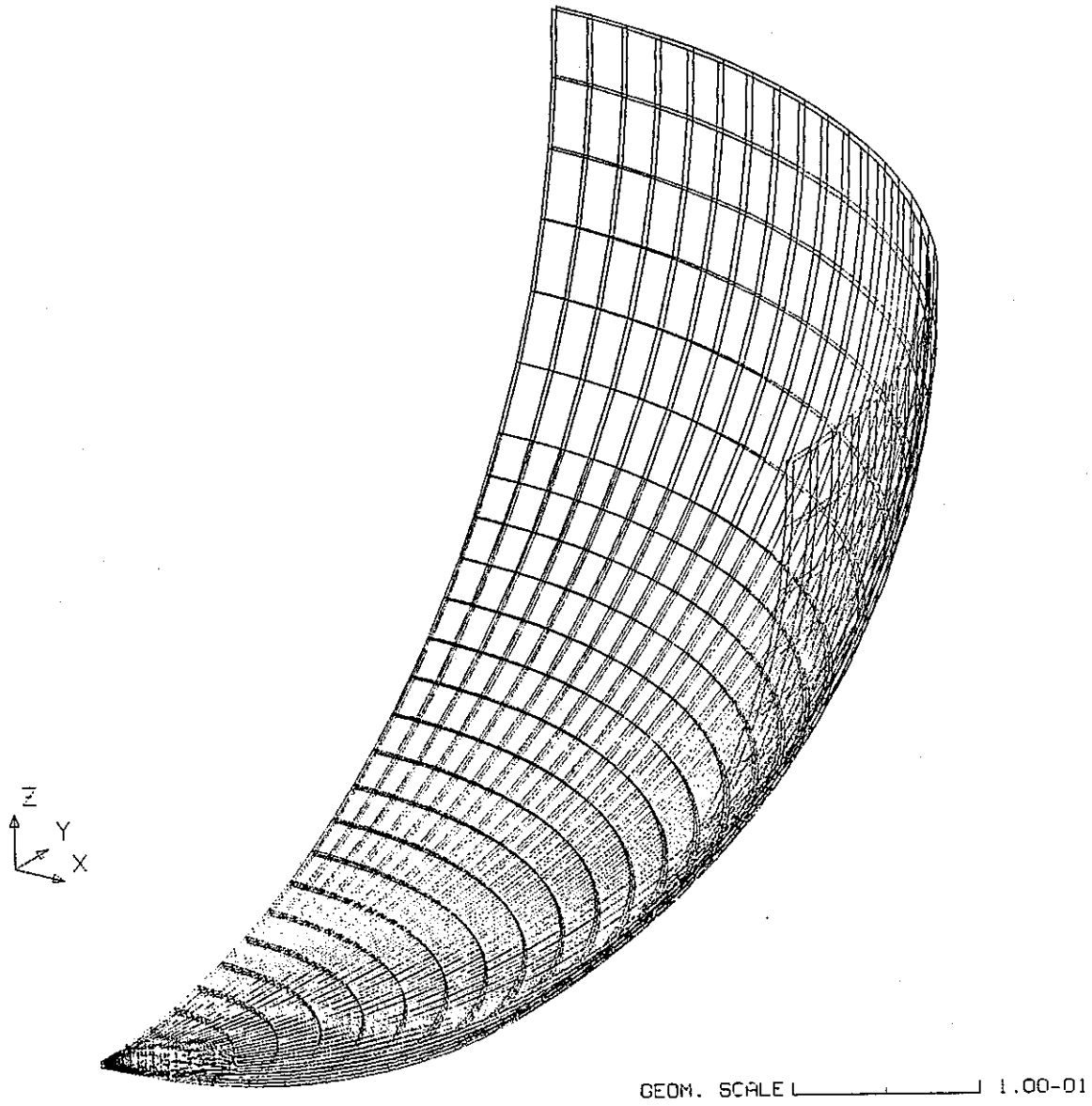

Fig. 3.1-2 3-D Analysis Model

agt9b\ch_3

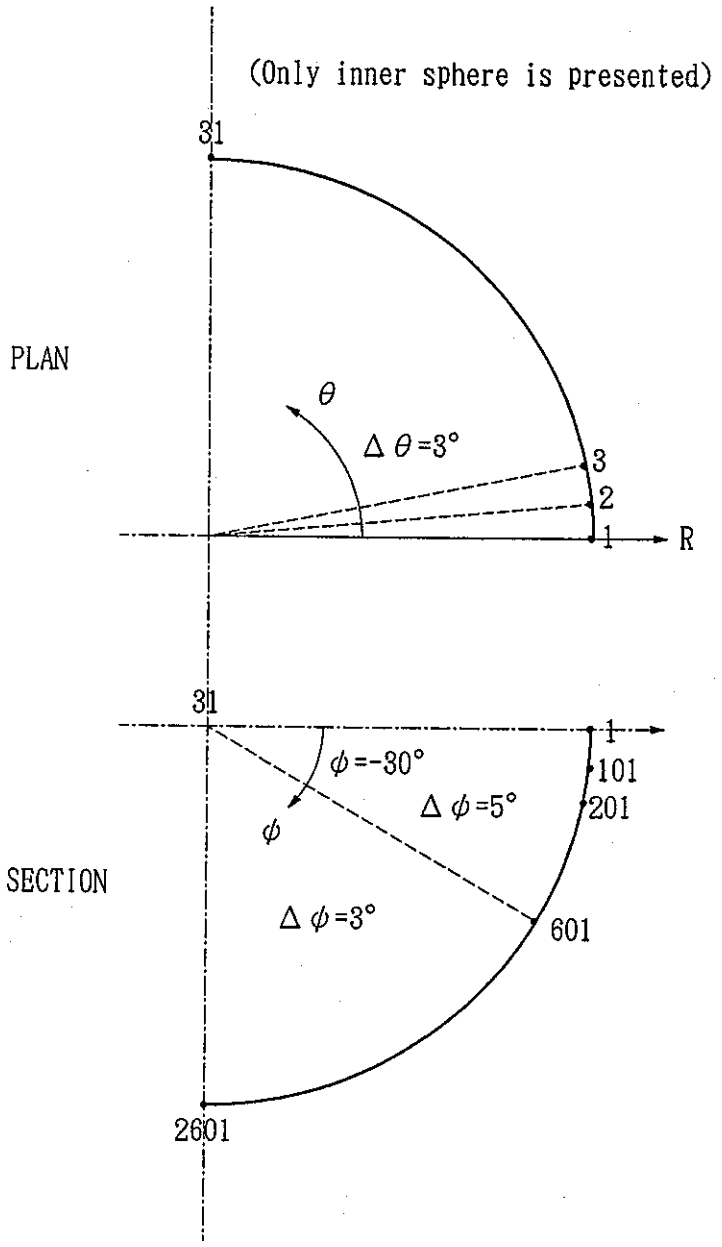

Fig. 3.1-3 Schematic of 3-D Analysis Model

agt9b\ch_3

3.2 RESULTS OF ANALYSIS

3.2.1 2-D Axi-symmetric Analysis

Fourteen runs were made with the 2-D model varying the circumferential wave number, n, to be 0, 1, 2, 3, 4, 5, 6, 8, 10, 12, 14, 16, 18, and 20. The results of the analyses are shown in the tables and figures listed below.

Table 3.2-1 Natural Frequencies by Axi-symmetric Model
Table 3.2-2 Participation Factors for Each Mode
Table 3.2-3 Effect of Thickness Variation on Natural Frequency
Table 3.2-4 Profile of Pressure Distribution (1st mode, n = 0)
Fig. 3.2-1 Distribution of Natural Frequencies
Fig. 3.2-2 Distribution of Participation Factors
Fig. 3.2-3 through Fig. 3.2-9 Vibration Modes

Since the fluid region and its free surface are directly incorporated in the analysis model, some sloshing modes with very low frequencies, as well as the shell vibration modes, are also included in the results. Here, these sloshing modes are excluded and the shell modes are re-sorted in ascending order.

From the analyses, 142 vibration modes were identified in a range of about 27 Hz through 300 Hz. Among these, the lowest one is 27.1 Hz and its mode shape is axi-symmetric. Figs. 3.2-1 and 3.2-2 show the natural frequencies and participation factors as functions of the ague wave number, respectively. From these figures, one can see that the axi-symmetric modes have lower frequencies and are easily excited in the case of a hemisphere subjected to an external fluid pressure. This is quite contrary to cylindrical shells whose fundamental mode usually has a higher order of circumferential wave number. One can also note from the mode shapes that only in the axi-symmetric modes the bottom point displaces in the vertical direction.

From these analysis results, it is presumed that the pressure profile appropriate for buckling analysis is the one that comes from the fundamental axi-symmetric mode. The normalized pressure distribution along a meridional line is listed in Table 3.2-3. The pressure takes its maximum at the bottom and gradually decreases toward the

free surface.

In the analyses mentioned above, the nominal value of wall thickness, in stead of the actual measured thickness distribution, was used. To see the effect of thickness variation, an analysis was done on the axi-symmetric modes using the actual thickness distribution. The results are compared with those with nominal thickness in Table 3.2-3. Although the natural freauencies decrease when the actual thickness variation is used, the difference from those with the nominal thickness is slight enough to be negligible. Since the deviation in the pressure profile is inferred to be also insignificant, the result with constatnt thickness is taken as the base case.

3.2.2 3-D Analysis

The results of the analyses are shown in the tables and figures listed below.

Table 3.2-5 List of Natural Frequencies
Table 3.2-6 Participation Factors
Table 3.2-7 Profile of Pewssure Distribution
Fig. 3.2-10 through 3.2-21 Vibration Modes

Referring to the results of 2-D axi-symmetric analyses, the 3-D analysis was carried out in the frequency range of 25 Hz through 160 Hz, and twelve shell modes were identified. Here, like in the cases of 2-D analysis, the sloshing modes are eliminated from the result. These twelve shell modes have even number of circumferential wave ranging 0 through 8, since a quater section is modeled using symmetry condition.

Compared in Table 3.2-5 are the natural frequencies obtained by 3-D and 2-D analyses. From the table, one can see the 3-D analysis gives quite close results compared with the 2-D results, both in terms frequency and mode shapes.

Fig. 3.2-22 shows the pressure distribution by the 3-D analysis along with the 2-D result for comparison. A quite good coincidence can be seen for the both results, and these profiles were judged applicable to buckling analysis.

Table 3.2-1

Natural Frequencies by 2-D Axi-symmetric Analysis

Unit : Hz

Circumferential Mode Number	Meriodinal Mode Number				
	1	2	3	4	5
0	27.1	59.3	92.6	126.6	161.4
1	38.0	73.4	107.8	142.5	177.8
2	54.9	89.9	124.6	159.6	195.4
3	69.8	105.4	140.6	176.2	212.7
4	84.4	120.8	156.6	192.8	230.0
5	98.8	136.0	172.4	209.3	247.6
6	113.2	151.2	188.3	226.0	265.5
8	141.8	181.4	220.2	260.2	302.7
10	170.4	211.9	252.9	295.9	342.4
12	199.3	243.2	287.1	334.0	385.6
14	228.8	275.7	323.5	375.3	433.0
16	259.4	310.1	362.7	420.5	485.6
18	291.4	347.0	405.6	470.6	544.1
20	325.6	387.2	452.9	526.2	609.1

Table 3.2-2

Participation Factors (1 of 2 : R D.O.F.)

Circumferential Mode Number	Meriodilal Mode Number				
	1	2	3	4	5
0	1.222E+02	3.300E+01	1.038E+01	4.500E+00	2.263E+00
1	4.454E+01	7.539E+00	2.459E+00	9.625E-01	3.882E-01
2	2.567E+01	3.474E+00	1.785E+00	6.642E-01	3.090E-01
3	1.665E+01	1.636E+00	1.217E+00	4.258E-01	1.591E-01
4	1.148E+01	8.329E-01	8.186E-01	3.121E-01	3.850E-02
5	8.150E+00	4.818E-01	5.011E-01	2.584E-01	6.860E-02
6	5.810E+00	3.414E-01	2.331E-01	2.345E-01	1.709E-01
8	2.712E+00	3.022E-01	2.180E-01	2.171E-01	3.724E-01
10	7.446E-01	3.549E-01	5.858E-01	2.110E-01	5.650E-01
12	5.655E-01	4.278E-01	8.761E-01	2.172E-01	7.331E-01
14	1.452E+00	5.073E-01	1.102E+00	2.364E-01	8.722E-01
16	2.072E+00	5.841E-01	1.276E+00	2.601E-01	1.016E+00
18	2.509E+00	6.544E-01	1.420E+00	2.894E-01	1.326E+00
20	2.836E+00	7.161E-01	1.535E+00	3.573E-01	1.704E+00

Table 3.2-2 (Continued)

Participation Factors (2 of 2 : ϕ D.O.F.)

Circumferential Mode Number	Meriodilal Mode Number				
	1	2	3	4	5
0	2.130E+02	2.418E+01	8.306E+00	3.354E+00	1.695E+00
1	6.333E+01	1.420E+00	2.534E+00	1.092E-01	1.823E-01
2	3.287E+01	1.912E+00	2.111E+00	1.359E-01	4.520E-02
3	1.972E+01	1.802E+00	1.434E+00	1.946E-01	1.628E-01
4	1.279E+01	1.354E+00	8.662E-01	3.139E-01	3.456E-01
5	8.628E+00	8.722E-01	3.962E-01	4.407E-01	5.059E-01
6	5.876E+00	4.424E-01	1.154E-02	5.561E-01	6.479E-01
8	2.513E+00	1.999E-01	5.712E-01	7.314E-01	8.880E-01
10	5.886E-01	6.024E-01	9.791E-01	8.406E-01	1.080E+00
12	5.856E-01	8.549E-01	1.261E+00	9.148E-01	1.228E+00
14	1.324E+00	1.021E+00	1.458E+00	9.709E-01	1.337E+00
16	1.809E+00	1.131E+00	1.592E+00	1.001E+00	1.460E+00
18	2.128E+00	1.205E+00	1.694E+00	1.033E+00	1.810E+00
20	2.351E+00	1.256E+00	1.764E+00	1.187E+00	2.227E+00

Table 3.2-3

Effect of Thickness Variation on Natural Frequency (N = 0)

Unit : Hz

MODE #	THICKNESS DISTRIBUTION		RATIO
	VARIABLE	UNIFORM	
1	26.1	27.1	0.96
2	55.6	59.3	0.94
3	86.9	92.6	0.94
4	119.0	126.6	0.94
5	152.0	161.4	0.94

Table 3.2-4

Normalized Pressure Profile by 2-D Analysis

(1 of 2)

NODE #	ϕ	PRESSURE
106	30	-7.909E-04
107	31	1.762E-02
108	32	3.658E-02
109	33	5.607E-02
110	34	7.604E-02
111	35	9.644E-02
112	36	1.172E-01
113	37	1.384E-01
114	38	1.598E-01
115	39	1.816E-01
116	40	2.036E-01
117	41	2.259E-01
118	42	2.483E-01
119	43	2.710E-01
120	44	2.937E-01
121	45	3.166E-01
122	46	3.396E-01
123	47	3.626E-01
124	48	3.857E-01
125	49	4.087E-01
126	50	4.317E-01
127	51	4.546E-01
128	52	4.774E-01
129	53	5.001E-01
130	54	5.226E-01
131	55	5.449E-01
132	56	5.670E-01
133	57	5.888E-01
134	58	6.103E-01
135	59	6.315E-01
136	60	6.524E-01

(2 of 2)

NODE #	ϕ	PRESSURE
137	61	6.729E-01
138	62	6.929E-01
139	63	7.126E-01
140	64	7.318E-01
141	65	7.505E-01
142	66	7.687E-01
143	67	7.863E-01
144	68	8.034E-01
145	69	8.199E-01
146	70	8.358E-01
147	71	8.511E-01
148	72	8.657E-01
149	73	8.797E-01
150	74	8.929E-01
151	75	9.055E-01
152	76	9.173E-01
153	77	9.284E-01
154	78	9.387E-01
155	79	9.483E-01
156	80	9.571E-01
157	81	9.651E-01
158	82	9.722E-01
159	83	9.786E-01
160	84	9.841E-01
161	85	9.889E-01
162	86	9.928E-01
163	87	9.958E-01
164	88	9.980E-01
165	89	9.994E-01
166	90	1.000E+00

Table 3.2-5

Natural Frequencies by 3-D Analysis

Unit : Hz

Circumferential Mode Number	Meriodinal Mode Number			
	1	2	3	4
0	27.1 (+0) *	60.1 (+1)	94.2 (+2)	129.1 (+2)
2	55.6 (+1)	91.7 (+2)	127.6	N.A.
4	86.0 (+2)	124.0 (+3)	N.A.	N.A.
6	115.9 (+2)	156.5 (+4)	N.A.	N.A.
8	146.0 (+3)	N.A.	N.A.	N.A.

* $(f_{3D} / f_{2D} - 1) * 100$ (%)

Table 3.2-6

Participation Factors by 3-D Analysis

R Degree of Freedom

Circumferential Mode Number	Meriodilal Mode Number			
	1	2	3	4
0	4.868E+03	1.258E+03	4.350E+02	2.042E+02
2	6.089E+02	8.836E+01	5.328E+01	N.A.
4	1.339E+01	1.086E+01	N.A.	N.A.
6	1.851E+00	3.949E-02	N.A.	N.A.
8	1.178E+01	N.A.	N.A.	N.A.

θ Degree of Freedom

Circumferential Mode Number	Meriodilal Mode Number			
	1	2	3	4
0	4.356E+03	1.194E+03	3.975E+02	1.971E+02
2	6.089E+02	8.835E+01	5.328E+01	N.A.
4	8.950E+01	6.294E+00	N.A.	N.A.
6	1.851E+00	2.599E-02	N.A.	N.A.
8	1.628E+01	N.A.	N.A.	N.A.

ϕ Degree of Freedom

Circumferential Mode Number	Meriodilal Mode Number			
	1	2	3	4
0	1.182E+04	1.361E+03	4.934E+02	2.324E+02
2	8.875E-03	3.515E-04	4.030E-04	N.A.
4	5.614E+01	8.596E+00	N.A.	N.A.
6	2.126E-03	8.478E-03	N.A.	N.A.
	1.948E+01	N.A.	N.A.	N.A.

Table 3.2-7

Normalized Pressure Profile by 3-D Analysis

Angle ϕ	Normalized Pressure
30°	-6.8810E-04
33°	5.8870E-02
36°	1.2260E-01
39°	1.8940E-01
42°	2.5850E-01
45°	3.2910E-01
48°	4.0030E-01
51°	4.7110E-01
54°	5.4080E-01
57°	6.0840E-01
60°	6.7300E-01
63°	7.3390E-01
66°	7.9030E-01
69°	8.4140E-01
72°	8.8640E-01
75°	9.2490E-01
78°	9.5610E-01
81°	9.7960E-01
84°	9.9460E-01
87°	1.0000E+00
90°	9.9150E-01

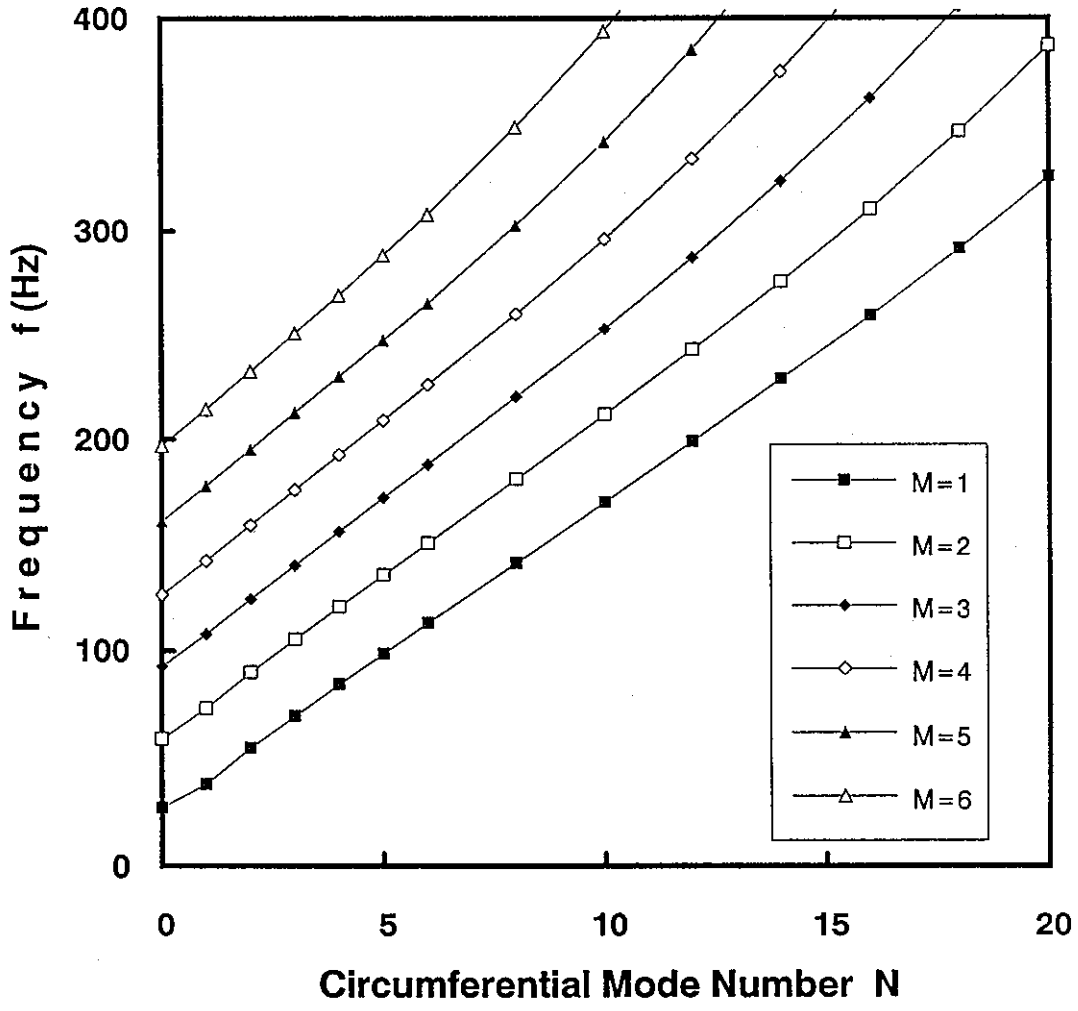

Fig. 3.2-1 Distribution of Natural Frequencies by 2-D Axi-symmetric Analysis

agt9b\ch_3

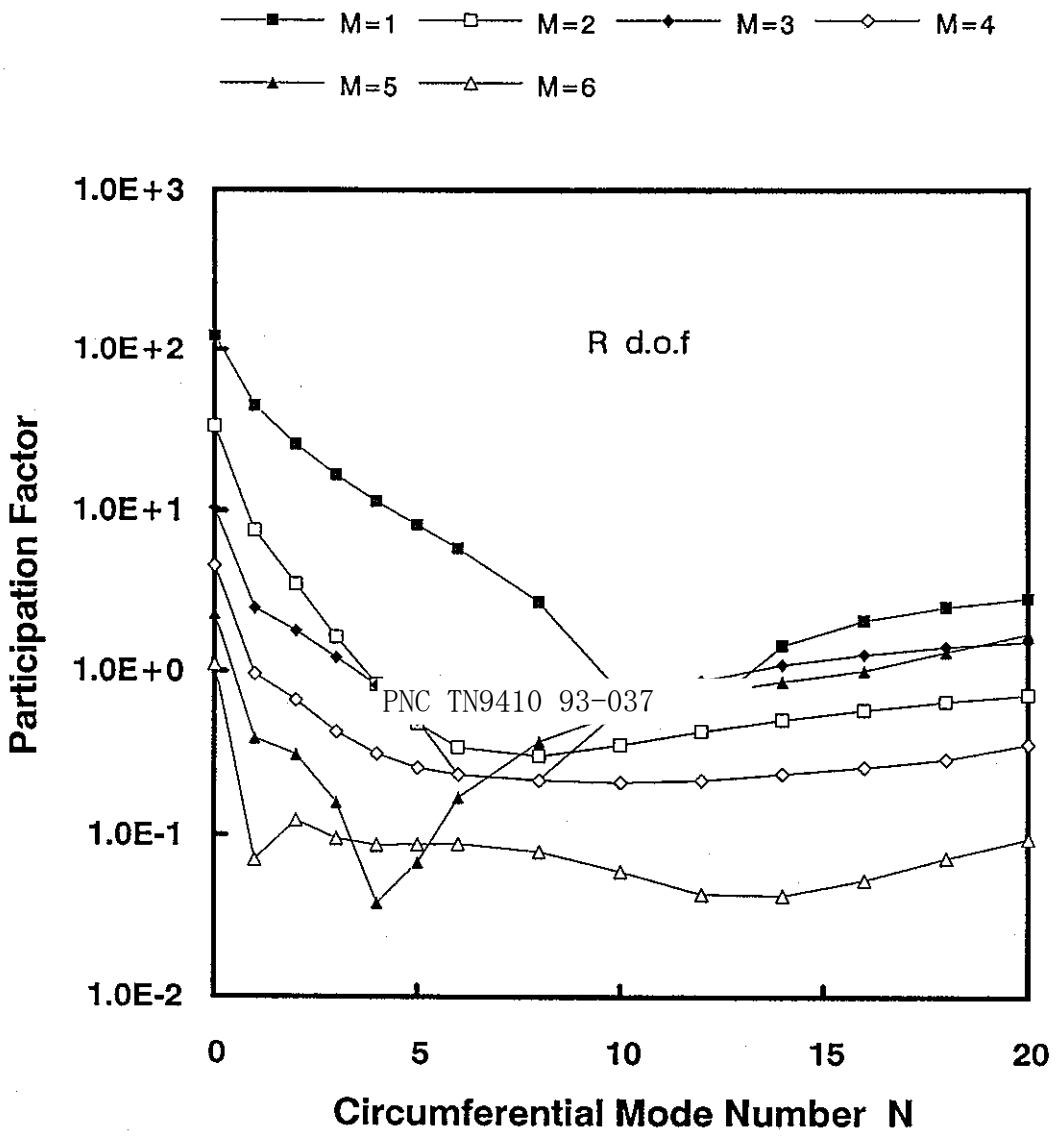

Fig. 3.2-2 Distribution of Participation Factors by 2-D Axi-symmetric Analysis (1 of 2: R d.o.f)

agt9b\ch_3

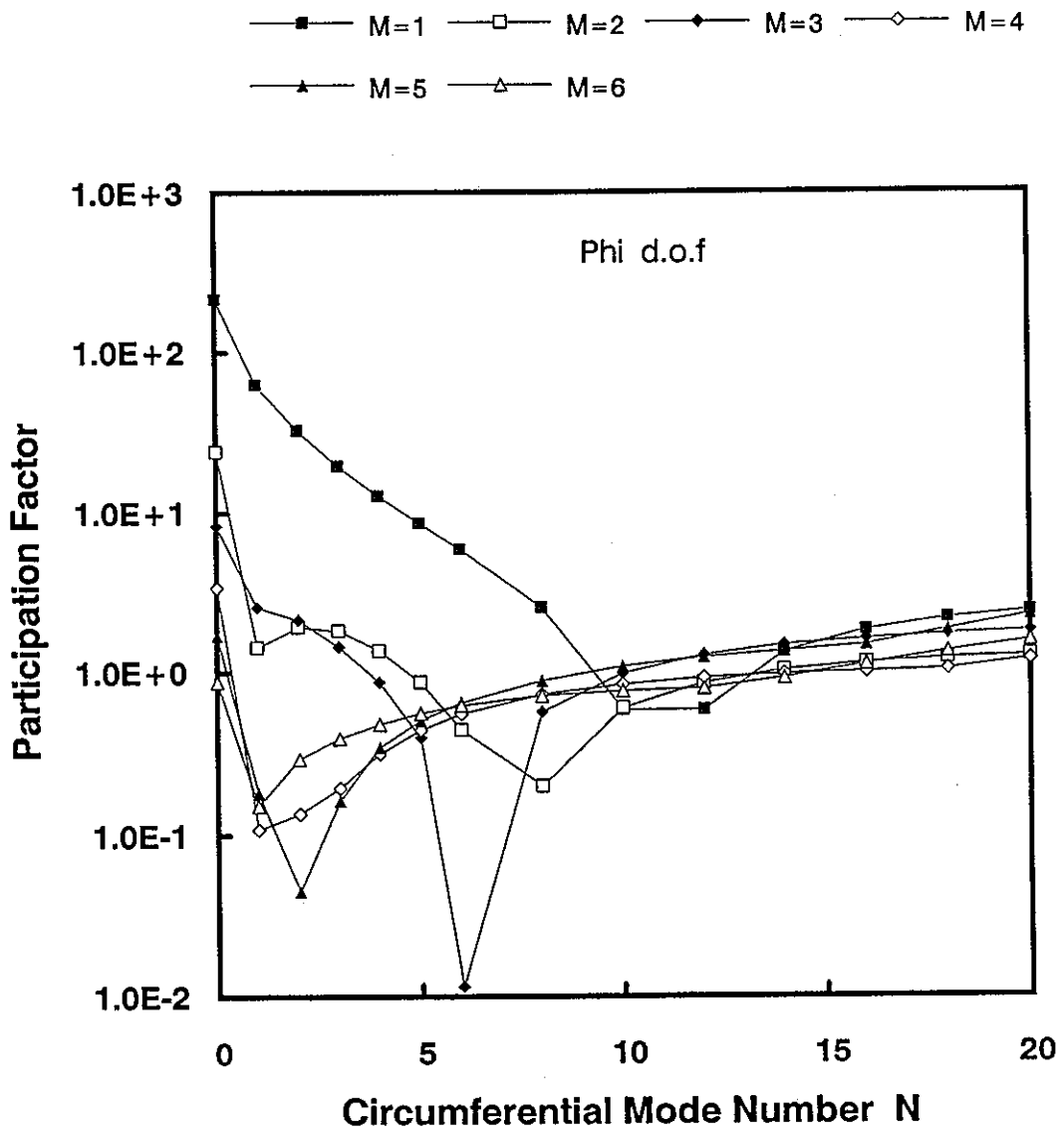

Fig. 3.2-2 Distribution of Participation Factors by 2-D Axi-symmetric Analysis (2 of 2: Phi d.o.f)

agt9b\ch_3

N = 0

m = 1
f = 27.1 Hz

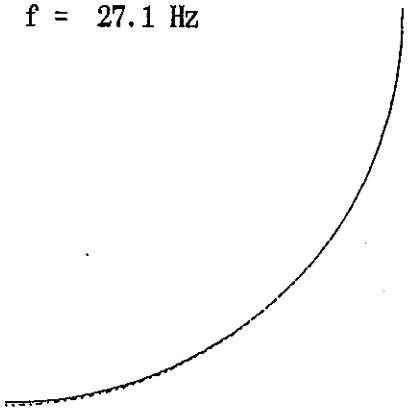

m = 2
f = 59.3 Hz

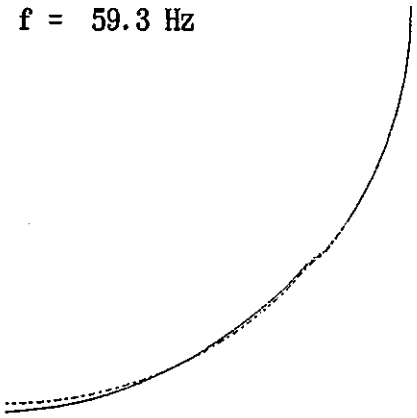

m = 3
f = 92.6 Hz

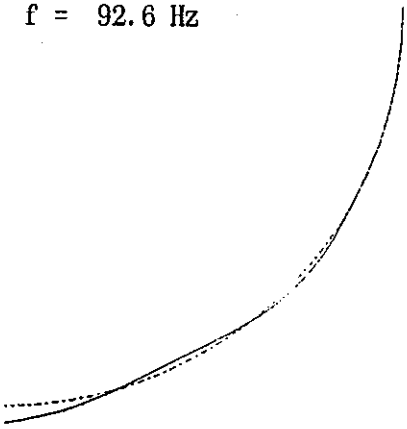

m = 4
f = 126.6 Hz

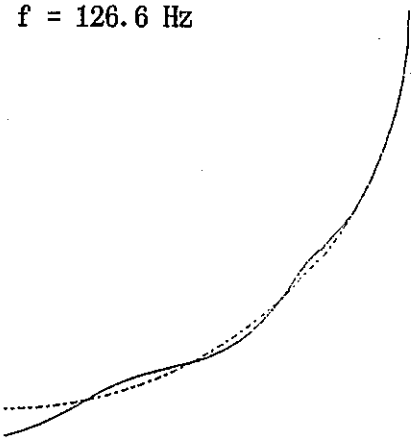

m = 5
f = 161.4 Hz

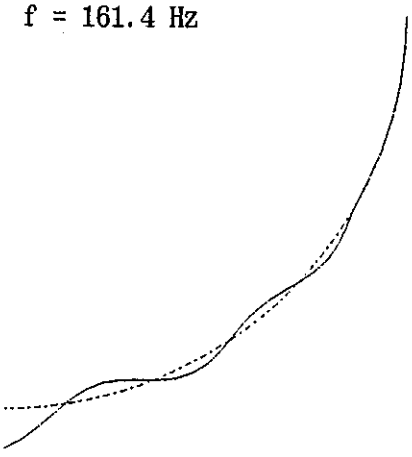

m = 6
f = 197.0 Hz

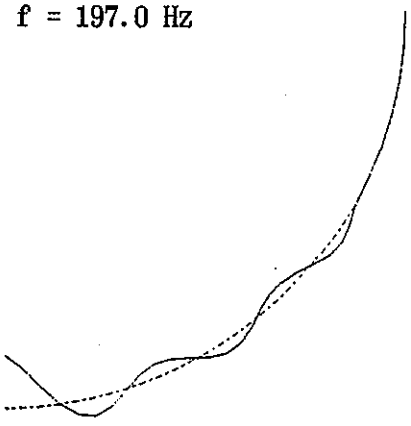

Fig. 3.2.3 Vibration Modes of Inner Shell - N = 0 -

N = 1

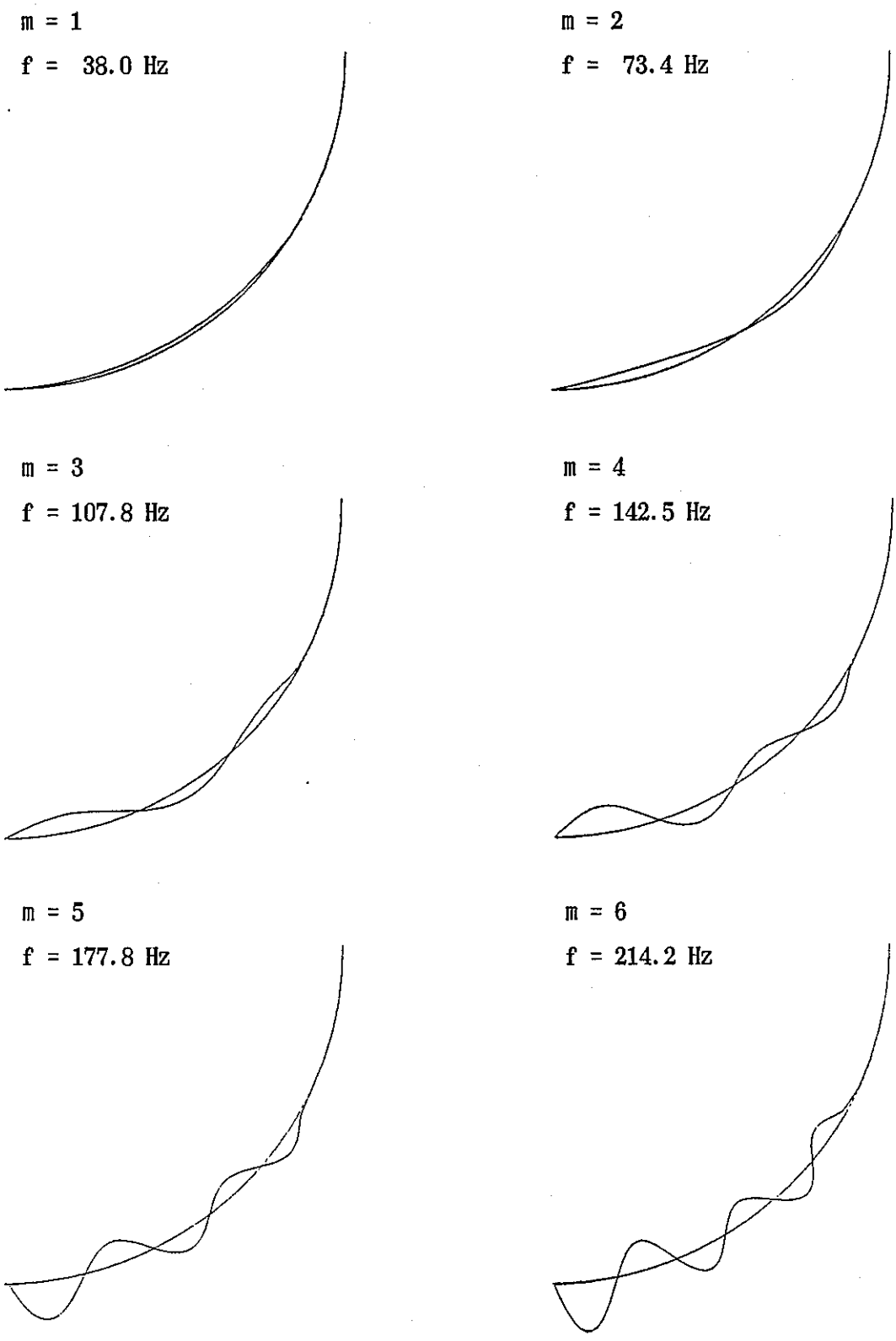

Fig. 3.2.4 Vibration Modes of Inner Shell - N = 1 -

N = 2

m = 1
f = 54.9 Hz

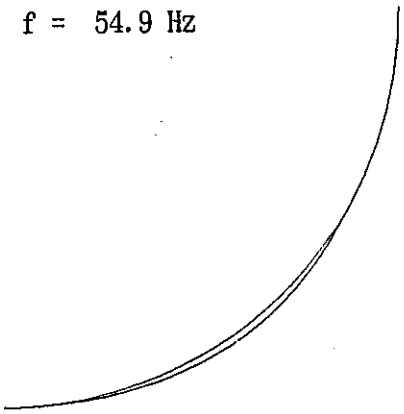

m = 2
f = 89.9 Hz

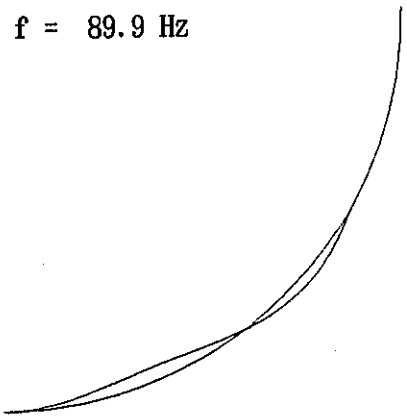

m = 3
f = 124.6 Hz

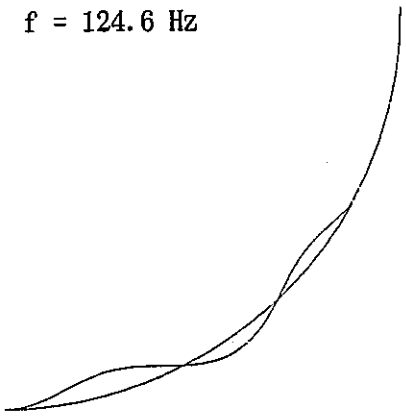

m = 4
f = 159.6 Hz

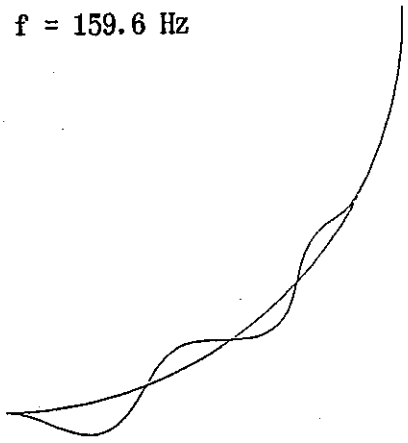

m = 5
f = 195.4 Hz

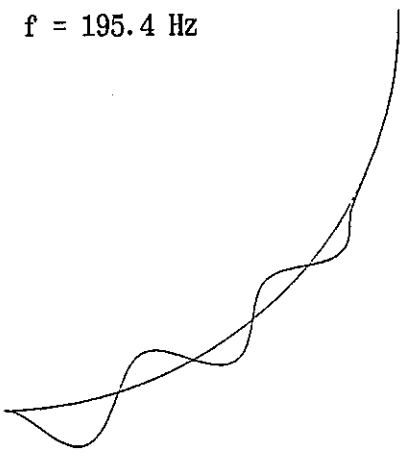

m = 6
f = 232.6 Hz

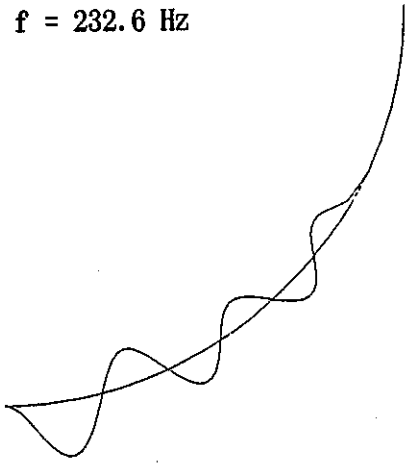

Fig. 3.2.5 Vibration Modes of Inner Shell - N = 2 -

N = 3

m = 1
f = 69.8 Hz

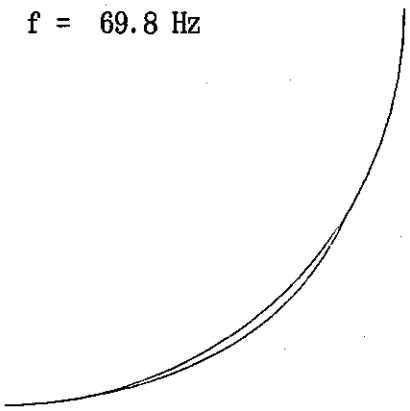

m = 2
f = 105.4 Hz

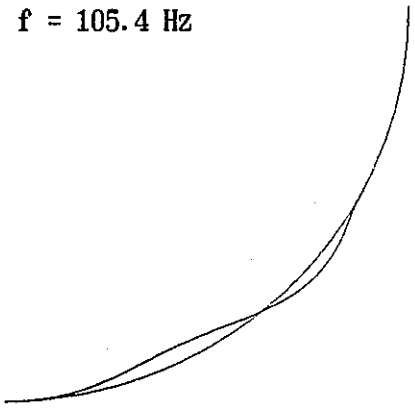

m = 3
f = 140.6 Hz

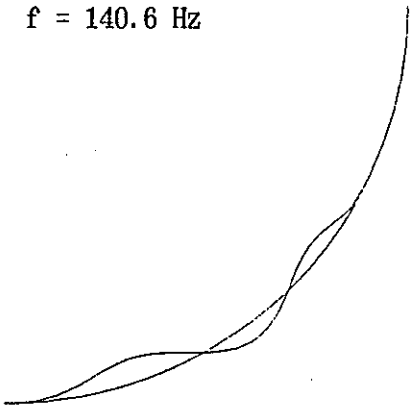

m = 4
f = 176.2 Hz

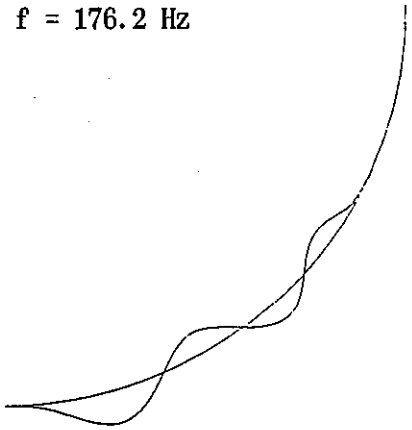

m = 5
f = 212.7 Hz

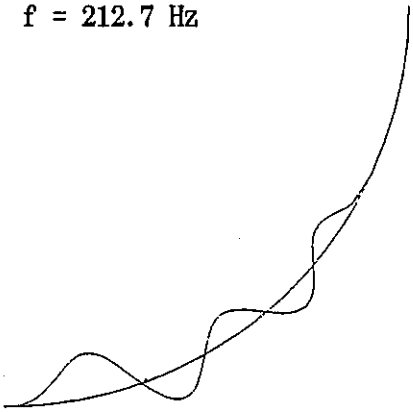

m = 6
f = 250.8 Hz

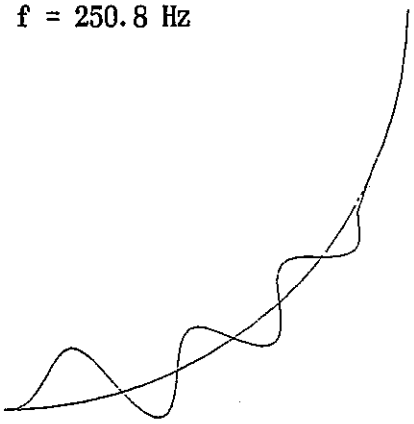

Fig. 3.2.6 Vibration Modes of Inner Shell - N = 3 -

N = 4

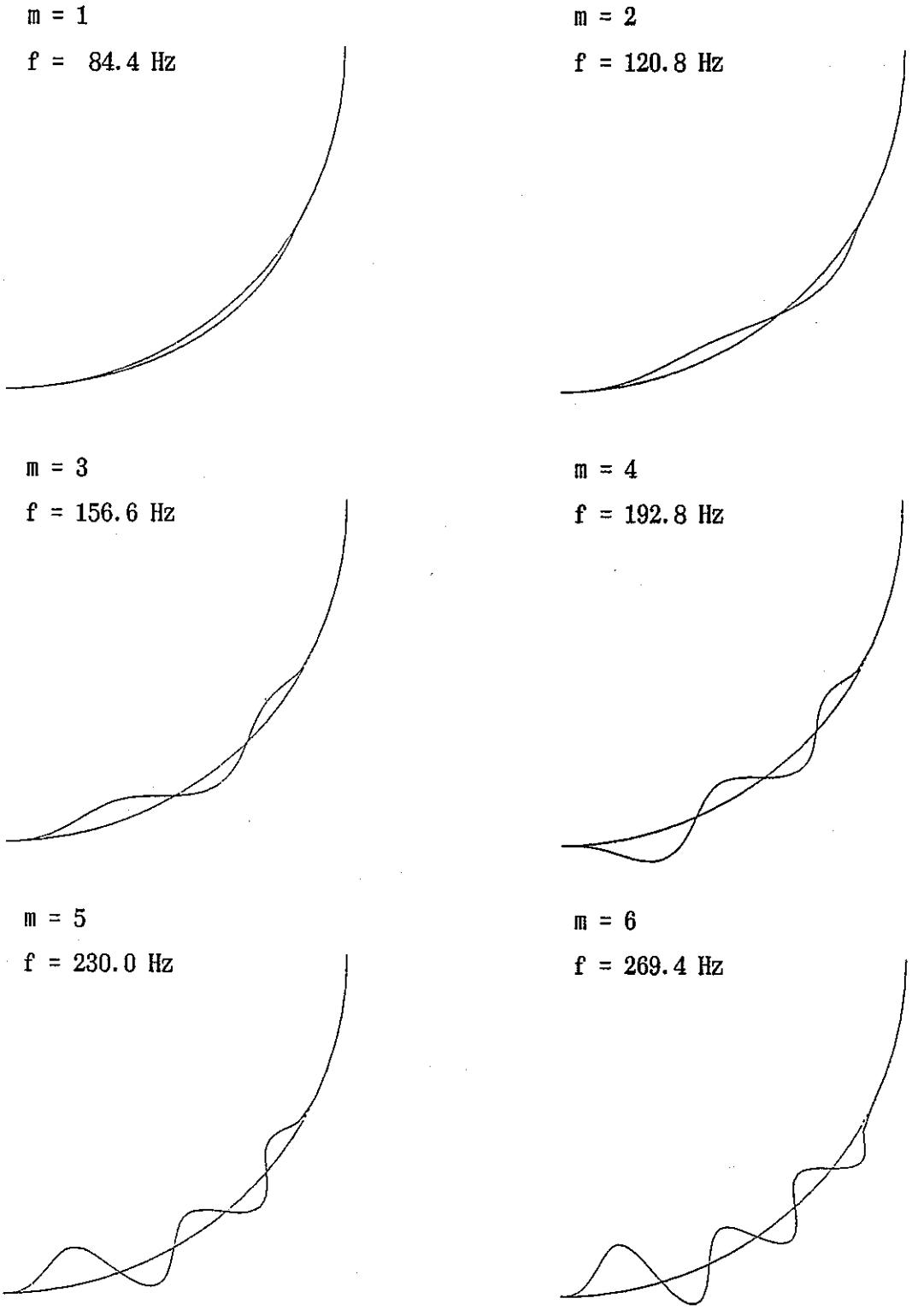

Fig. 3.2.7 Vibration Modes of Inner Shell - N = 4 -

N = 5

m = 1
f = 98.8 Hz

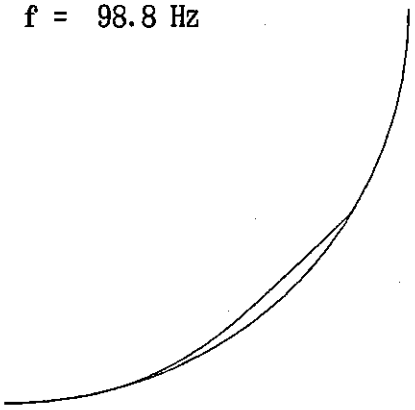

m = 2
f = 136.0 Hz

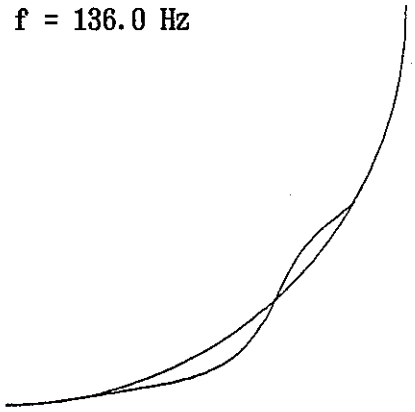

m = 3
f = 172.4 Hz

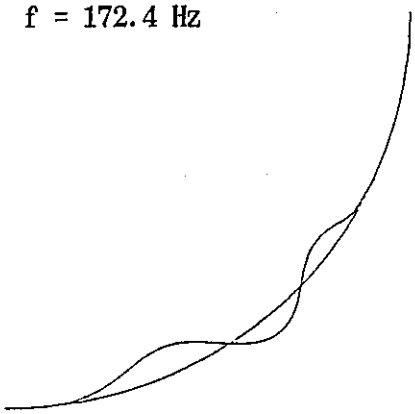

m = 4
f = 209.3 Hz

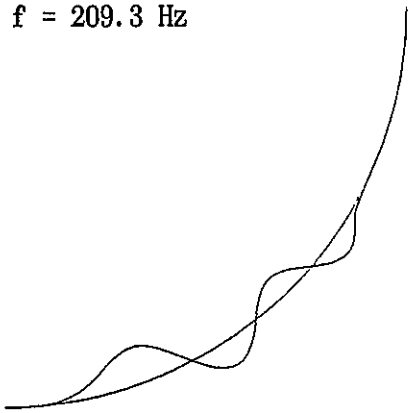

m = 5
f = 247.6 Hz

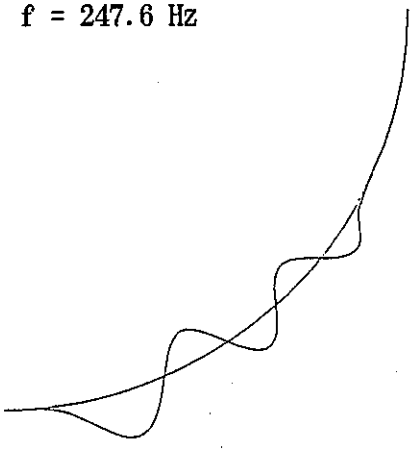

m = 6
f = 288.4 Hz

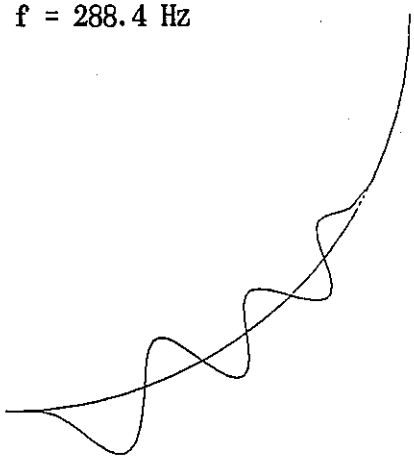

Fig. 3.2.8 Vibration Modes of Inner Shell - N = 5 -

N = 6

m = 1
f = 113.2 Hz

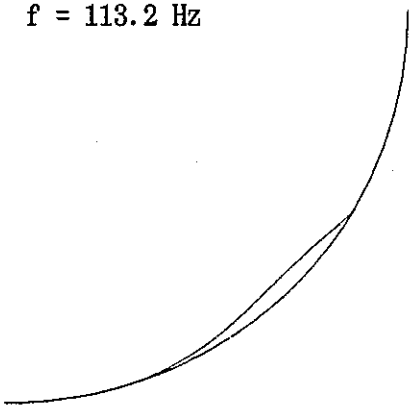

m = 2
f = 151.2 Hz

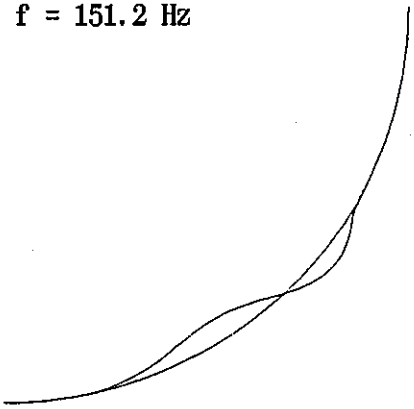

m = 3
f = 188.3 Hz

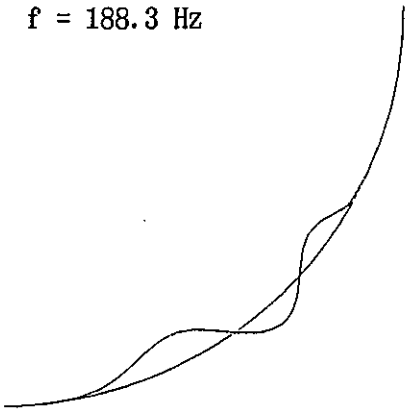

m = 4
f = 226.0 Hz

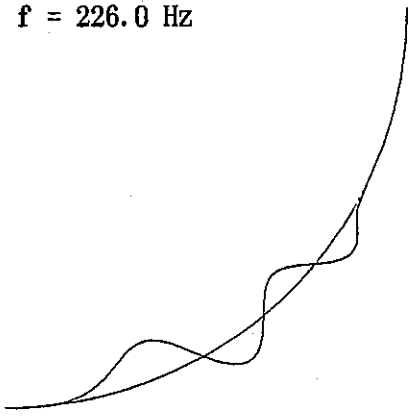

m = 5
f = 265.5 Hz

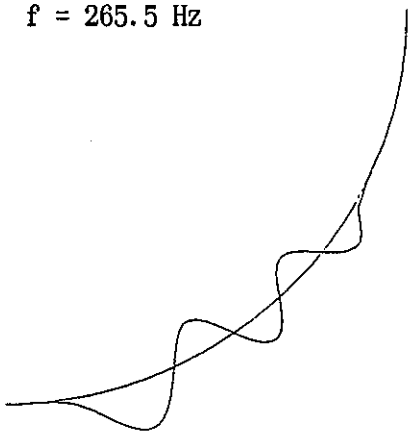

m = 6
f = 307.9 Hz

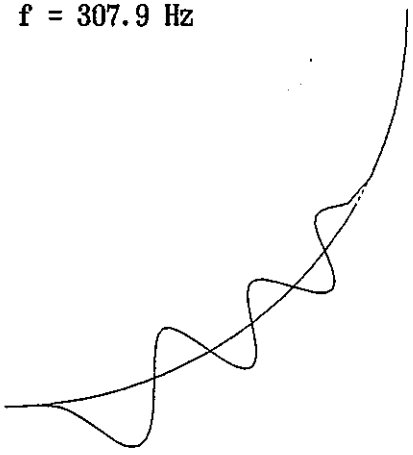

Fig. 3.2.9 Vibration Modes of Inner Shell - N = 6 -

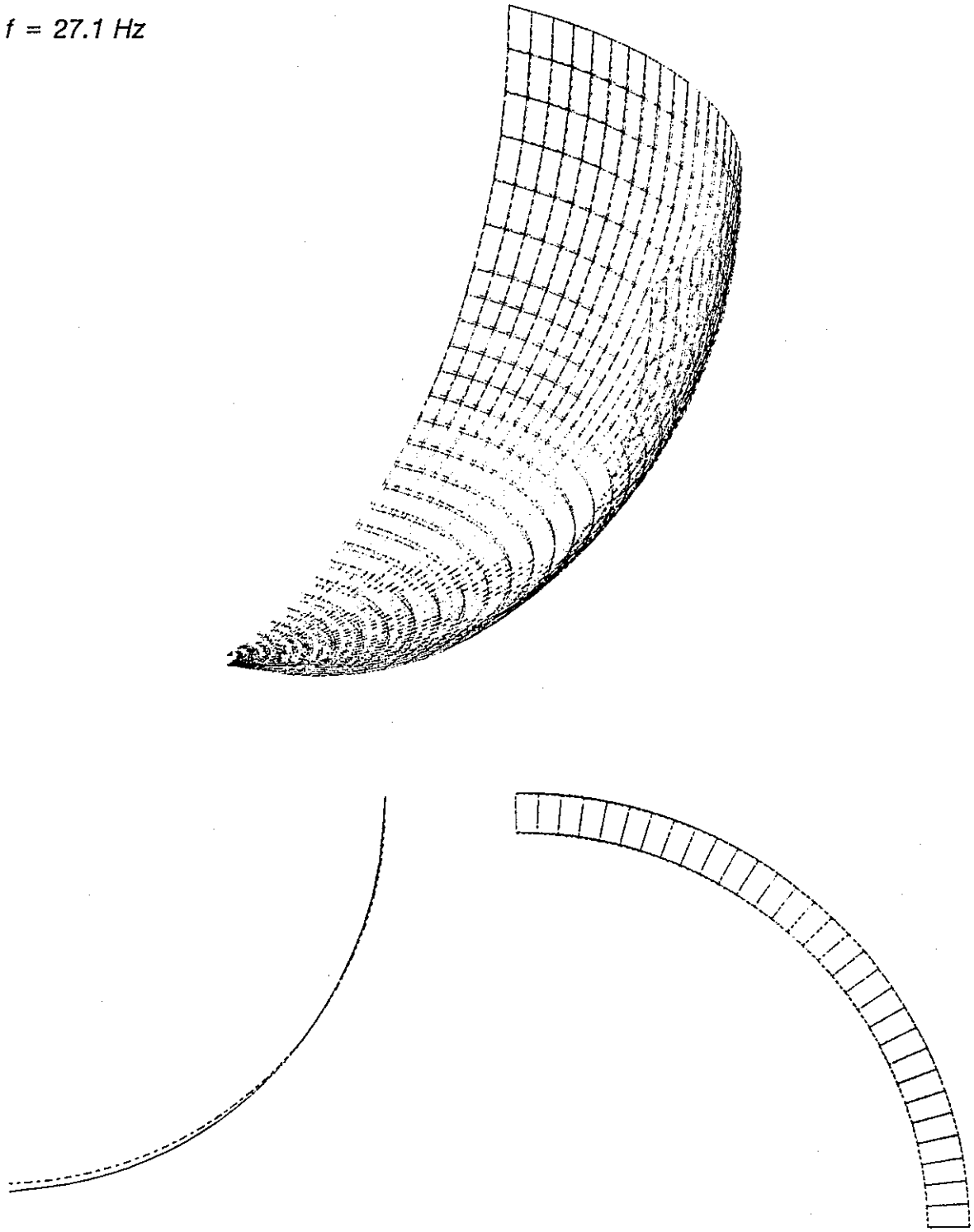

Fig. 3.2.10 3-D Vibration Mode of Inner Shell - N=0, M=1 -

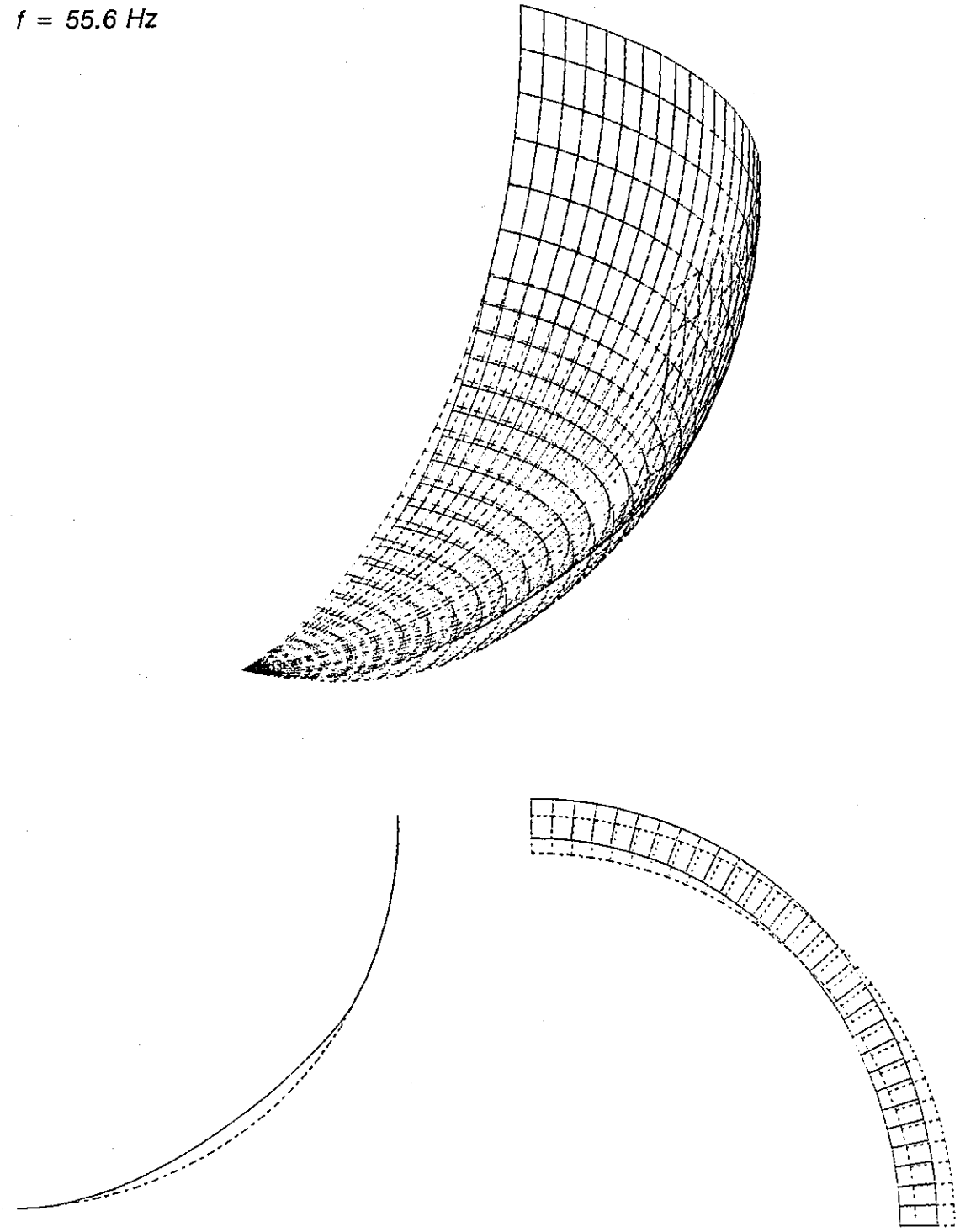

Fig. 3.2.11 3-D Vibration Mode of Inner Shell - N=2, M=1 -

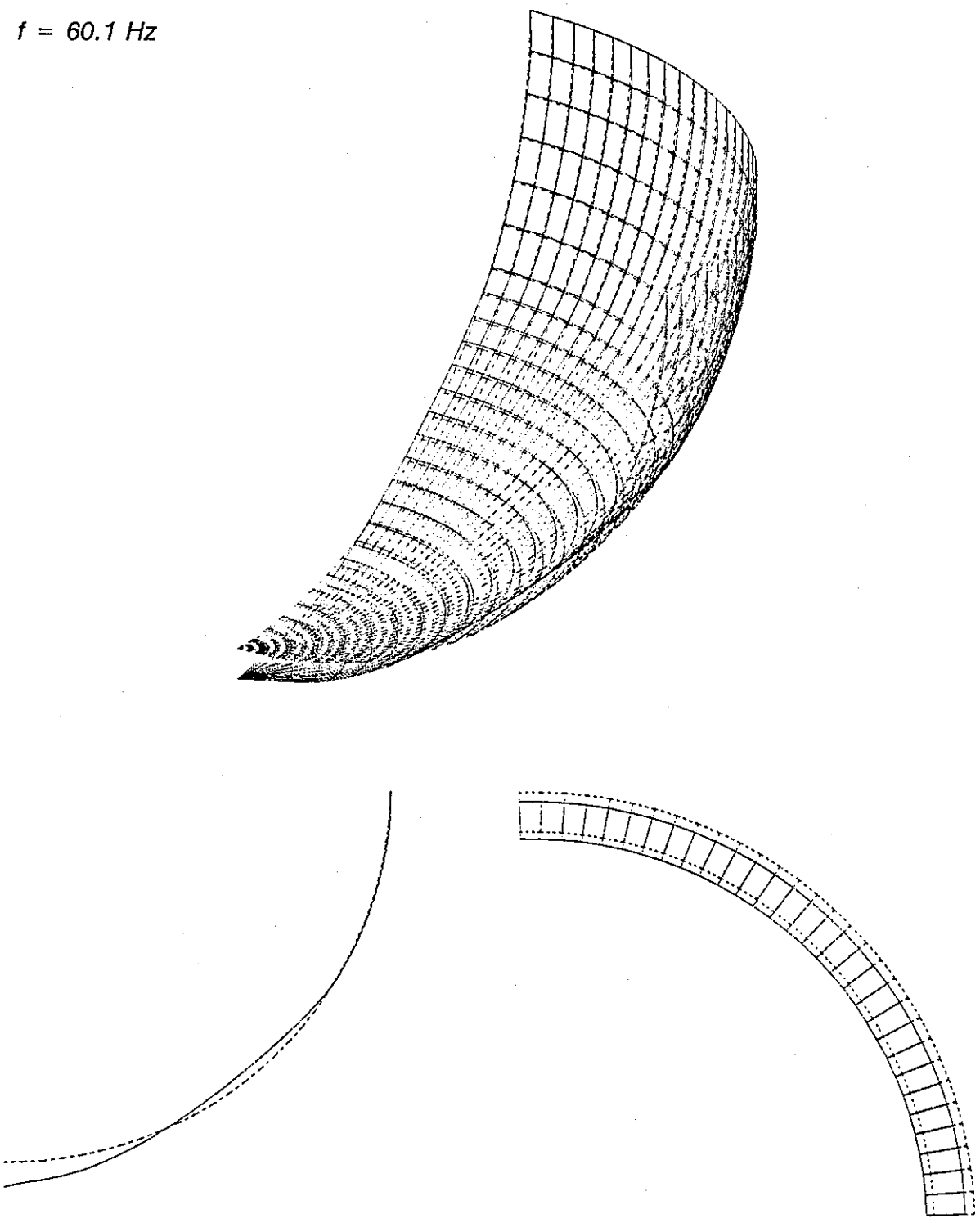

Fig. 3.2.12 3-D Vibration Mode of Inner Shell - N=0, M=2 -

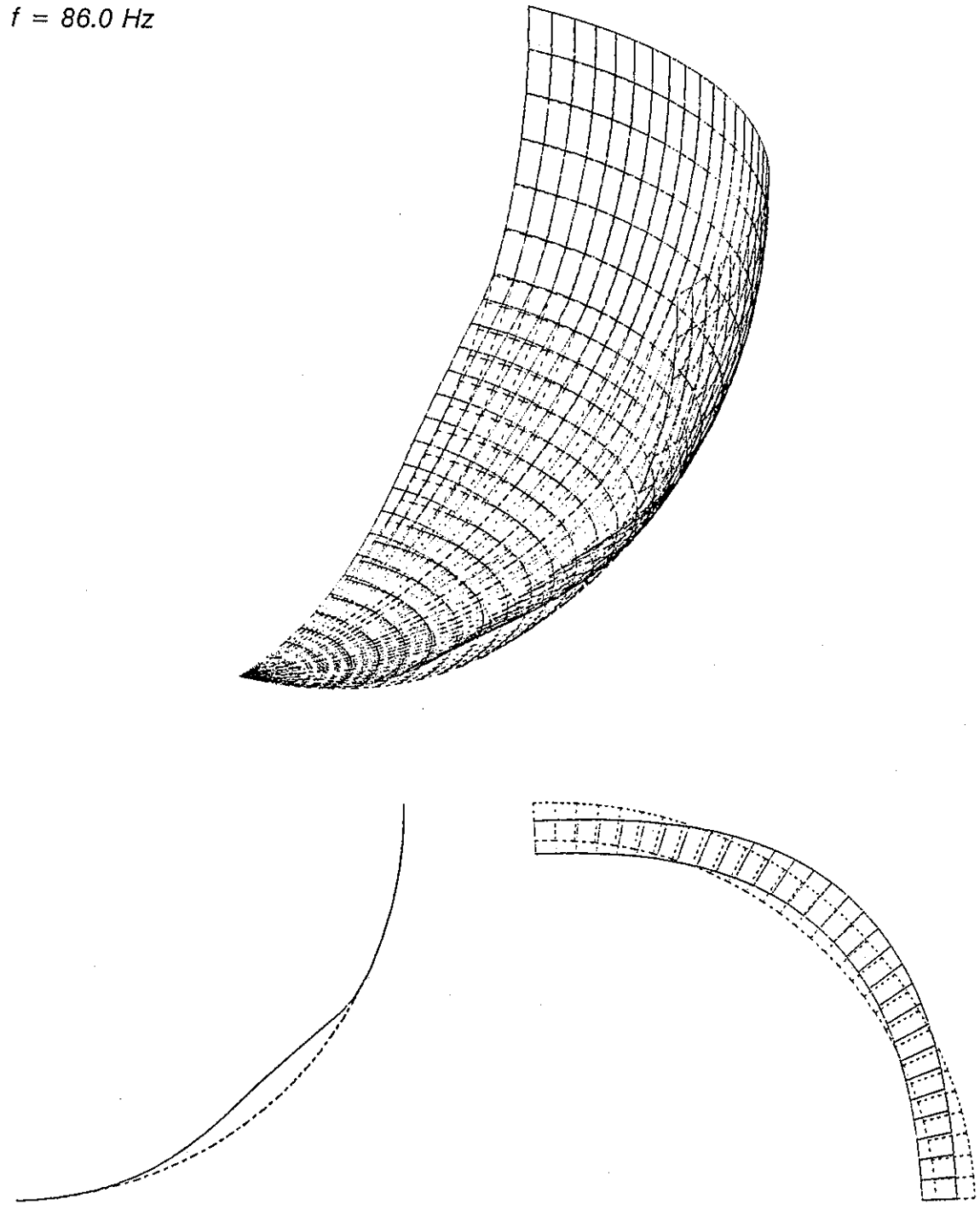

Fig. 3.2.13 3-D Vibration Mode of Inner Shell - N=4, M=1 -

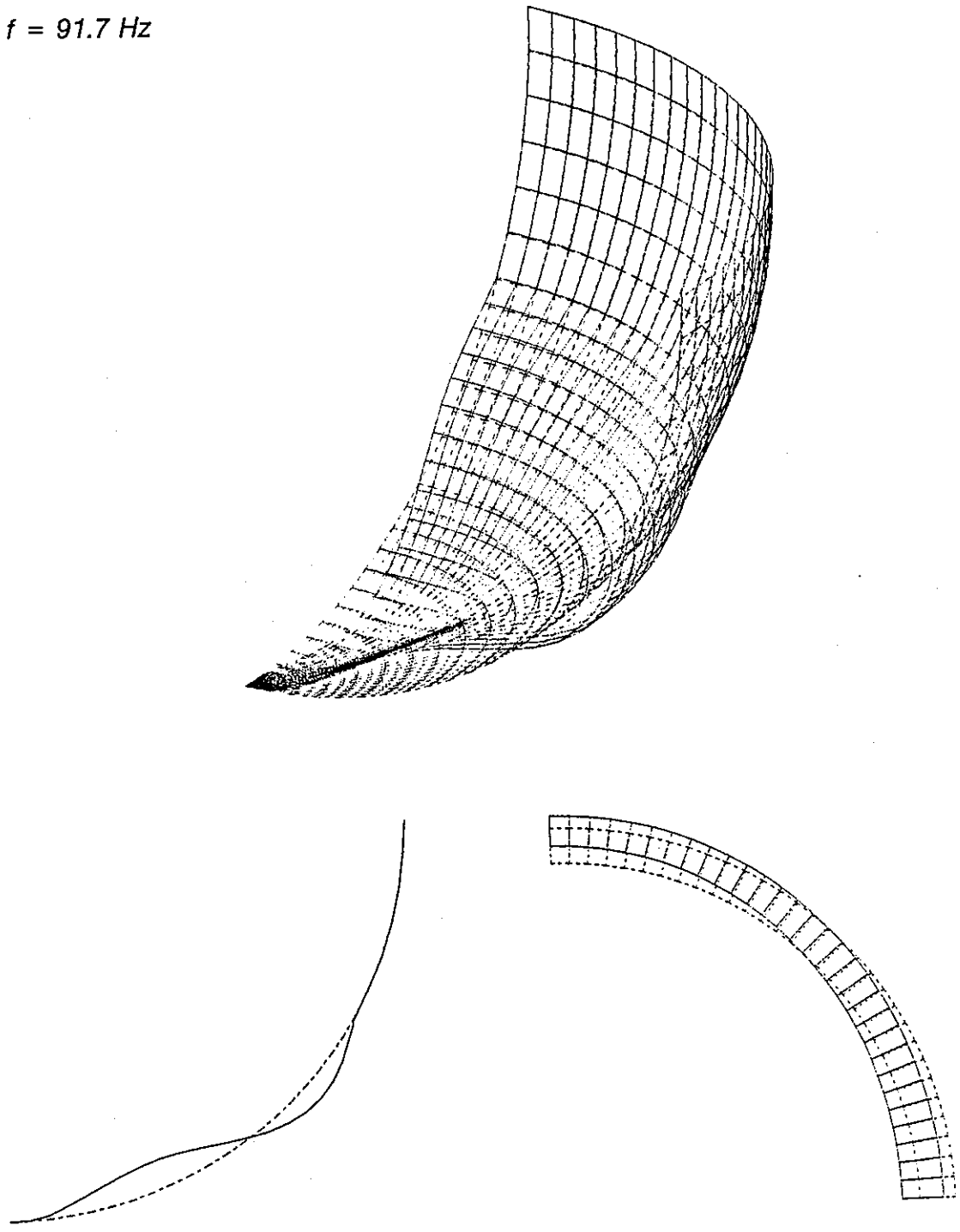

Fig. 3.2.14 3-D Vibration Mode of Inner Shell - N=2, M=2 -

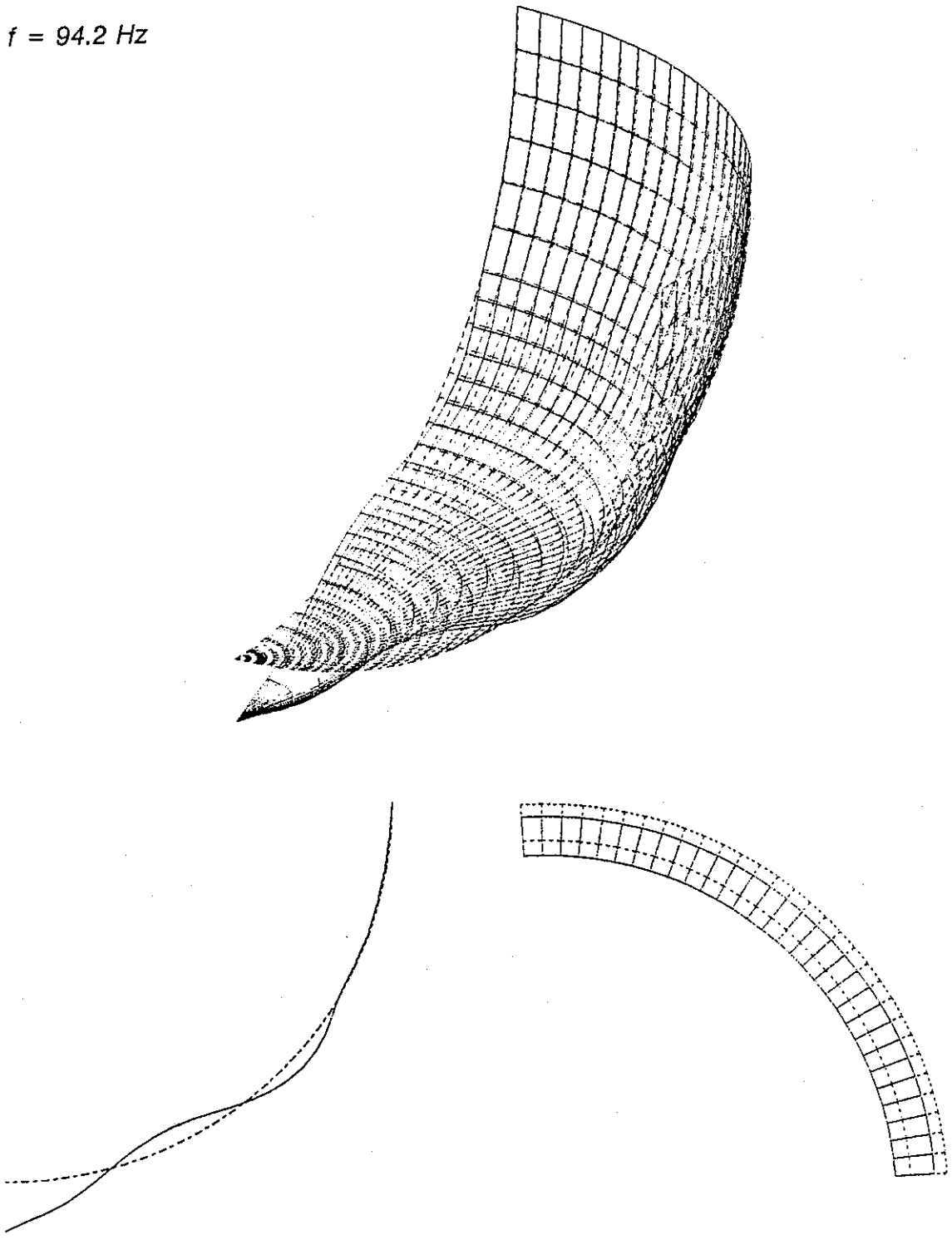

Fig. 3.2.15 3-D Vibration Mode of Inner Shell - N=0, M=3 -

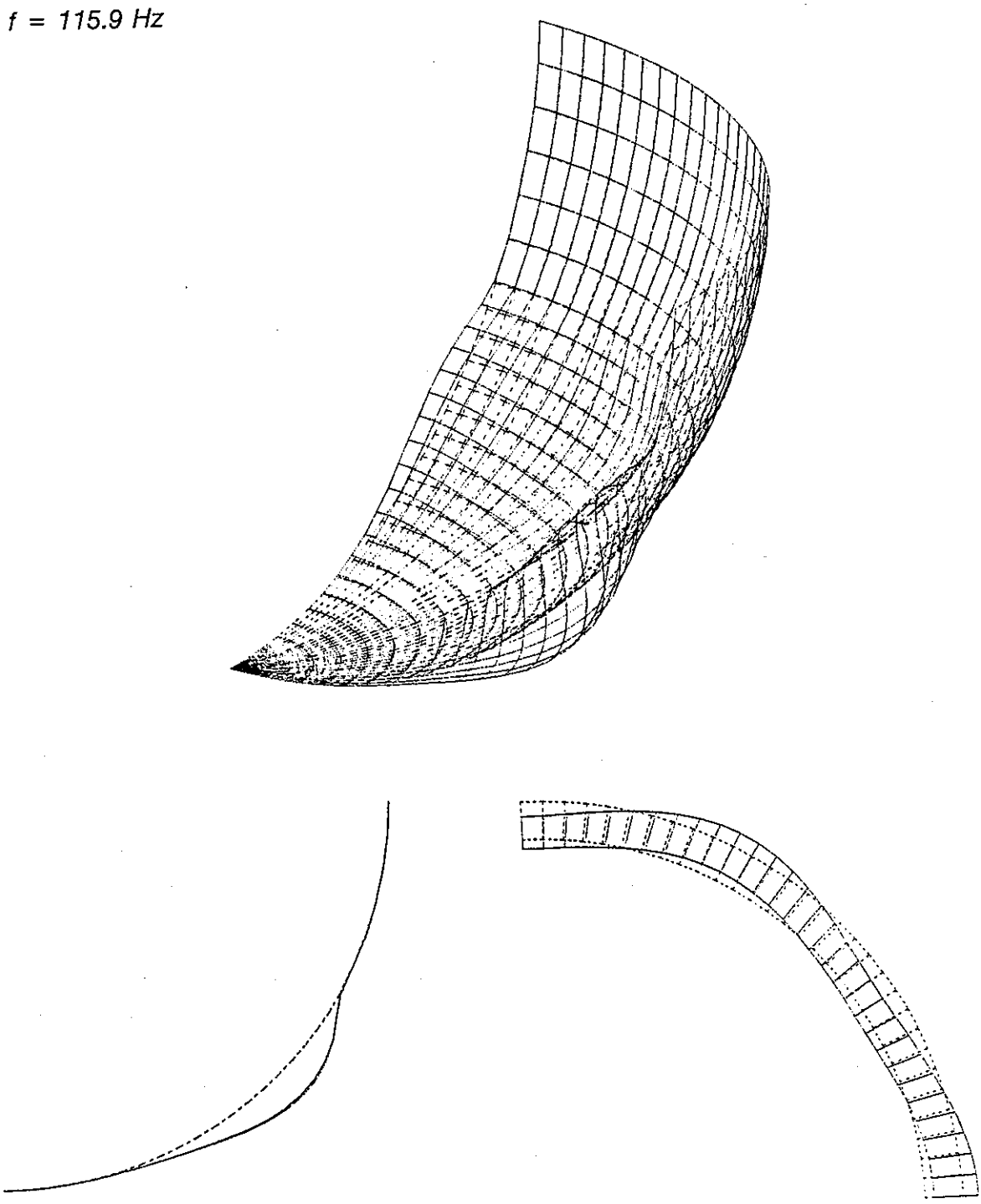

Fig. 3.2.16 3-D Vibration Mode of Inner Shell - N=6, M=1 -

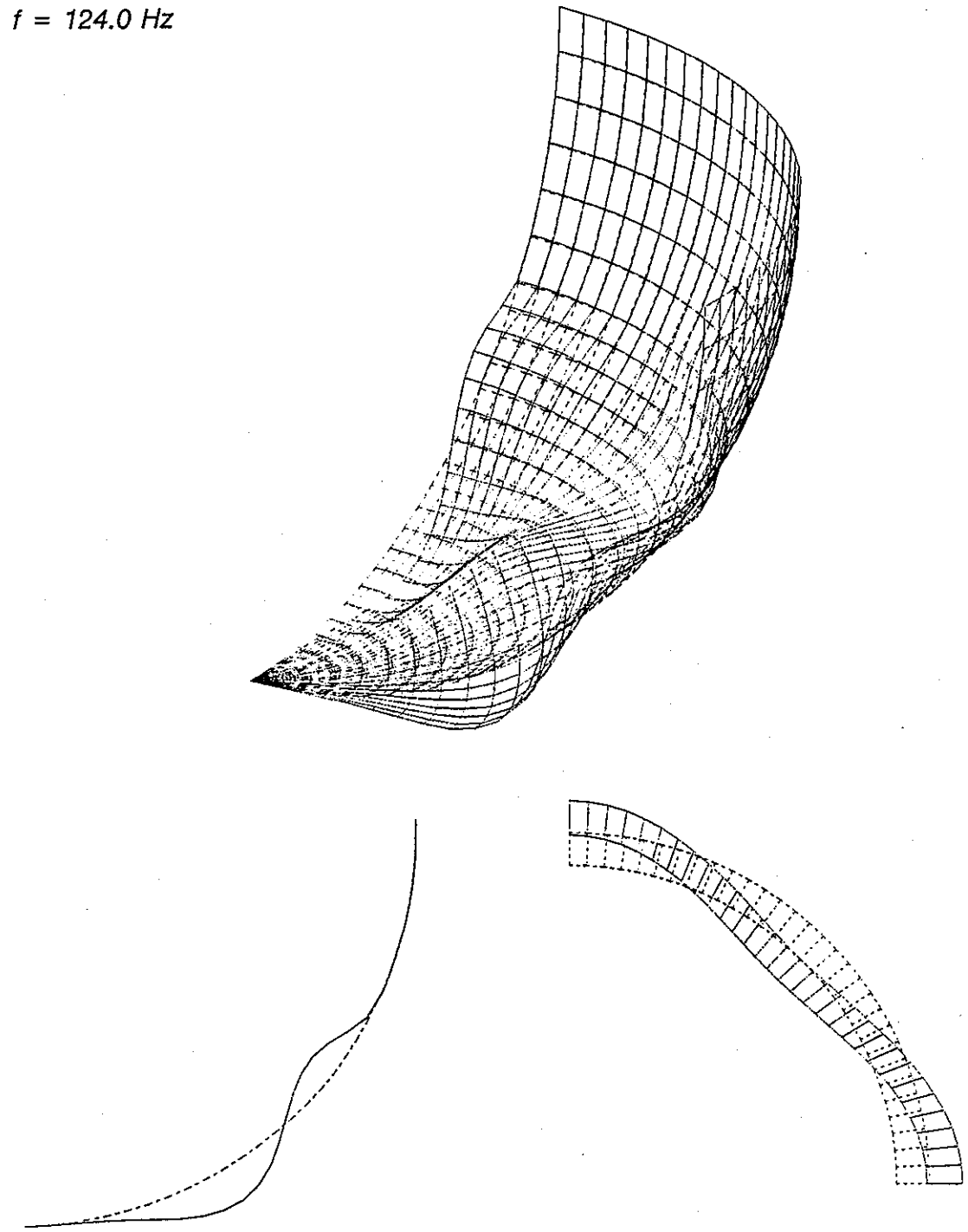

Fig. 3.2.17 3-D Vibration Mode of Inner Shell - N=4, M=2 -

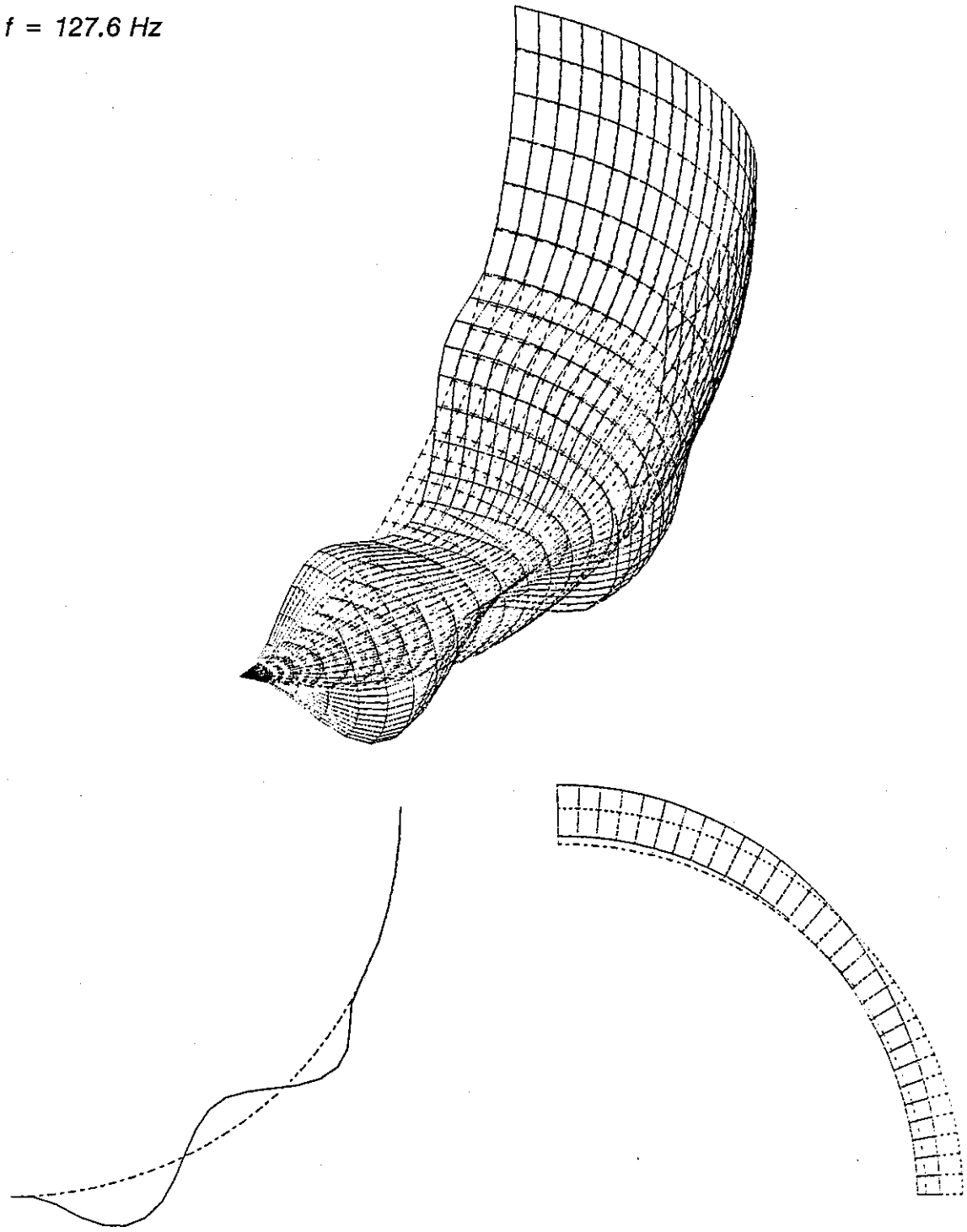

Fig. 3.2.18 3-D Vibration Mode of Inner Shell - N=2, M=3 -

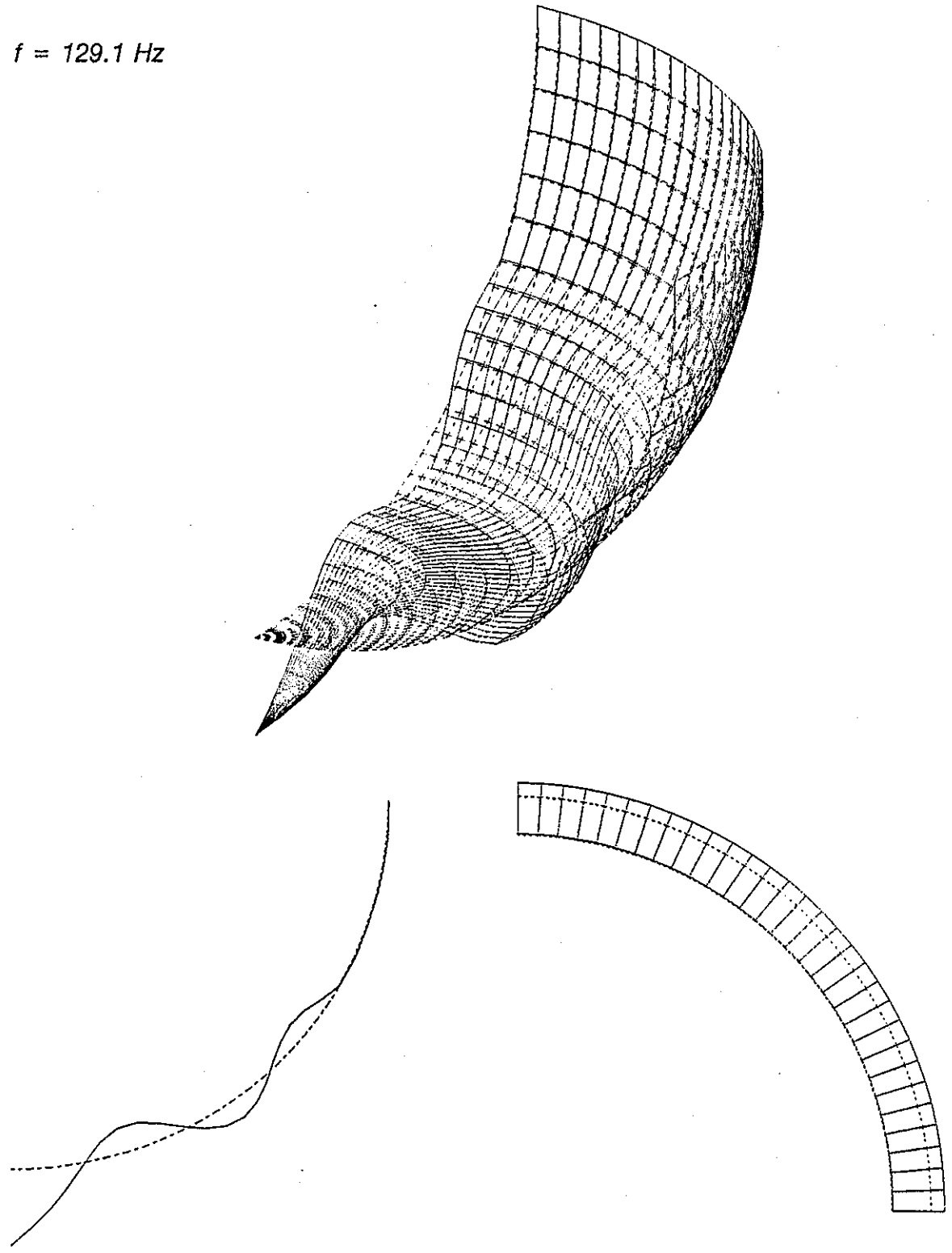

Fig. 3.2.19 3-D Vibration Mode of Inner Shell - N=0, M=4 -

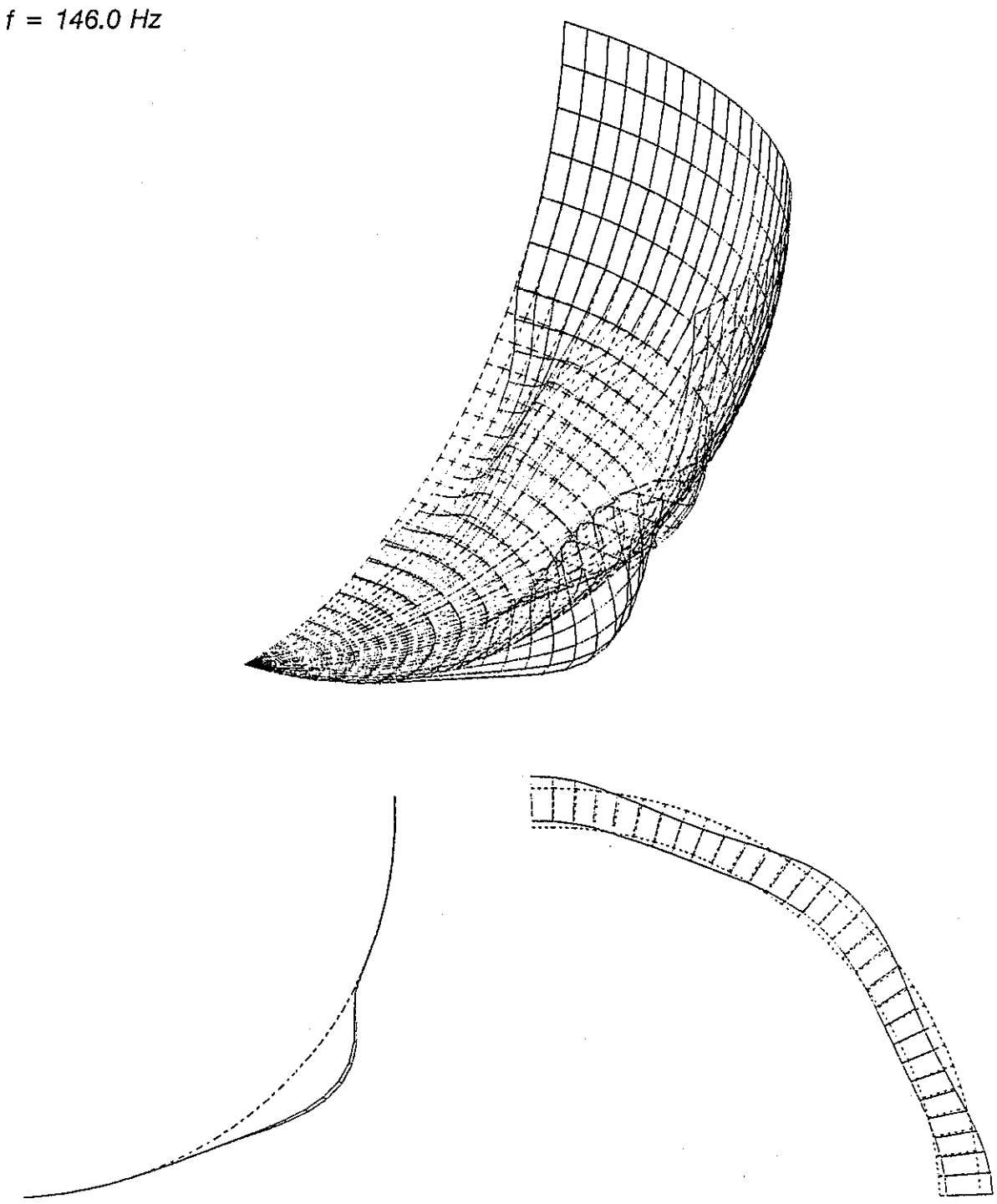

Fig. 3.2.20 3-D Vibration Mode of Inner Shell - N=8, M=1 -

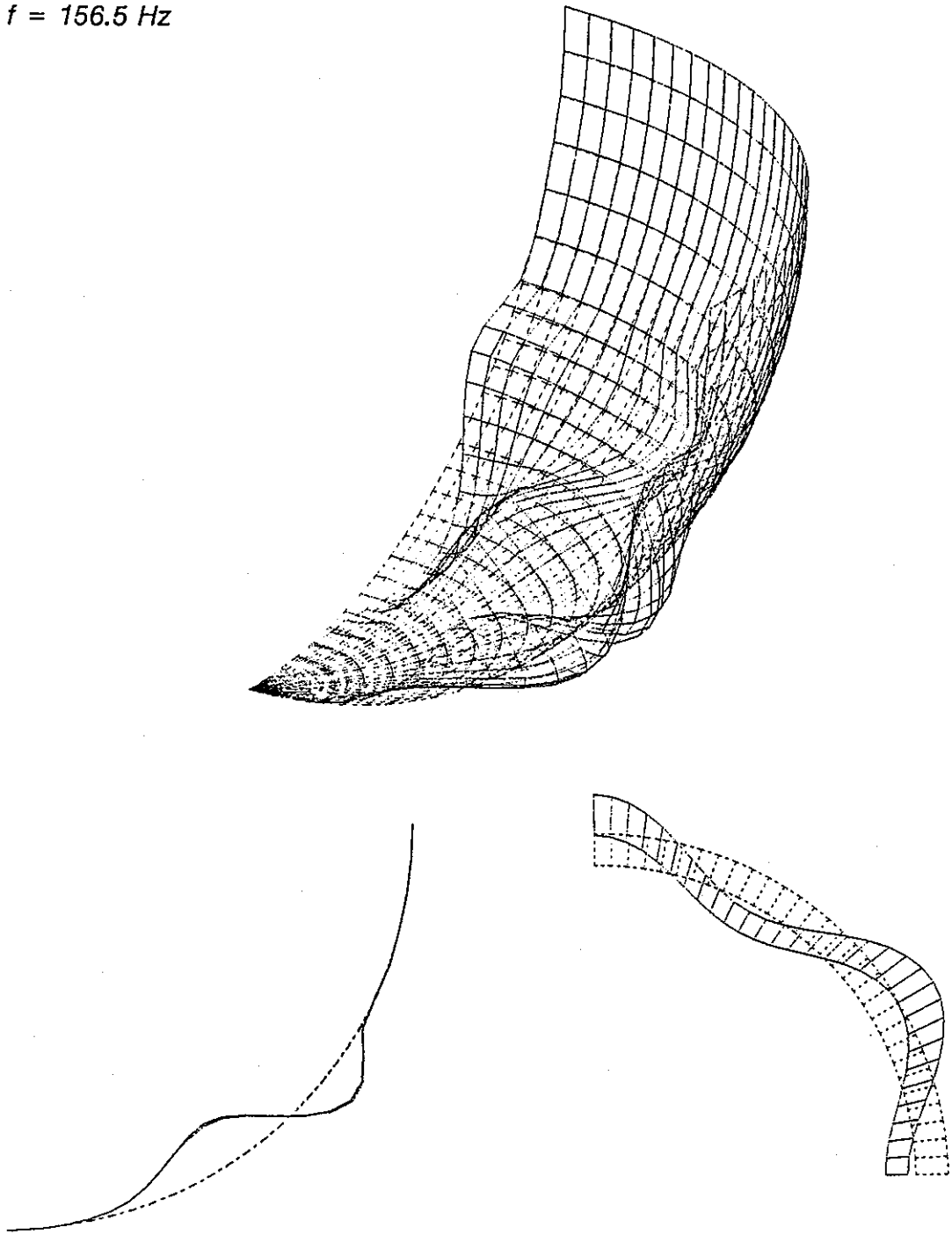

Fig. 3.2.21 3-D Vibration Mode of Inner Shell - N=6, M=2 -

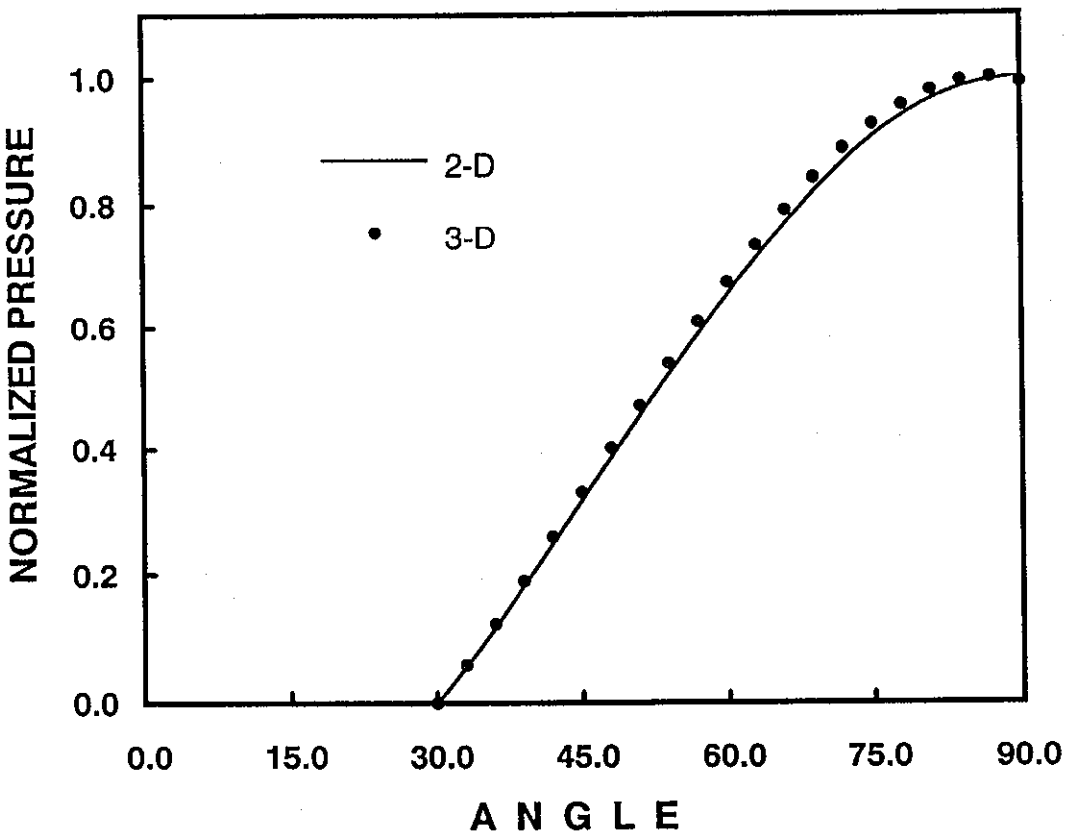

Fig. 3.2-22 Profile of Pressure Distribution by 2-D and 3-d Analysis

agt9b\ch_3

4. BUCKLING ANALYSIS

A series of static stress and buckling analyses was performed on the thin inner hemisphere. Since the fundamental mode of fluid pressure mode is axi-symmetric, analyses using a 2-D model were first carried out. Then, some detailed 3-D analyses were also done, because it was not ascertained that the axi-symmetric buckling mode to be prevailing even the pressure is applied in an axi-symmetric mode. Although the nominal uniform thickness was used in the dynamic analyses, the actually measured thickness distribution was used in the static analyses.

4.1 METHOD OF ANALYSIS

4.1.1 2-D Axi-symmetric Analysis

ANALYSIS MODEL : The analysis model for the inner hemisphere is identical with the model used in the dynamic analysis, as shown in Fig. 4.1-1.

number of nodes	67
total degree of freedom	199
number of elements	66 (66 * NCONC2)

GEOMETRY : The actually measured thickness distribution shown in Table 4.1-1 (same as Table 2.1-1) and Fig. 4.1-2 (Fig. 2.1-2), in stead of the nominal value, was used.

MATERIAL CONSTANTS : The material constants used in the analysis are as follows.

Young's modulus	6.60 E+10 Pa
Poisson's ratio	0.30
stress-strain curve	Table 4.1-2 (Table 2.1-1) and Fig. 4.1-3 (Fig. 2.1-3)

In case of elasto-plastic analysis, a multi-linear approximation for the inelastic stress-strain relationship given above. Work hardening coefficient, H', was calculated based on the given stress-strain relationship, which is listed in Table 4.1-3 and also shown in Fig. 4.1-4 (Fig. 2.1-4). Although there is some discontinuity in H' which may be attributed to a measurement error, these values were used in the analysis without

modification. von Mises' yield condition and isotropic hardening rule were adopted.

For the geometrical non-linearity due to large deformation, the updated Lagrangian formulation was used.

BOUNDARY CONDITION : The shell is clamped at its upper edge; i.e., all d.o.f except for the rotation around θ axis are fixed.

ANALYSIS CONDITION : Axi-symmetric deformation is assumed.

4.1.2 3-D Analysis

ANALYSIS MODEL : The whole hemisphere was modeled as shown in Fig. 4.1-5. The upper part above the water level ($0° \leq \rho \leq 30°$) was divided at 5° pitch, while the lower part below the water level ($30° \leq \rho \leq 90°$) was divided at 1.5° pitch. Finite elements used are ;

four node quadrilateral shell elements, QFLA4RT

The summary of overall analysis model is as follows.

number of nodes	2325	
total degree of freedom	6520	
number of elements	4020	(1560 * QFLA4RT)

GEOMETRY AND MATERIAL CONSTANTS : The geometry and the material constatns are identical with those used in the 2-D axi-symmetric analysis.

BOUNDARY CONDITION : The shell is clamped at its upper edge; i.e., all d.o.f except for the rotation around θ axis are fixed.

Table 4.1-1

Measured Thickness Variation of Inner Hemisphere

ZONE	THICKNESS (mm)
$0.0 \leq \phi \leq 5.4$	7.1
$5.4 \leq \phi \leq 16.2$	8.1
$16.2 \leq \phi \leq 25.2$	7.7
$25.2 \leq \phi \leq 36.0$	8.3
$36.0 \leq \phi \leq 45.0$	7.6
$45.0 \leq \phi \leq 55.8$	6.8
$55.8 \leq \phi \leq 64.8$	6.9
$64.8 \leq \phi \leq 73.6$	6.4
$73.6 \leq \phi \leq 86.4$	7.2
$86.4 \leq \phi \leq 90.0$	6.8

Table 4.1-2

Stress-strain Relation of Inner Hemisphere Material (pure Al)

σ 10^7 Pa	ϵ 10^{-3}
5.00	0.750
6.23	0.960
6.77	1.125
7.09	1.292
7.45	1.625
7.68	2.208
7.75	3.100
7.84	4.125
8.00	2000.

Table 4.1-3

Work Hardening Coefficient

ϵ_p	H' (Pa)
0.0	6.60E+10
9.924E-5	2.70E+10
2.178E-4	1.29E+10
4.962E-4	4.20E+09
1.044E-3	7.94E+08
1.926E-3	8.90E+08
2.937E-3	8.02E+05

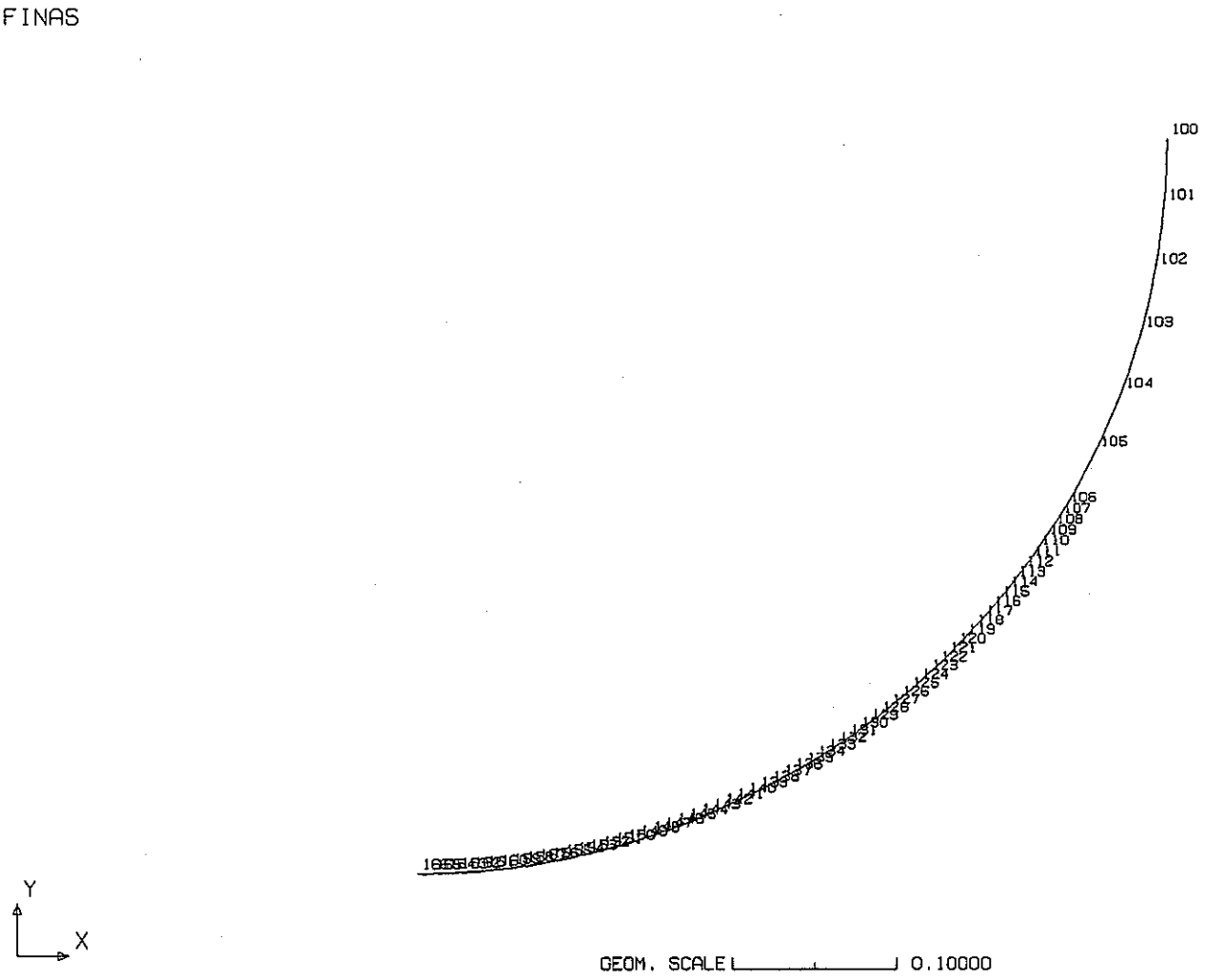

Fig. 4.1-1 2-D Axisymmetric Model for Stress Analysis

agt9b\ch_4

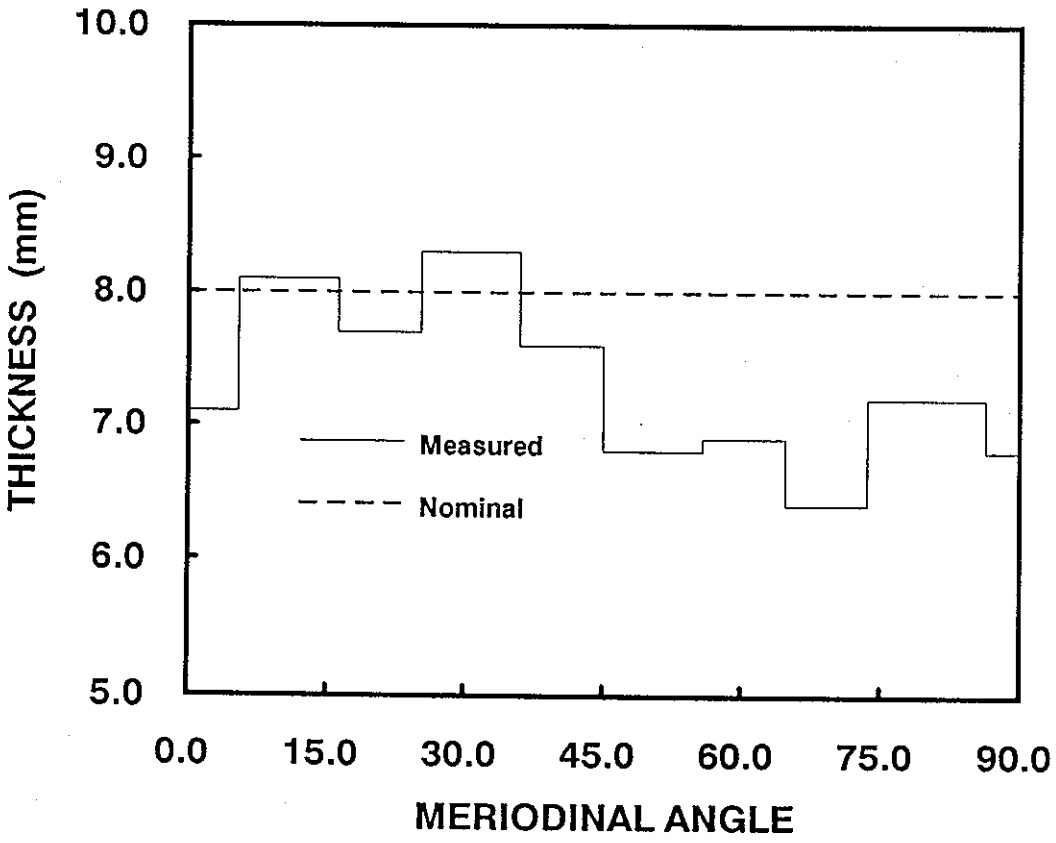

Fig. 4.1-2 Measured Thickness Distribution of Inner Hemisphere

agt9b\ch_4

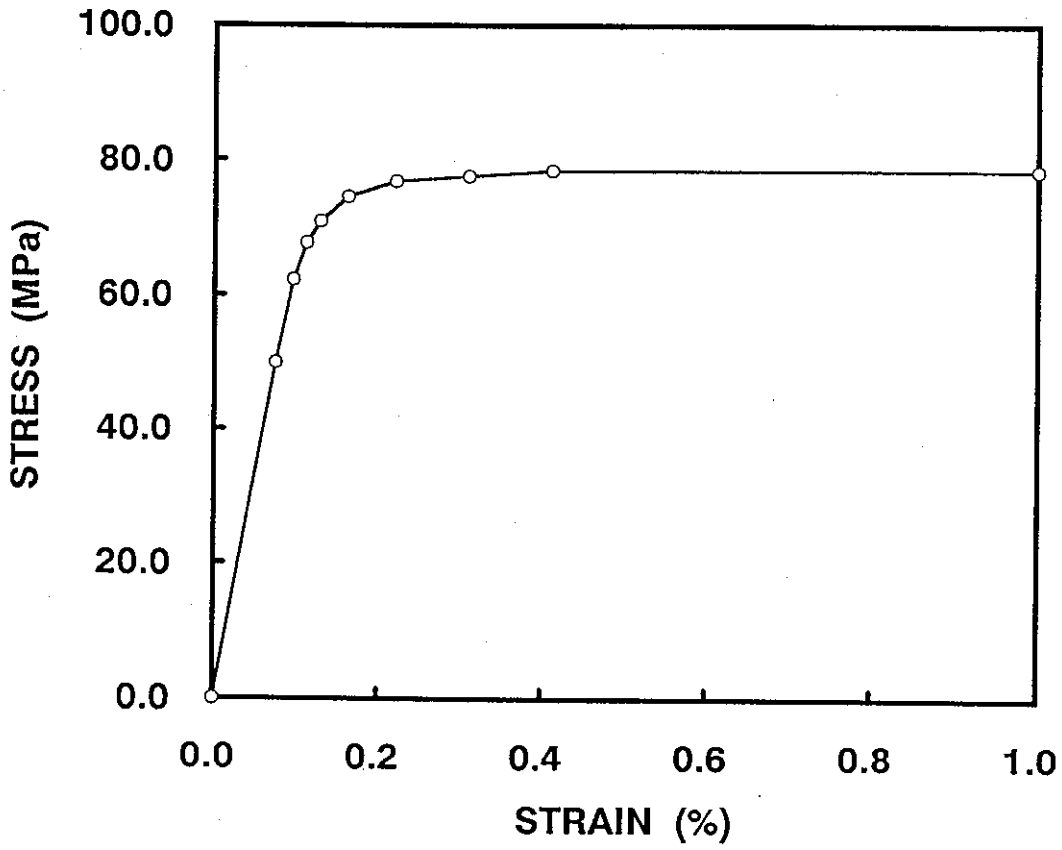

Fig. 4.1-3 Stress-strain Curve of Pure Aluminum

agt9b\ch_4

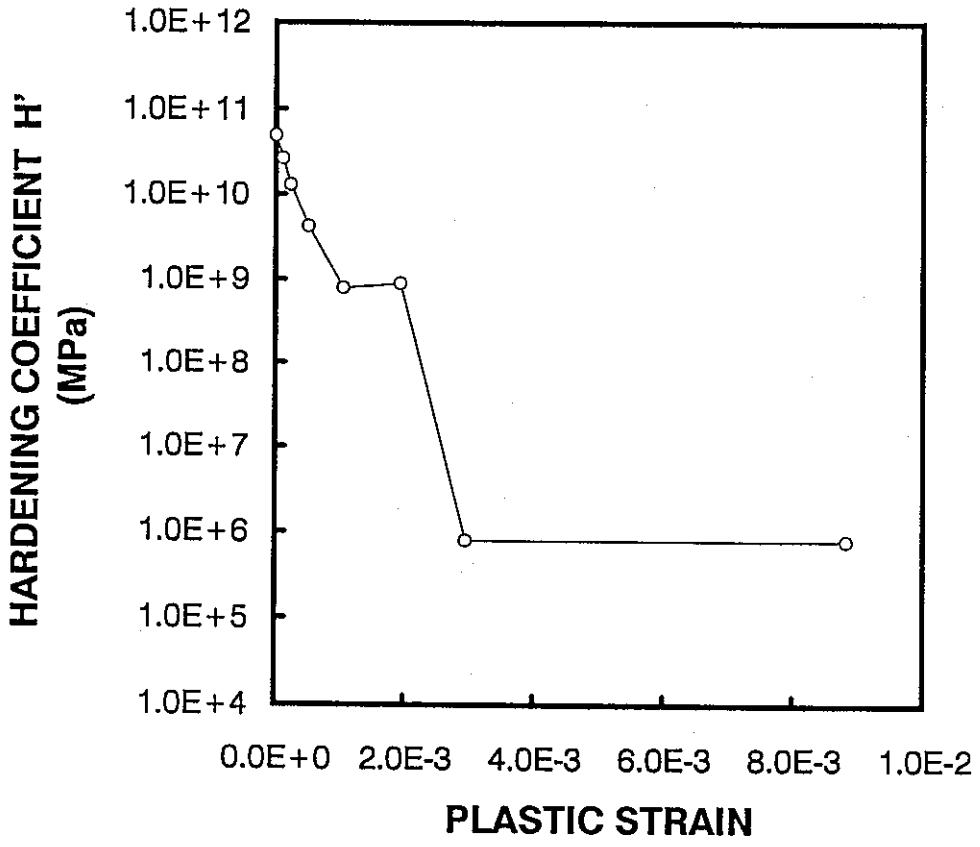

Fig. 4.1-4 Work Hardening Coefficient of Pure Aluminum

agt9b\ch_4

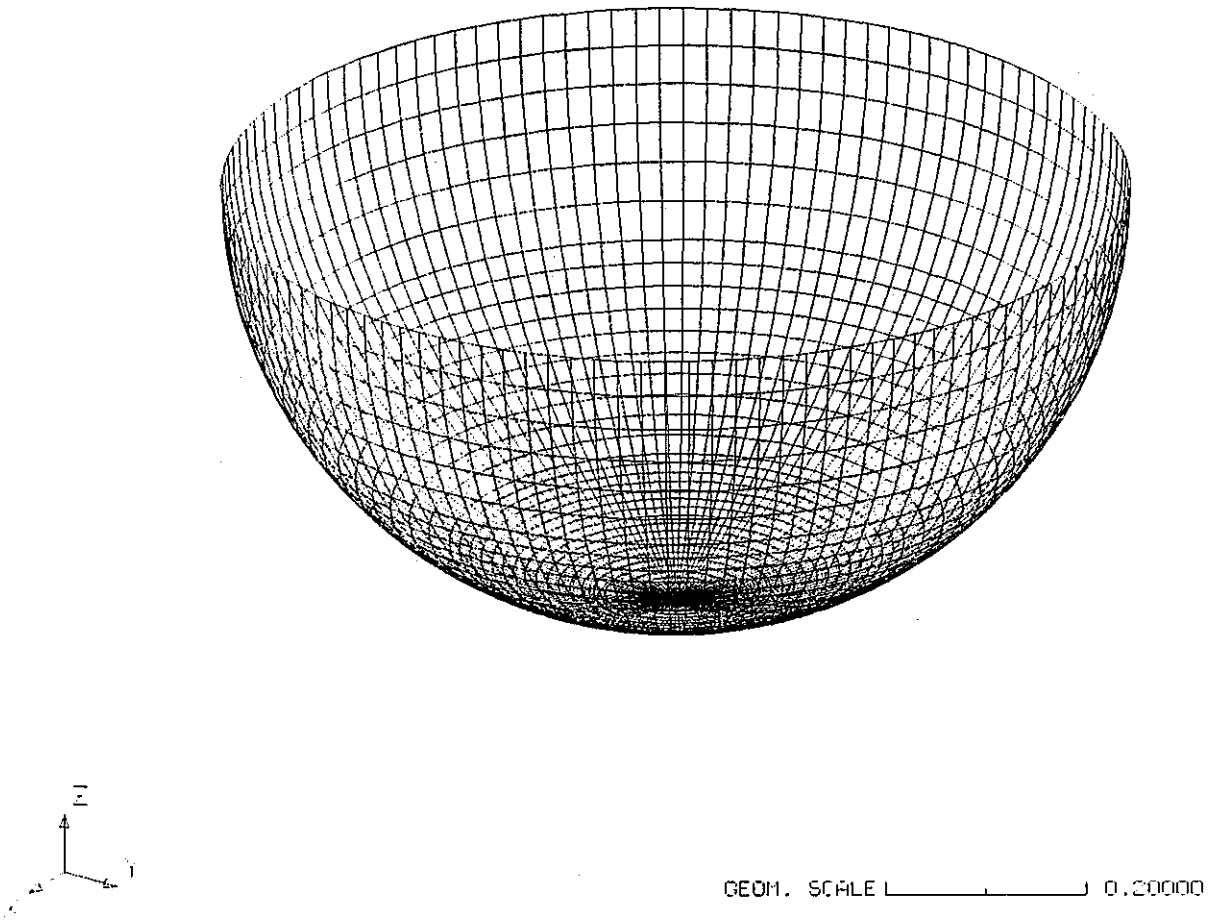

Fig. 4.1-5 3-D Model for Stress Analysis

agt9b\ch_4

4.2 PRELIMINARY STRESS ANALYSIS

Prior to the buckling analysis, elastic stress analyses with small deformation theory were conducted using both the axi-symmetric and 3-D models. The load applied is the distributed pressure with the maximum value of 1 MPa whose profile was obtained by the dynamic analysis.

Fig. 4.2-1 shows the deformation profile of the hemisphere subjected to the external pressure. Fig. 4.2-2 compares the nodal displacements in the radial direction along a meridional line obtained by axi-symmetric and 3-D analyses. The deflection of the shell takes its maximum value at the bottom point and gradually decreases, and the sign of the displacement turns from negative (shrinkage) to positive (dilatation) just before the water level. Although the overall deflection profiles by the axi-symmetric and 3-D analyses coincides each other, some differences can be seen at around the water level and the bottom point. These are attributed to the difference of mesh division and a kind of singularity of the 3-D elements including the bottom point.

In Fig. 4.2-3 shown are the distribution of membrane stress components (circumferential, meridional, and von Mises equivalent) along a meridional line. Here again, the overall stress distributions by the axi-symmetric and 3-D analyses are almost identical. The maximum of each stress component takes place at the bottom point, which are listed below.

Location	Meridional	Circum.	von Mises
Inner surface	-279.5	-277.5	278.5
Mid plane	-284.4	-284.0	284.4
Outer surface	-289.3	-291.0	291.0

The tangential stress of a sphere subjected to a pressure is given by

$$\sigma_t = \frac{pr}{2t} \tag{4.2-1}$$

Letting p = 1 MPa, r = 0.455 m, and t = 0.0008 m, and substituting these into eq. (4.2-1), one gets the theoretical value of tangential stress σ_t = 284.4 MPa, which is close enough to the analysis results.

agt9b\ch_4

The yielding stress, σ_y, of the material is assumed to be about 78 MPa from a bi-linear approximation of the stress-strain curve (Fig. 4.1-3). The stress level at which work hardening coefficient is first defined is 62.3 MPa. The maximum values of the pressure giving these stresses are about 0.27 MPa and 0.22 MPa, respectively.

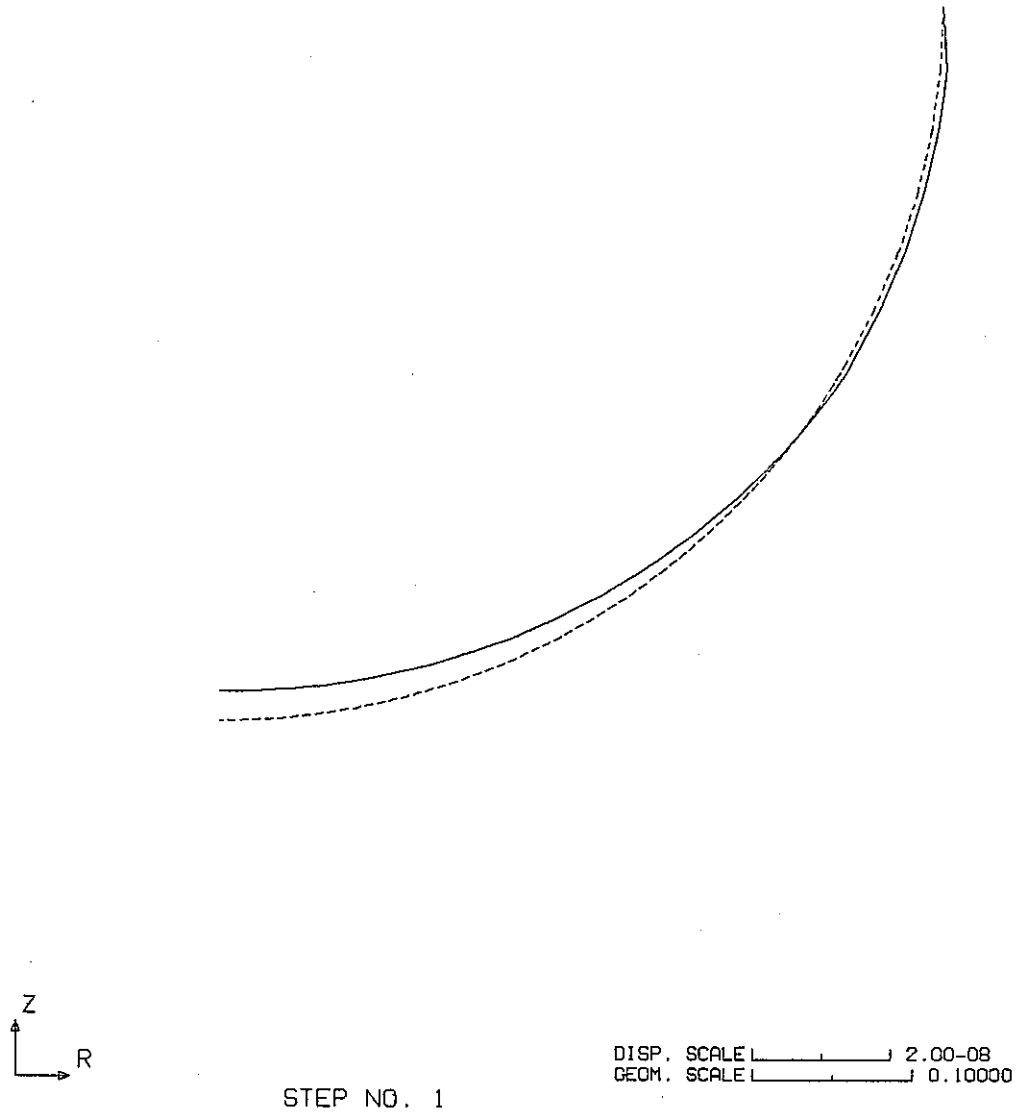

Fig. 4.2-1 Deformation of Hemisphere by Elastic Analysis

agt9b\ch_4

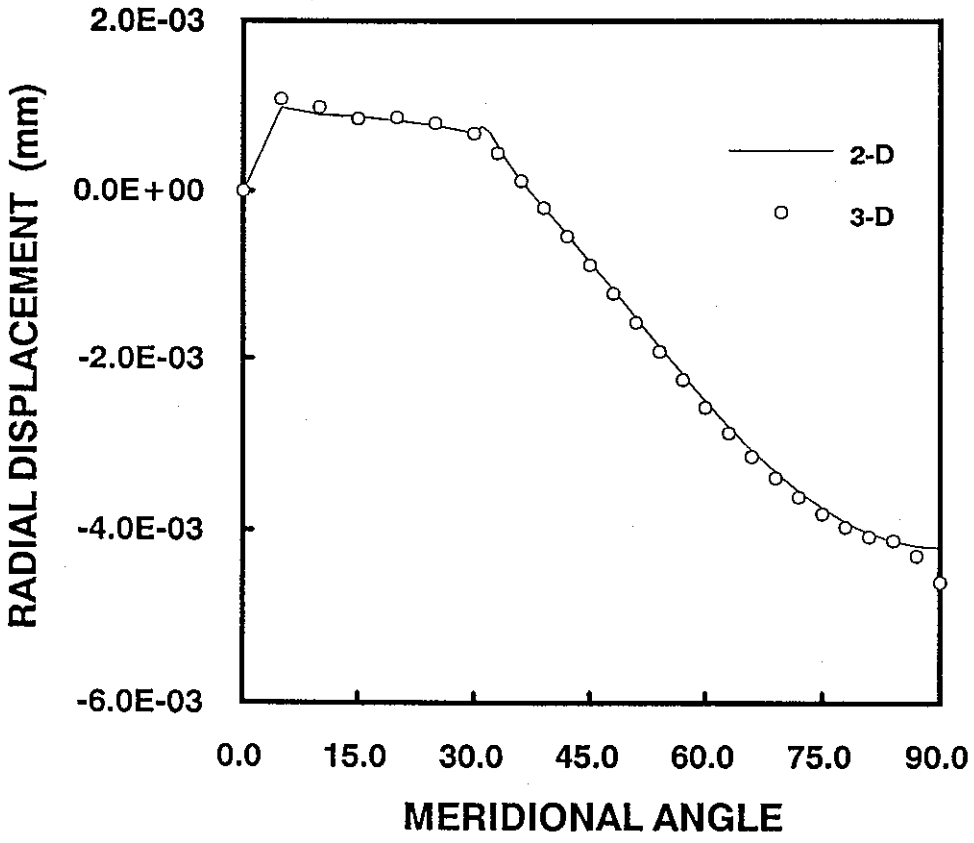

Fig. 4.2-2 Nodal Displacement by Axi-symmetric and 3-D Analysis

agt9b\ch_4

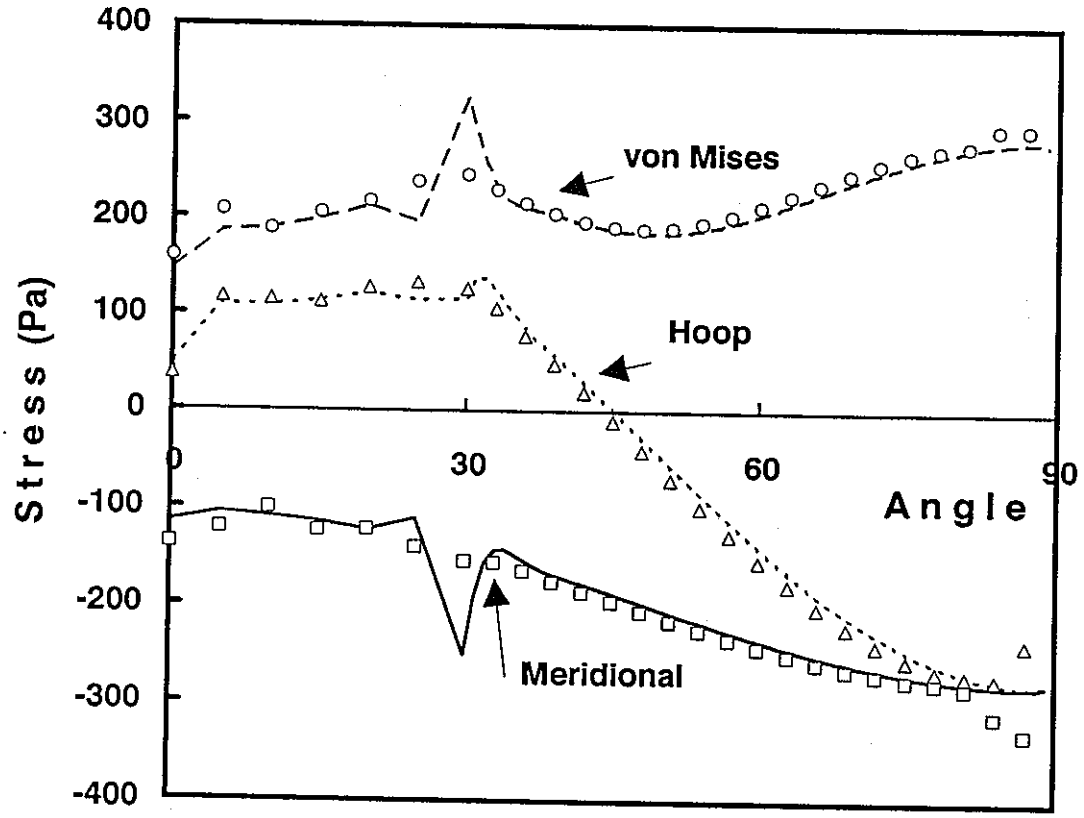

Fig. 4.2-3 Stress Distribution by Axi-symmetric and 3-D Analysis

agt9b\ch_4

4.3 2-D AXI-SYMMETRIC ANALYSIS

4.3.1 Elastic Eigenvalue Analysis

Two cases of elastic eigenvalue analyses using the 2-D axisymmetric model were carried out applying the pressure with maximum value of 1 MPa. In one case, the pressure load vector was kept normal to the shell referring to the geometry before deformation. In the other case, the following load option was adopted; i.e., the pressure load vector is modified to be always normal to the shell during deformation.

The critical buckling pressures obtained are listed in Table 4.3-1. The corresponding buckling modes are shown in Fig. 4.3-1 and 4.3-2.

The lowest buckling pressures are 0.189 MPa and 0.188 MPa, for the cases without and with the following load option, respectively. As far as elastic eigenvalue analysis is concerned, the following load option has insignificant effect on the result in terms of buckling pressure. However, the buckling modes obtained by each analysis does not correspond with each other.

A theoretical critical buckling pressure for a perfect thin sphere subjected to a uniform external pressure load is given by

$$p_{cr}=\frac{2E}{\sqrt{3(1-\nu^2)}}\left(\frac{t}{R}\right)^2 \qquad (4.3\text{-}1)$$

Letting E = 6.60E10 Pa, ν = 0.3, R = 0.455 m, and letting t = 0.8 mm (nominal value) or t = 0.7 mm (actual thickness at the bottom), the equation gives critical buckling pressures as p_{cr} = 0.247 MPa and 0.189 MPa, respectively. The latter value is in a good accordance with the lowest analysis results.

4.3.2 Incremental Large Deformation Analysis

Incremental large deformation and buckling analyses were performed. Here again, the following load option was not used in one case and was used in the other case. In

the former case, the inelastic material property described in Section 4.1 was used. The incremental pressure was applied in the following manner;

from 0.120 MPa to 0.160 MPa : $\Delta p = 0.01$ MPa
from 0.161 MPa to 0.170 MPa : $\Delta p = 0.001$ MPa

Buckling eigenvalue extraction was done in every step.

CASE 1 : Fig. 4.3-3 shows the history of nodal displacement at the bottom point of the hemisphere in the vertical direction. The sphere deforms linearly up to about 0.169 MPa, and then the displacement diverges at this pressure. Fig. 4.3-4 is the histories of the stresses in the element including the bottom point. Here again, each stress component increases linearly up to 0.169 MPa, and a large amount of bending stress is suddenly produced at this point. From these figures, one can judge that the critical pressure is 0.169 MPa.

Since the result of the elastic stress analysis noted in Section 4.2 that the pressure at which the bottom element start to yield is about 0.22 MPa, the above mentioned critical pressure implies that the buckling occur in the elastic range.

Fig. 4.3-5 is a relationship between the applied pressure versus critical buckling pressure obtained by the eigenvalue analysis at each pressure. This figure also depicts that the critical buckling pressure is around 0.17 MPa.

The deformed shape and the buckling modes at this pressure are shown in Figs. 4.3-6 and 4.3-7, respectively. The buckling mode and the deformation shape right after buckling are similar, and one can note that the deformation is highly concentrated to the bottom region of the hemisphere.

CASE 2 : Since it has been found that the buckling is likely to occur in the elastic range, the analysis with the following load option was done elastically.

Fig. 4.3-8 shows the nodal displacement history at the bottom point of the hemisphere in the vertical direction. Unlike the CASE 1, the displacement increased linearly and a numerical instability occurred at 0.163 MPa, and an structural instability in terms of

sudden increase of deformation was not attained in he analysis. Fig. 4.3-9 is the history of stresses at the bottom element. A large amount of bending stress, which was seen right after buckling occurred in the CASE 1, was not seen in this case.

Fig. 4.3-10 is a relationship between the applied pressure versus critical buckling pressure obtained by the eigenvalue analysis at some pressure steps. This figure also depicts that the critical buckling pressure is around 0.16 MPa.

The deformed shape and the buckling modes at this pressure are shown in Figs. 4.3-11 and 4.3-12, respectively. The buckling mode is concentrated to the bottom region of the hemisphere. The deformation shape right after the buckling remains stable in this case.

Table 4.3-1
Critical Buckling Pressure by
2-D Elastic Eigenvalue Analysis

Unit : MPa

Mode #	RUN 1	RUN 2
1	0.189	0.188
2	0.194	0.192
3	0.196	0.194
4	0.219	0.217
5	0.230	0.228
6	0.239	0.237

RUN 1: w/o follwing load option
RUN 2: with follwing load option

agt9b\ch_4

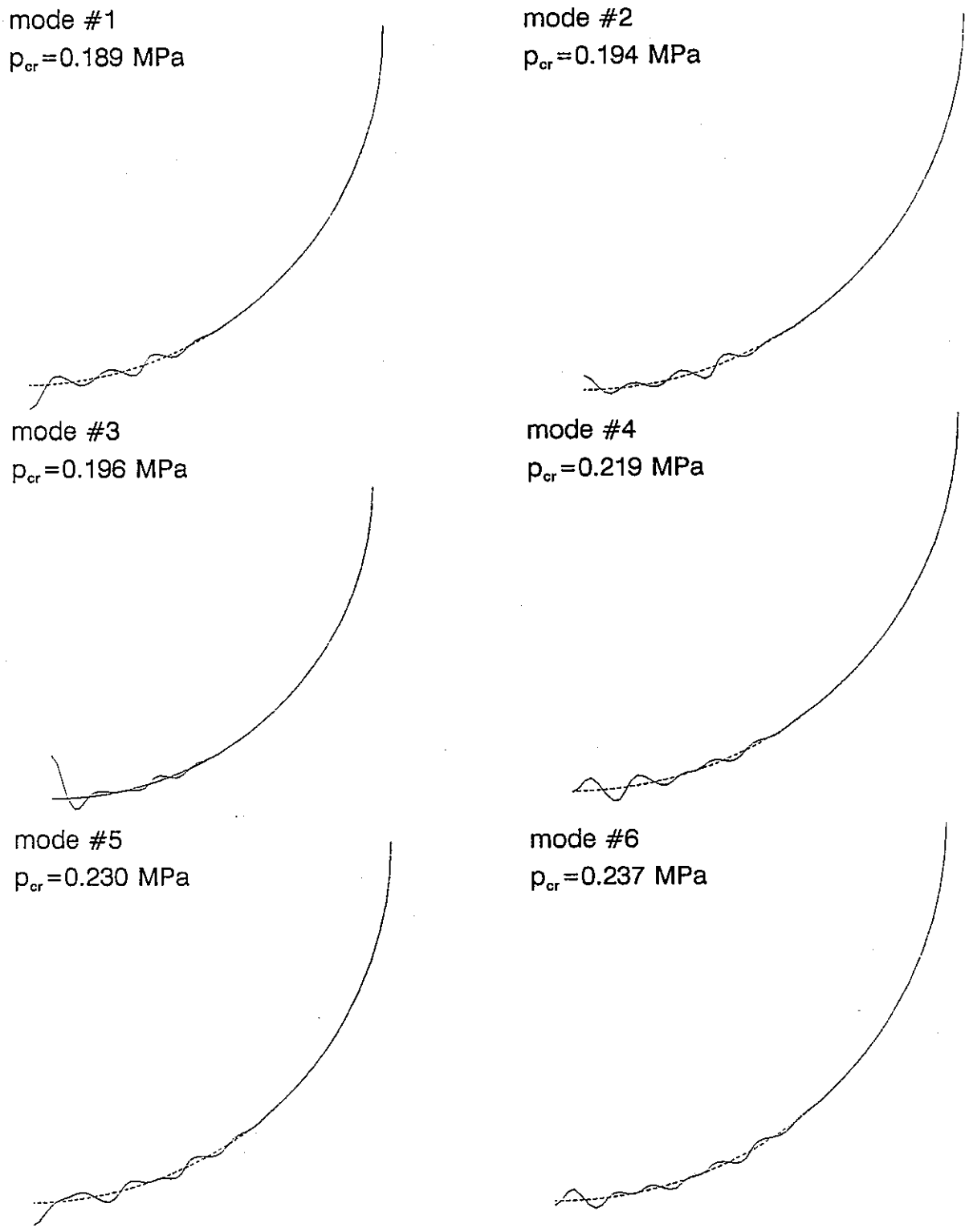

Fig. 4.3-1 Buckling Modes by Elastic Eigenvalue Analysis (w/o Following Load Option)

agt9b\ch_4

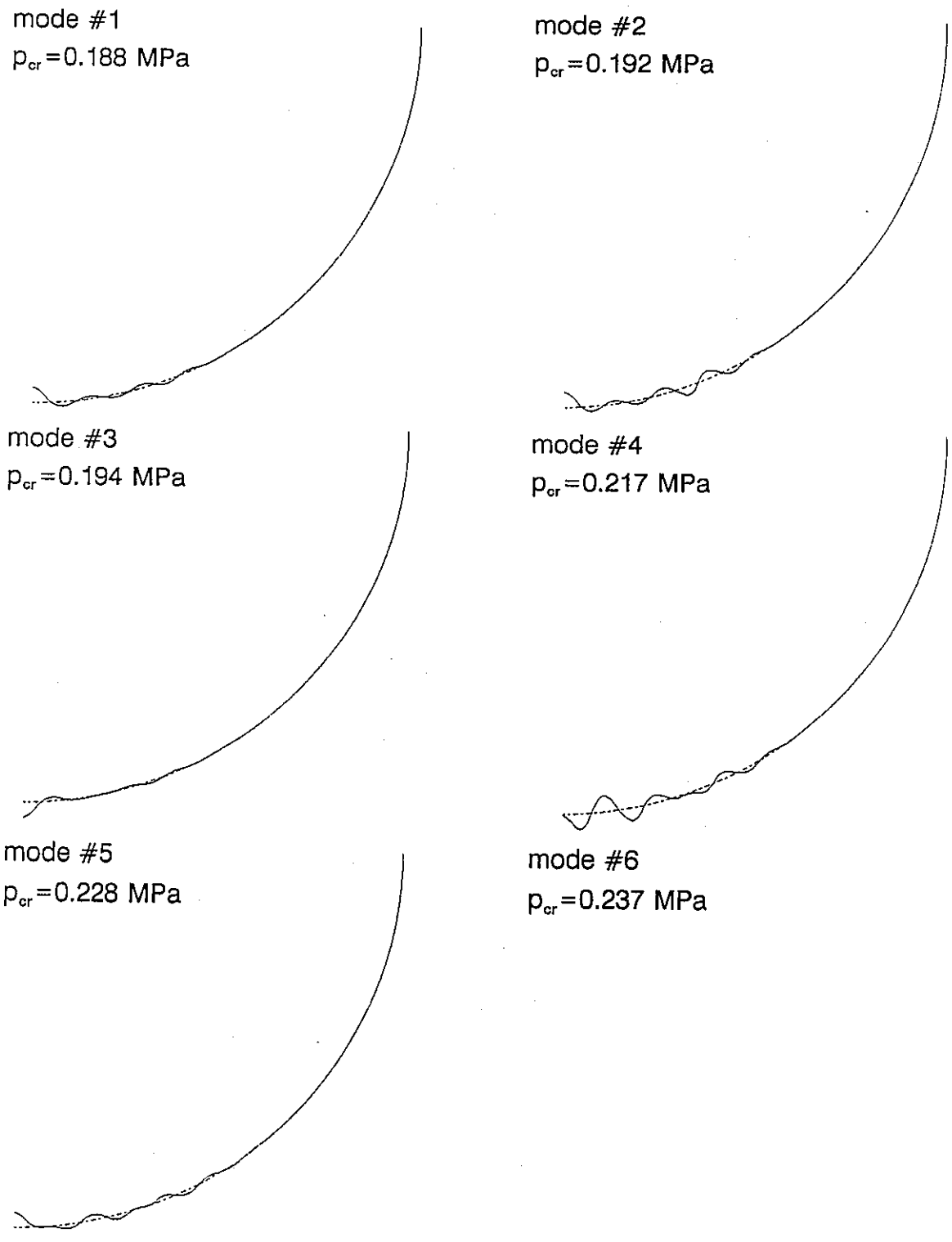

Fig. 4.3-2 Buckling Modes by Elastic Eigenvalue Analysis (with Following Load Option)

agt9b\ch_4

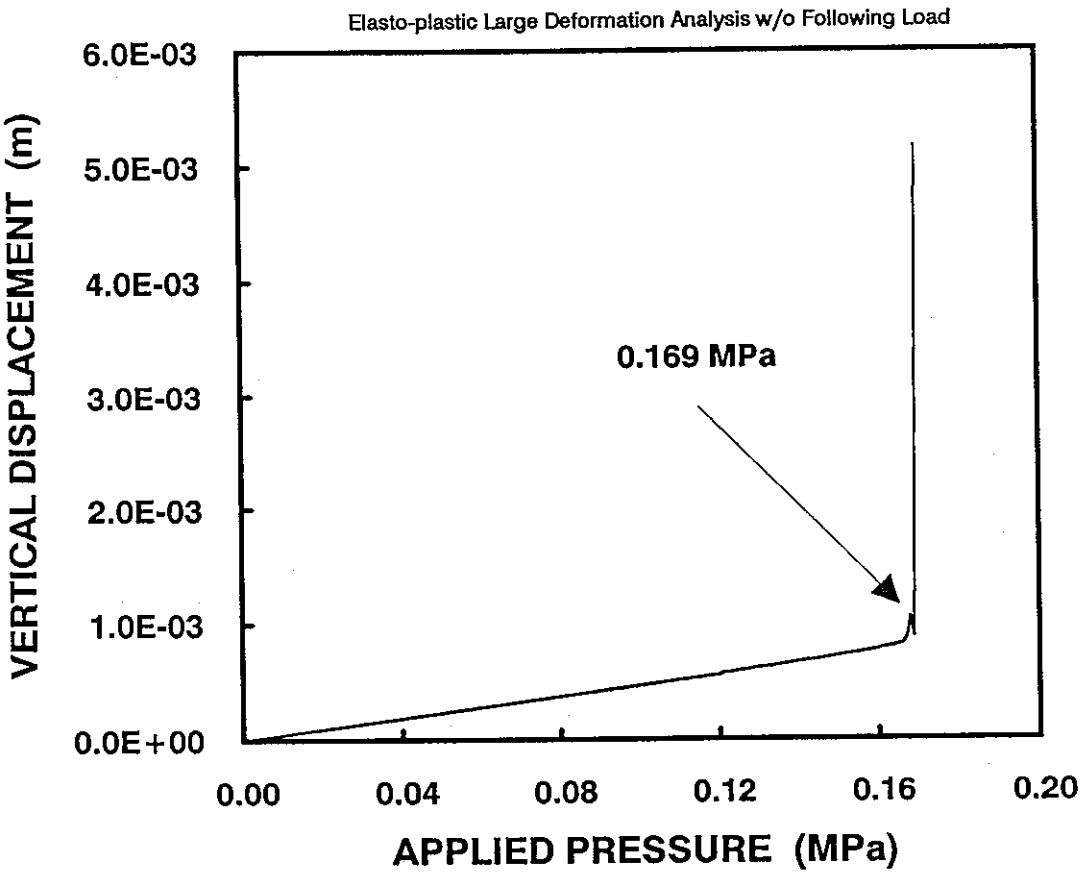

Fig. 4.3-3 Nodal Displacement vs. Applied Pressure (Elastoc-plstic Large deformation w/o Following Load)

agt9b\ch_4

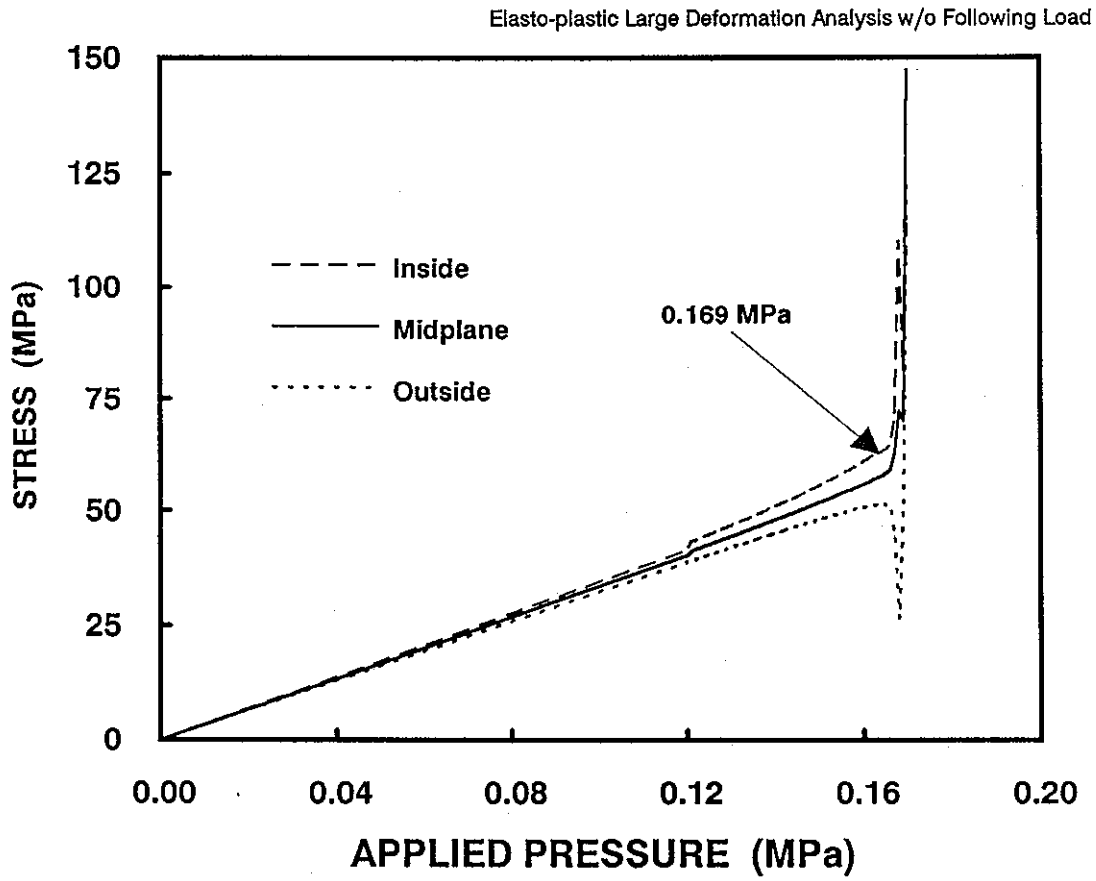

Fig. 4.3-4 Stress vs. Applied Pressure
(Elasto-plastic Large Deformation Analysis w/o Following Load)

agt9b\ch_4

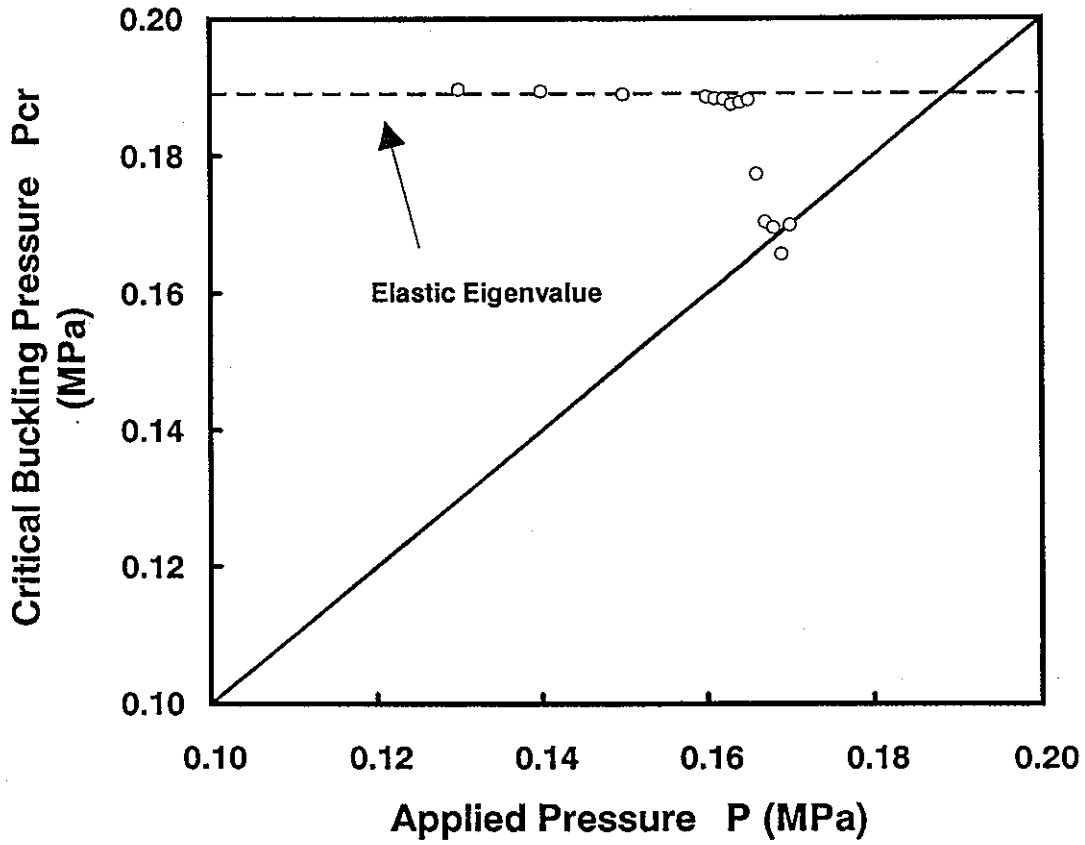

Fig. 4.3-5 Critical Buckling Pressure vs. Applied Pressure (Elasto-plastic Large Deformation Analysis w/o Following Load)

agt9b\ch_4

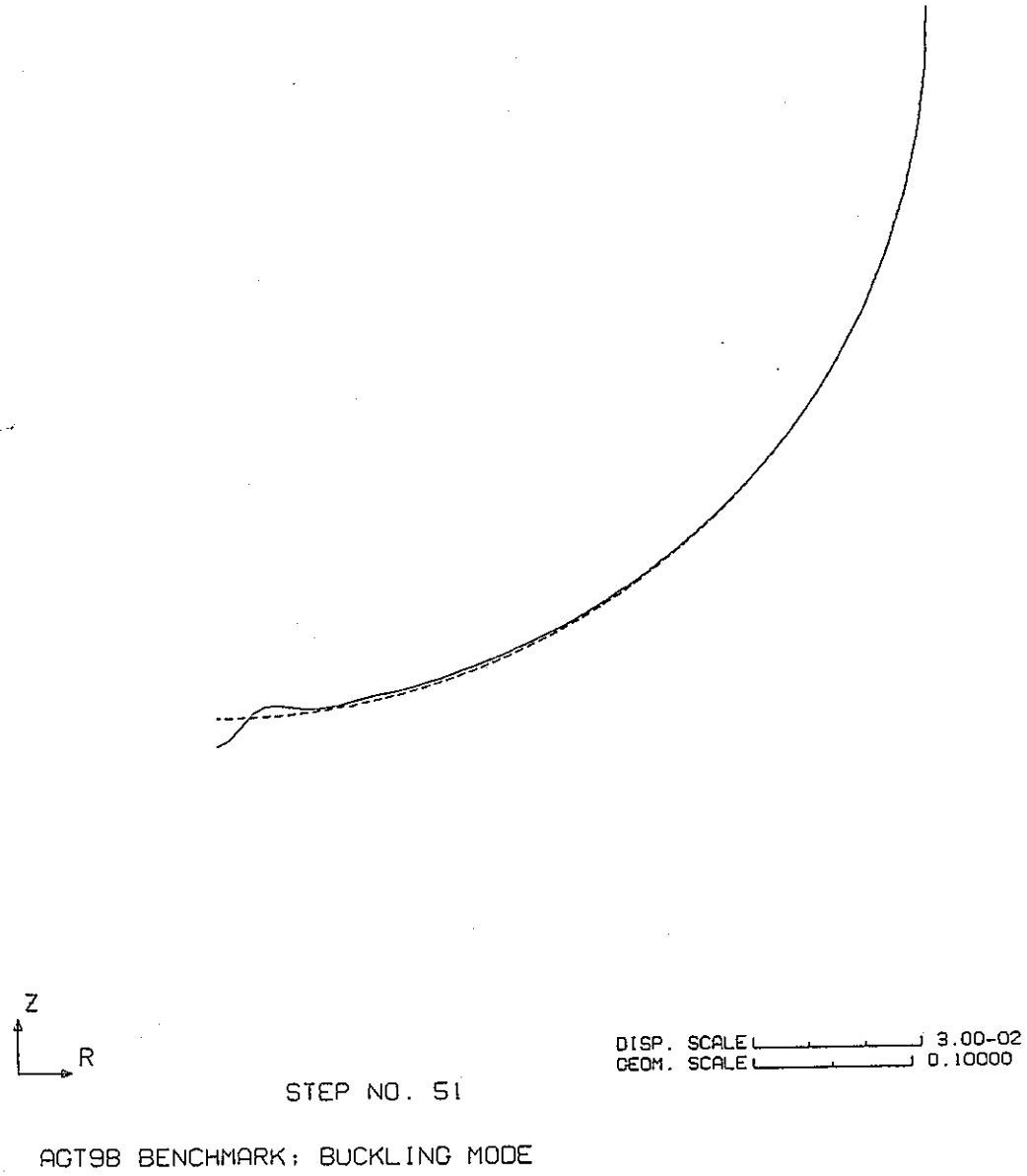

Fig. 4.3-6 Deformation of Hemisphere at Critical Buckling Pressure (Elasto-plastic Large Deformation w/o Following Load)

agt9b\ch_4

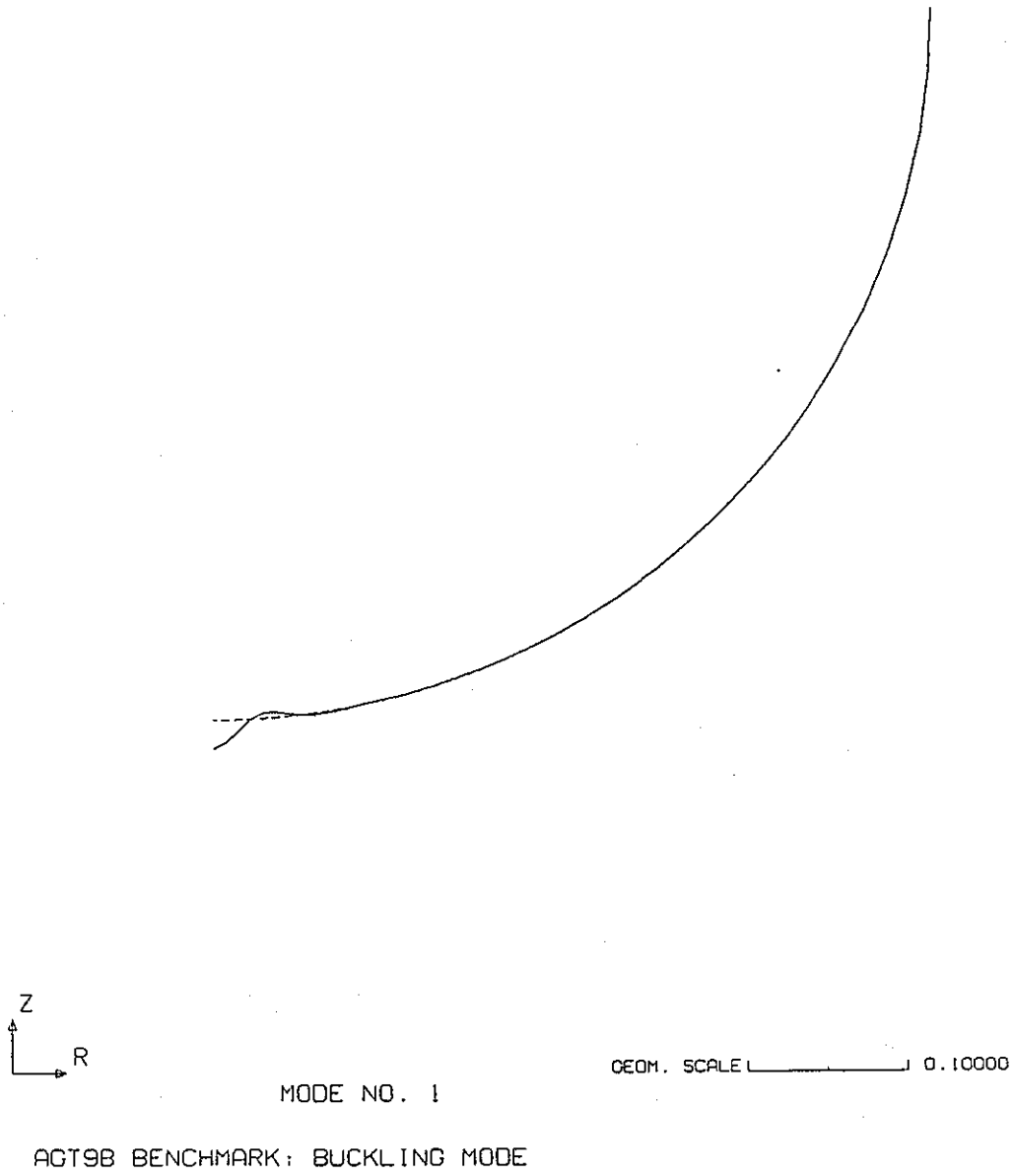

Fig. 4.3-7 Buckling Modes at Critical Pressure (Elasto-plastic Large Deformation w/o Following Load)

agt9b\ch_4

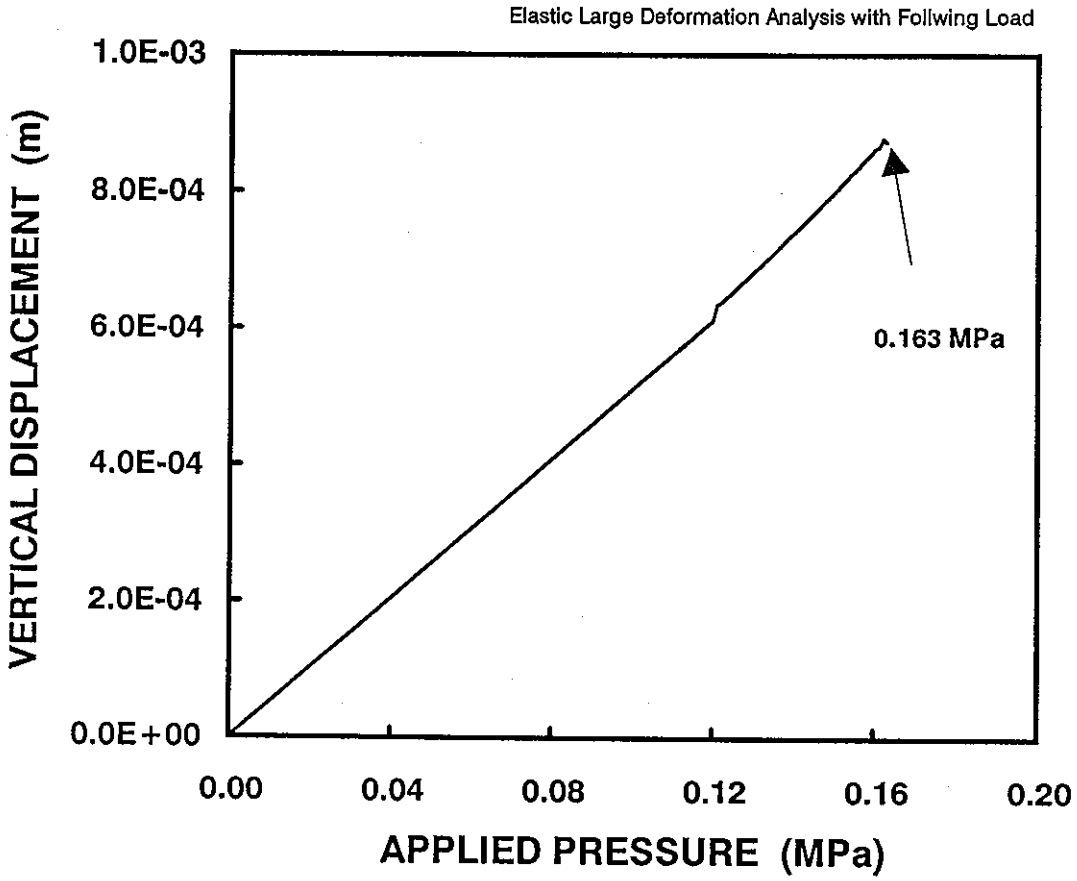

Fig. 4.3-8 Nodal Displacement vs. Applied Pressure (Elastic Large Deformation with Following Load)

agt9b\ch_4

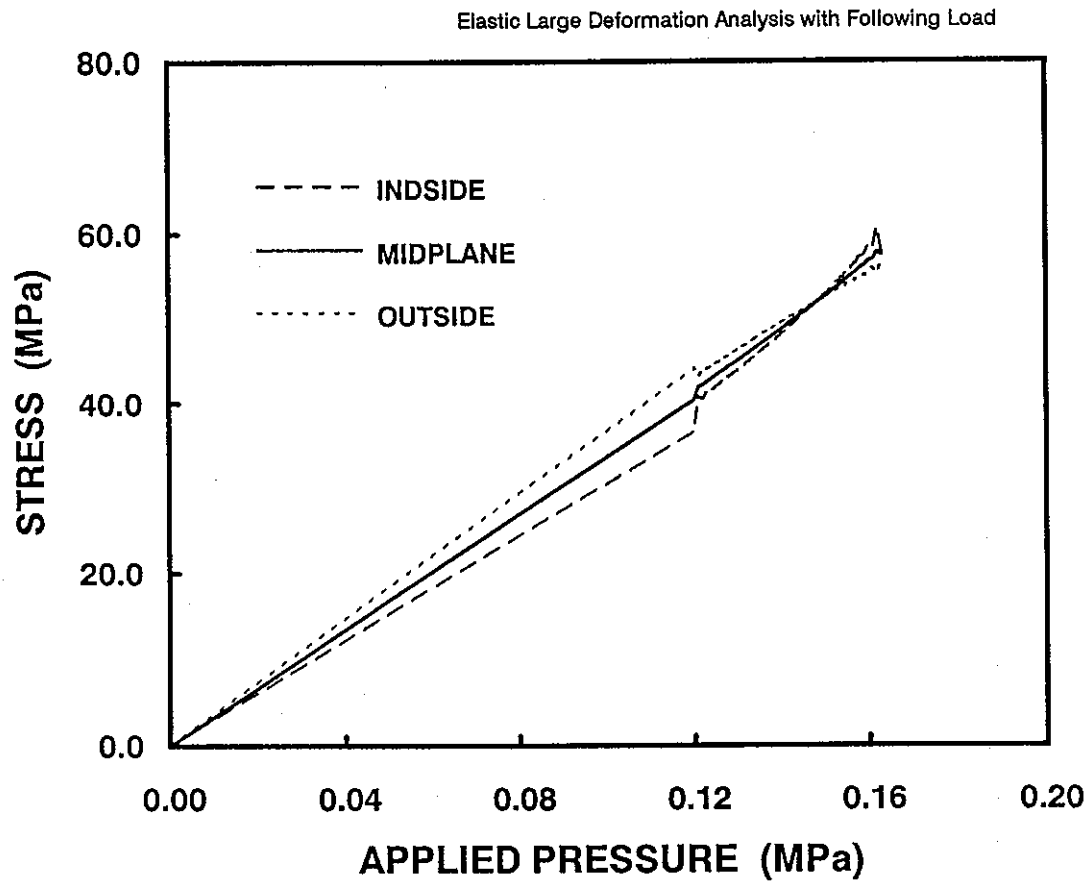

Fig. 4.3-9 Stress vs. Applied Pressure (Elastic Large Deformation with Following Load)

agt9b\ch_4

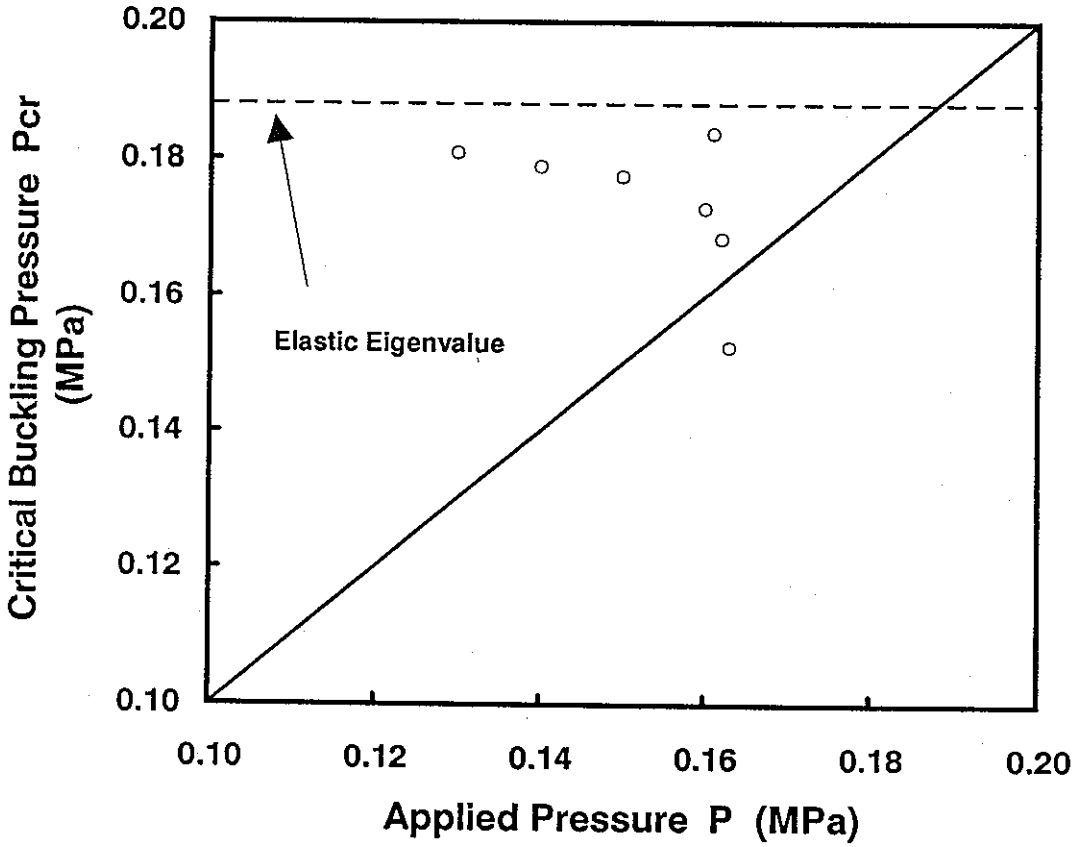

Fig. 4.3-10 Critical Buckling Pressure vs. Applied Pressure (Elastic Large Deformation Analysis with Following Load)

agt9b\ch_4

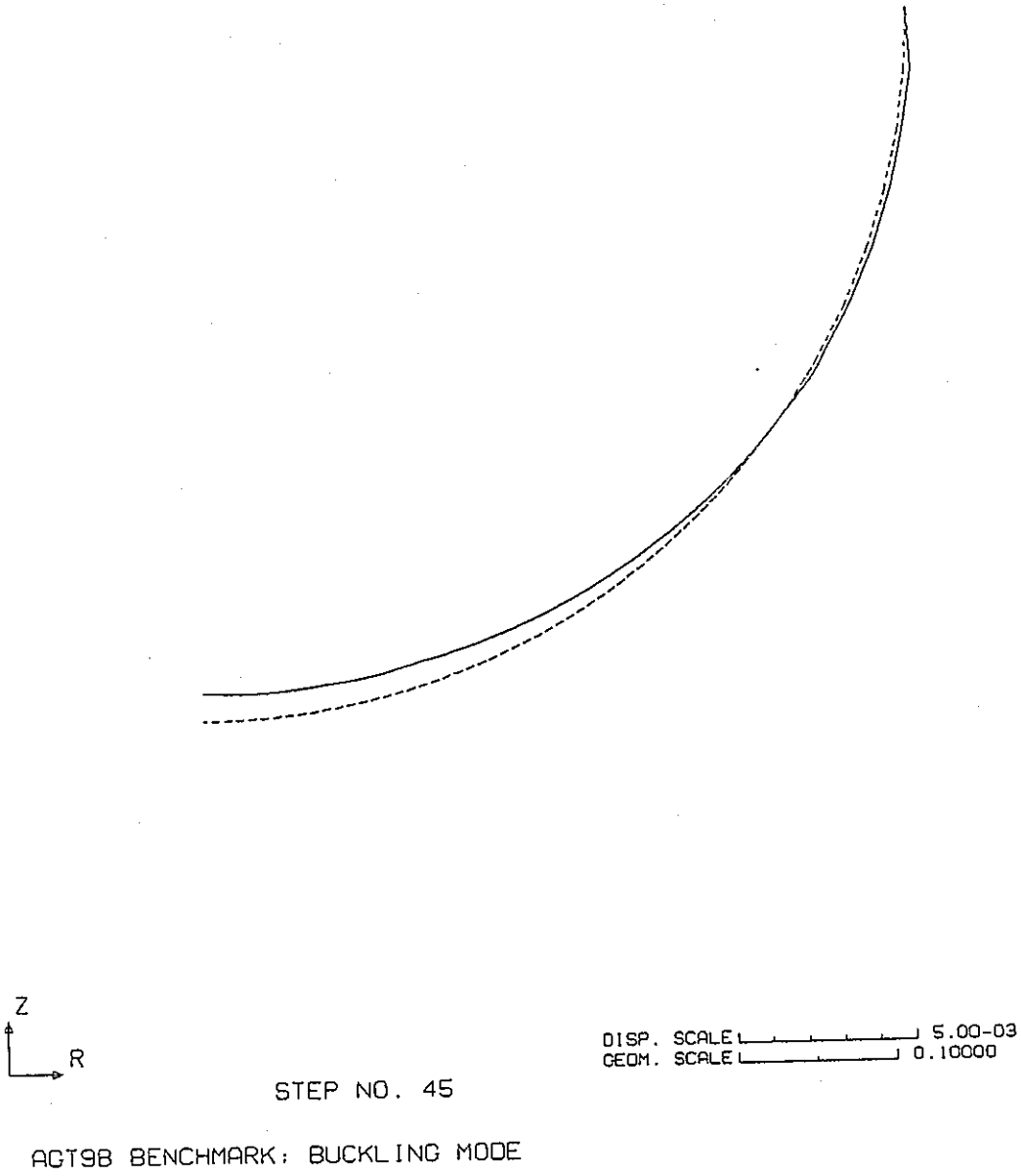

Fig. 4.3-11 Deformation of Hemisphere at Critical Buckling Pressure (Elastic Large Deformation with Following Load)

agt9b\ch_4

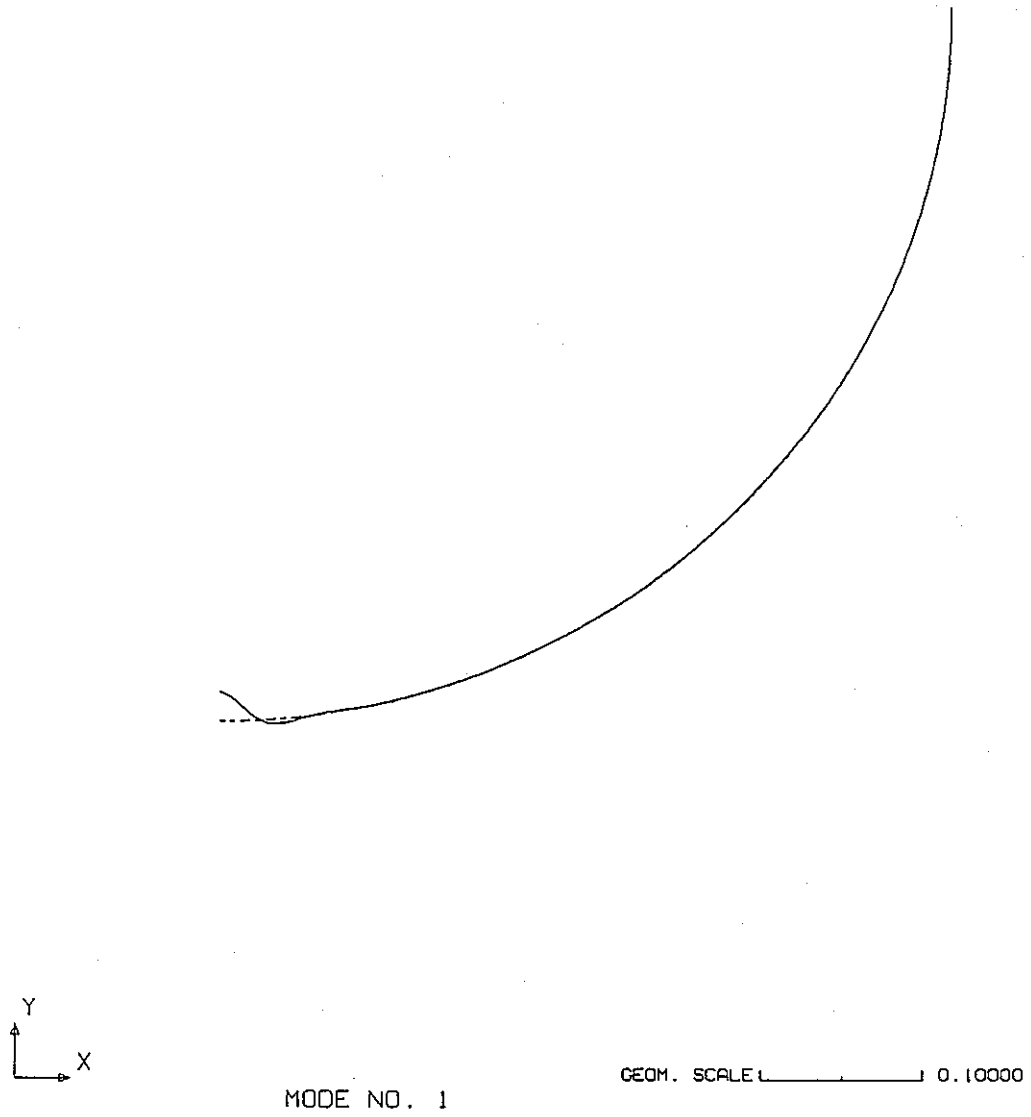

Fig. 4.3-12 Buckling Modes at Critical Pressure (Elastic Large Deformation with Following Load)

agt9b\ch_4

4.4 3-D ANALYSIS

Since it was found by the 2-D analyses that buckling is likely to occur in the elastic range, two cases of elastic large deformation and buckling analyses were performed with the full 3-D model. The following load option was not used in the CASE 1 and was used in the CASE 2. The pressure distribution obtained by the 2-D dynamic fluid-structure interaction analysis was developped in the circumferential direction assuming axia symmetry and applied. The pressure increment is as follows;

from 0.110 MPa to 0.140 MPa : Δp = 0.01 MPa
from 0.140 MPa to 0.170 MPa : Δp = 0.002 MPa

Buckling eigenvalue extraction was done at some typical pressure steps.

CASE 1 : Fig. 4.4-1 shows the history of the nodal displacement at the bottom point of the hemisphere in the vertical direction. The deformation of the hemisphere gradually increases more than the linear relation due to the large deformation effect up to about 0.16 MPa, and then the displacement behavior becomes unstable. Fig. 4.4-2 is the histories of the stresses in the element including the bottom point. Each stress component increases gradually up to about 0.16 MPa, and a large amount of bending stress is suddenly produced at this point. From these figures, one can judge that the critical pressure is 0.160 MPa.

Fig. 4.4-3 is a relationship between the applied pressure versus critical buckling pressure obtained by the eigenvalue analysis at each pressure. This figure also depicts that the critical buckling pressure is around 0.16 MPa.

The buckling mode and the deformed shape at this pressure are shown in Figs. 4.4-4 and 4.4-5 respectively. The deformation in the buckling mode is highly concentrated in the bottom region and axi-symmetric. The deformation shape right after buckling are also axi-symmetric, but the overall deofrmation still prevails.

CASE 2 : Fig. 4.4-6 shows the nodal displacement history at the bottom point of the hemisphere in the vertical direction. Like the CASE 1, the displacement increases up to about 0.16 MPa, and then the displacement becomes unstable. Fig. 4.4-7 is the

history of stresses at the bottom element. A large amount of bending stress is produces at about 0.16 MPa.

Fig. 4.4-8 is a relationship between the applied pressure versus critical buckling pressure obtained by the eigenvalue analysis at some pressure steps. This figure also depicts that the critical buckling pressure is also around 0.16 MPa.

The buckling mode and the deformed shape at this pressure are shown in Figs. 4.4-9 and 4.4-10, respectively. The buckling mode is concentrated to the bottom region of the hemisphere. The deformation shape right after the buckling remains almost stable. Here again, the buckling mode is axi-symmetric and the mode shape is very similar to that obtained by the 2-D analysis.

Contrary to the 2-D analysis, the difference of the buckling pressures with and without the following load is not significant in the 3-D analysis.

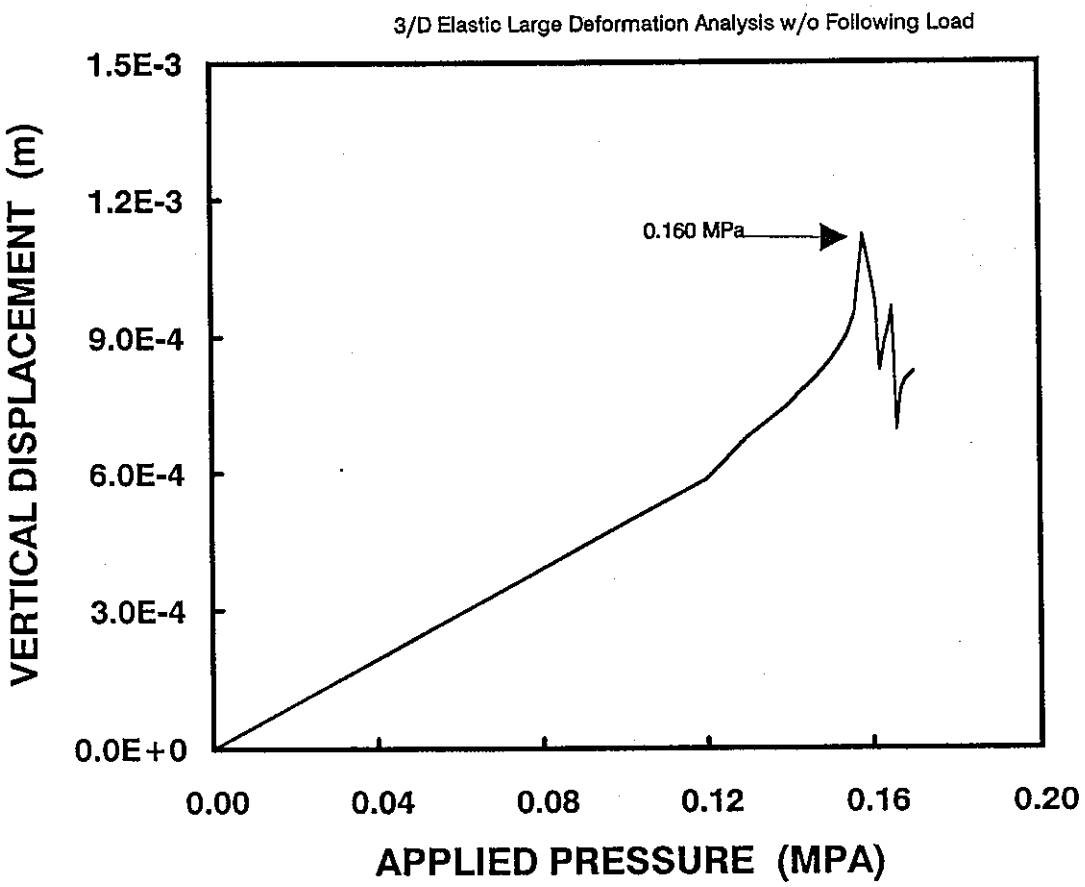

Fig. 4.4-1 Nodal Displacement vs. Applied Pressure (Elastic Large deformation w/o Following Load)

agt9b\ch_4

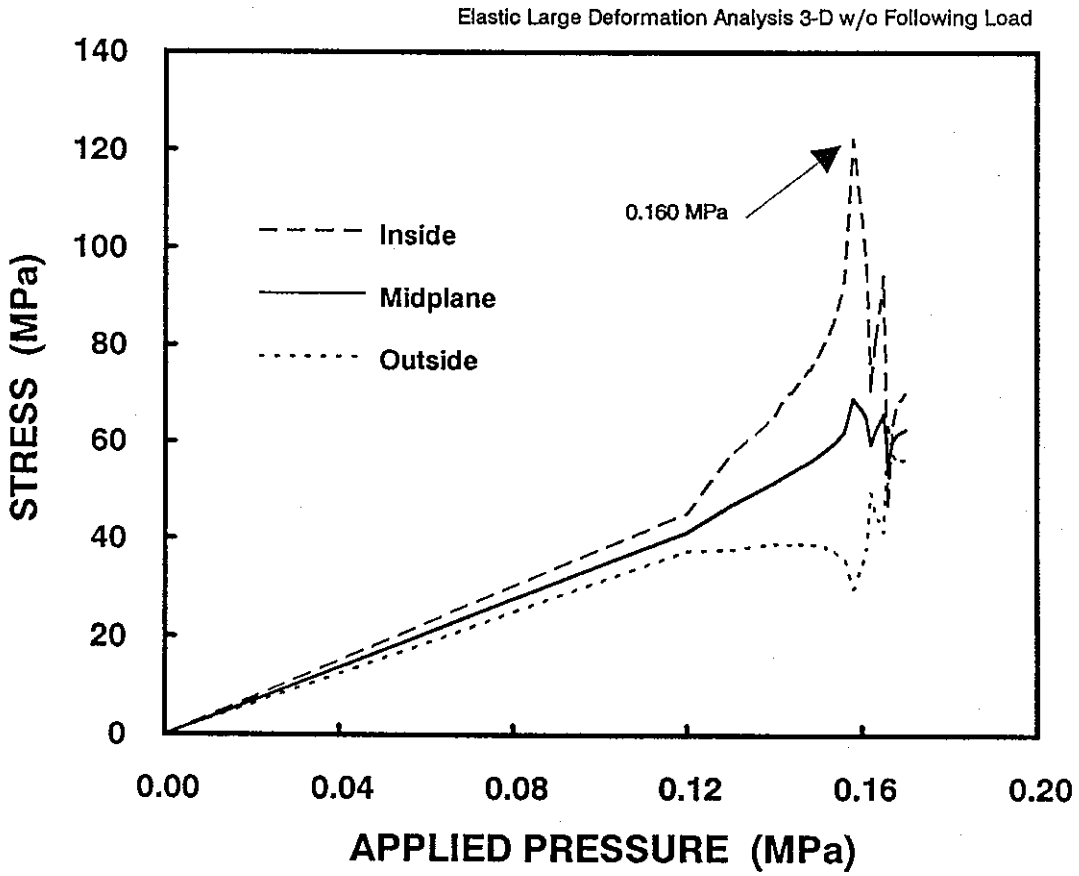

Fig. 4.4-2 Stress vs. Applied Pressure
(Elastic Large Deformation Analysis w/o Following Load)

agt9b\ch_4

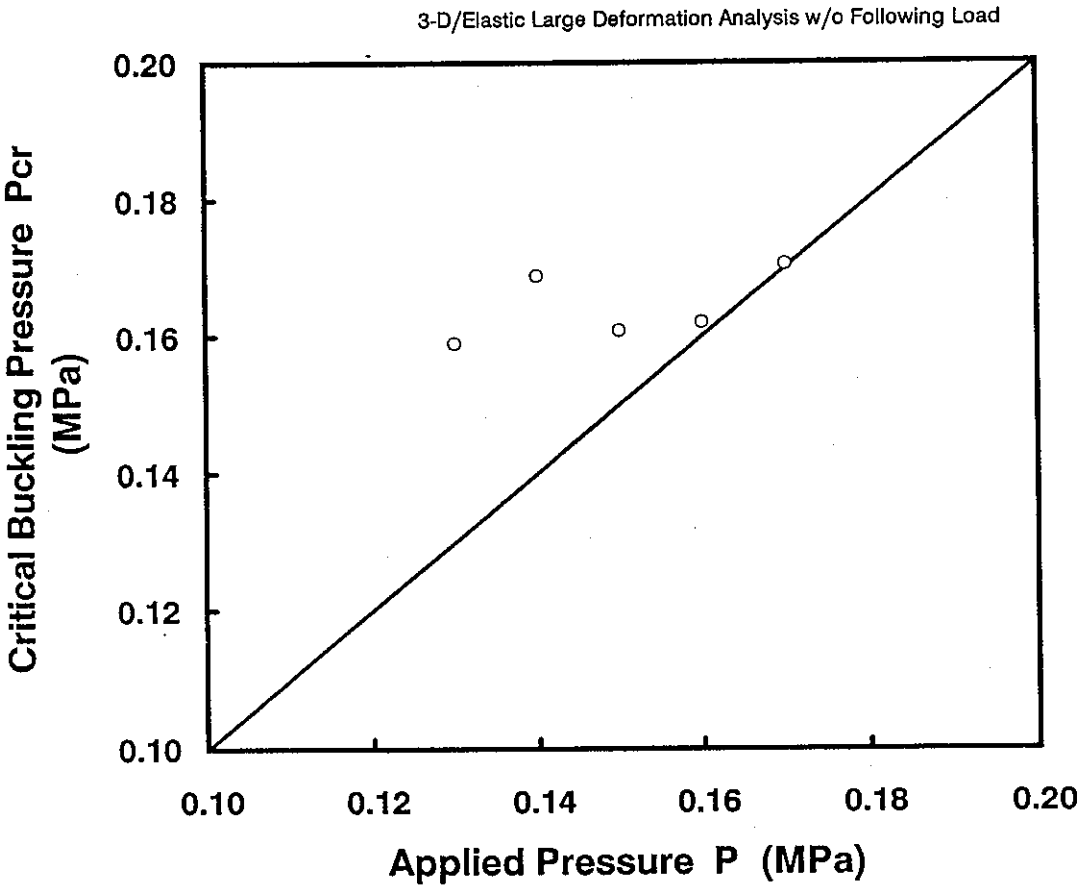

Fig. 4.4-3 Critical Buckling Pressure vs. Applied Pressure (Elastic Large Deformation Analysis w/o Following Load)

agt9b\ch_4

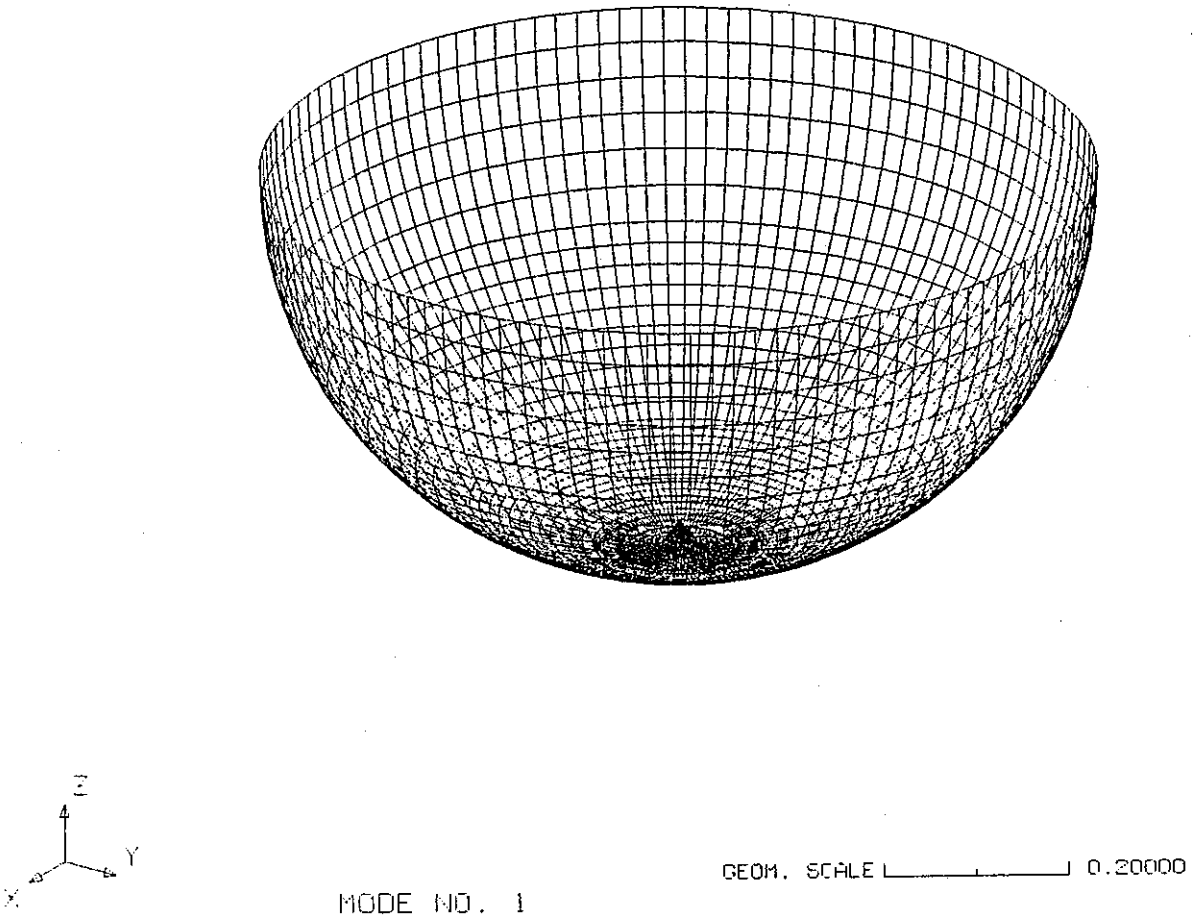

Fig. 4.4-4 Buckling Mode at Critical Pressure (1 of 3 : whole view)
(Elastic Large Deformation w/o Following Load)

agt9b\ch_4

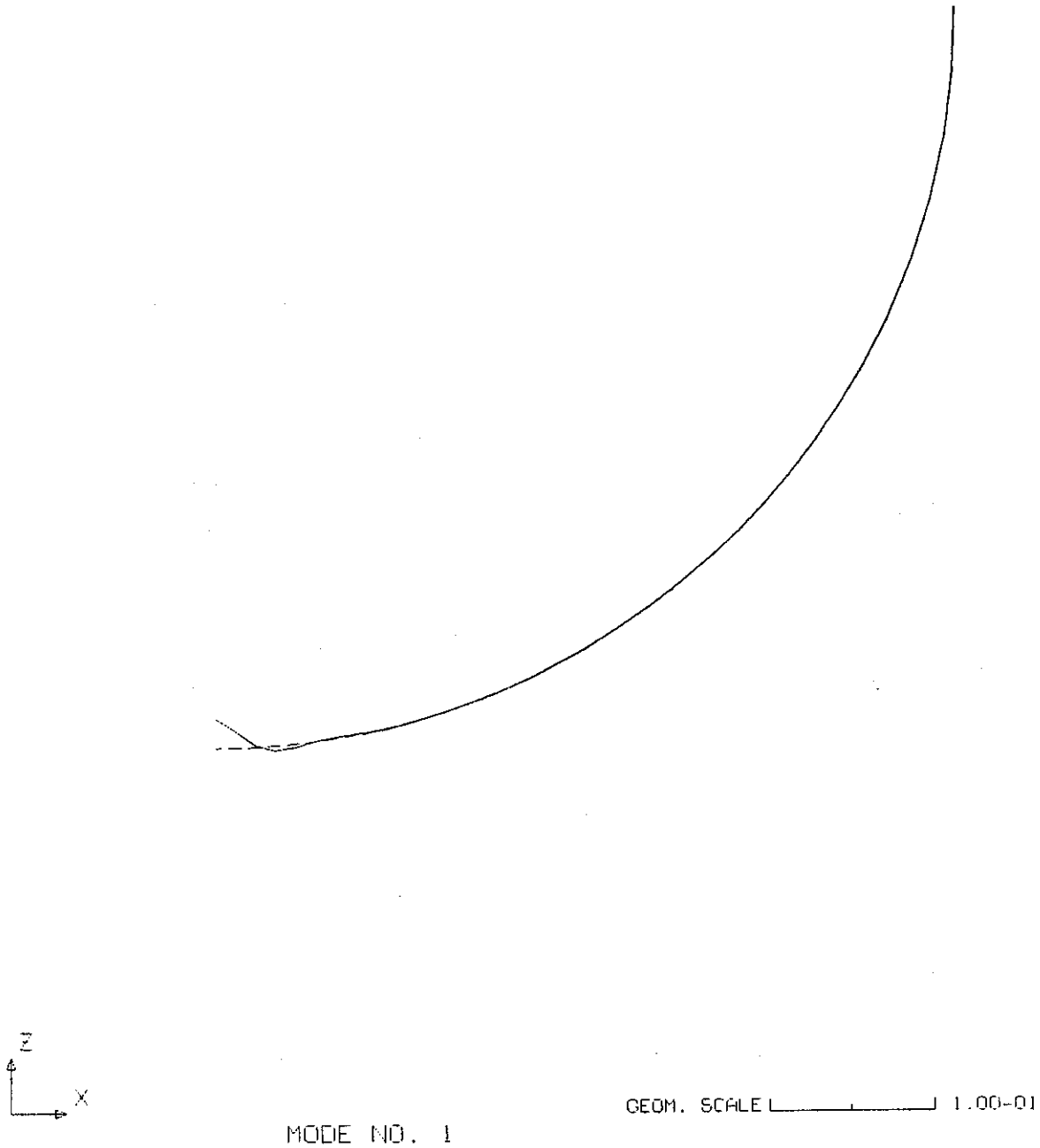

Fig. 4.4-4 Buckling Mode at Critical Pressure (2 of 3 : section)
(Elastic Large Deformation w/o Following Load)

agt9b\ch_4

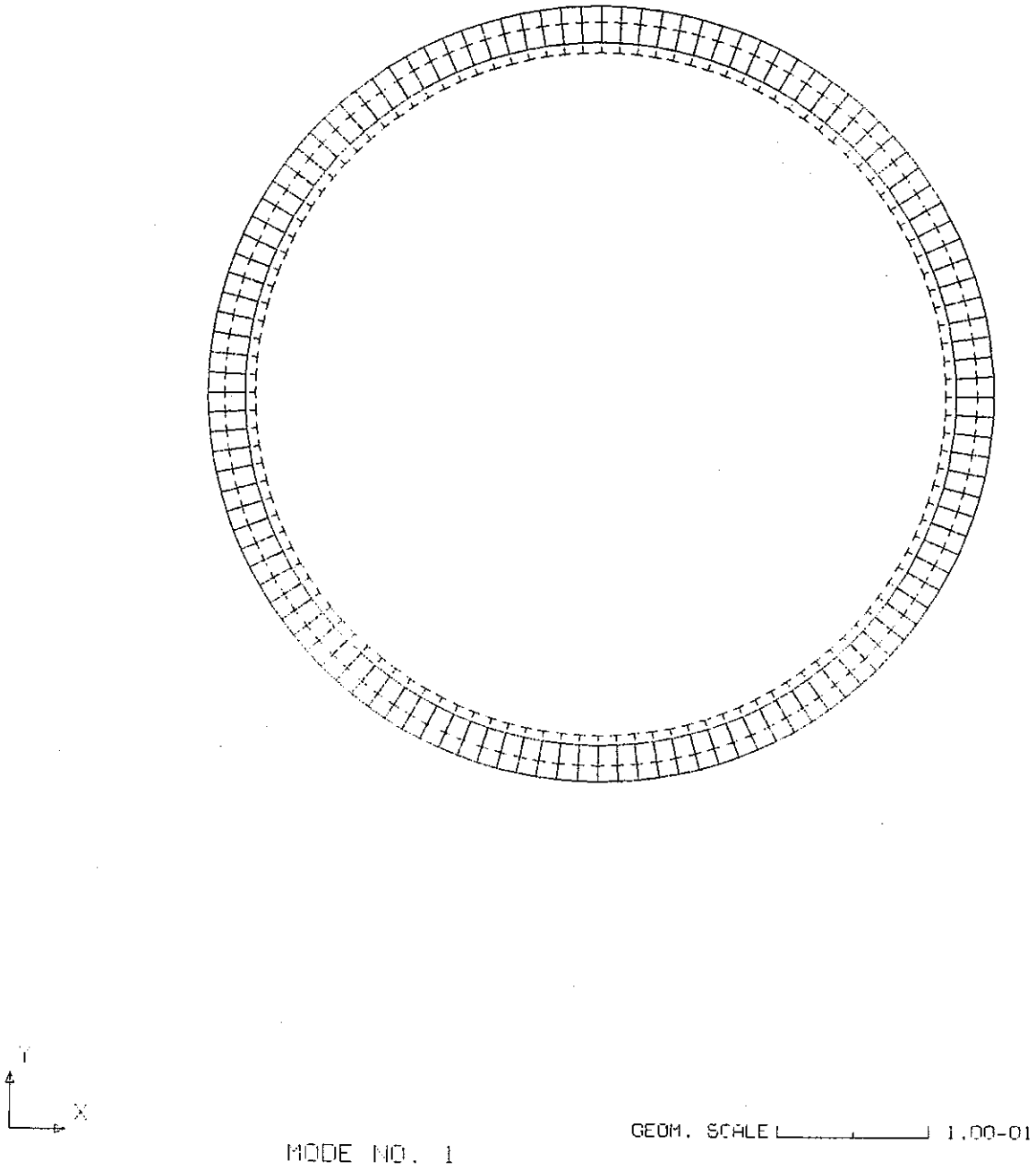

Fig. 4.4-4 Buckling Mode at Critical Pressure (3 of 3 : plan)
(Elastic Large Deformation w/o Following Load)

agt9b\ch_4

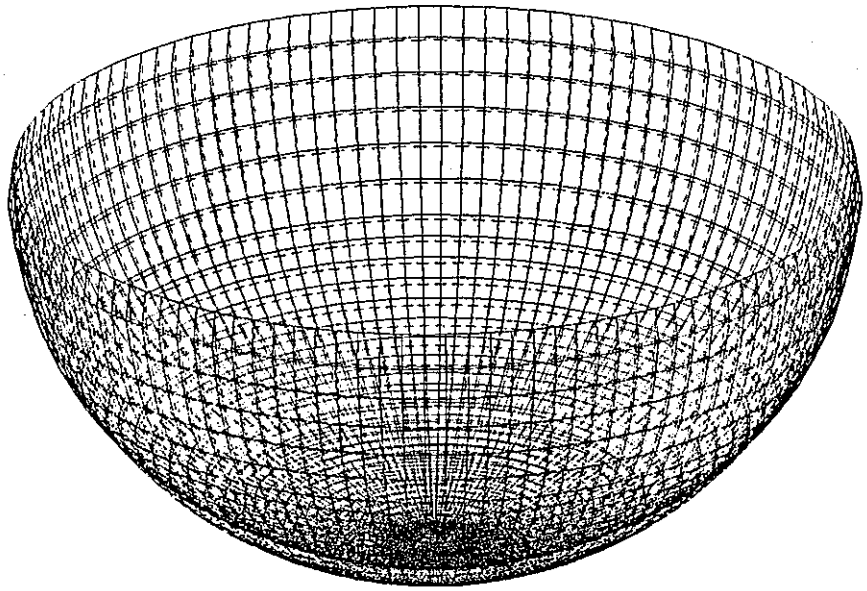

Fig. 4.4-5 Deformation at Critical Buckling Pressure (1 of 3 : whole view) (Elastic Large Deformation w/o Following Load)

agt9b\ch_4

Fig. 4.4-5 Deformation at Critical Buckling Pressure (2 of 3 : section)
(Elastic Large Deformation w/o Following Load)

agt9b\ch_4

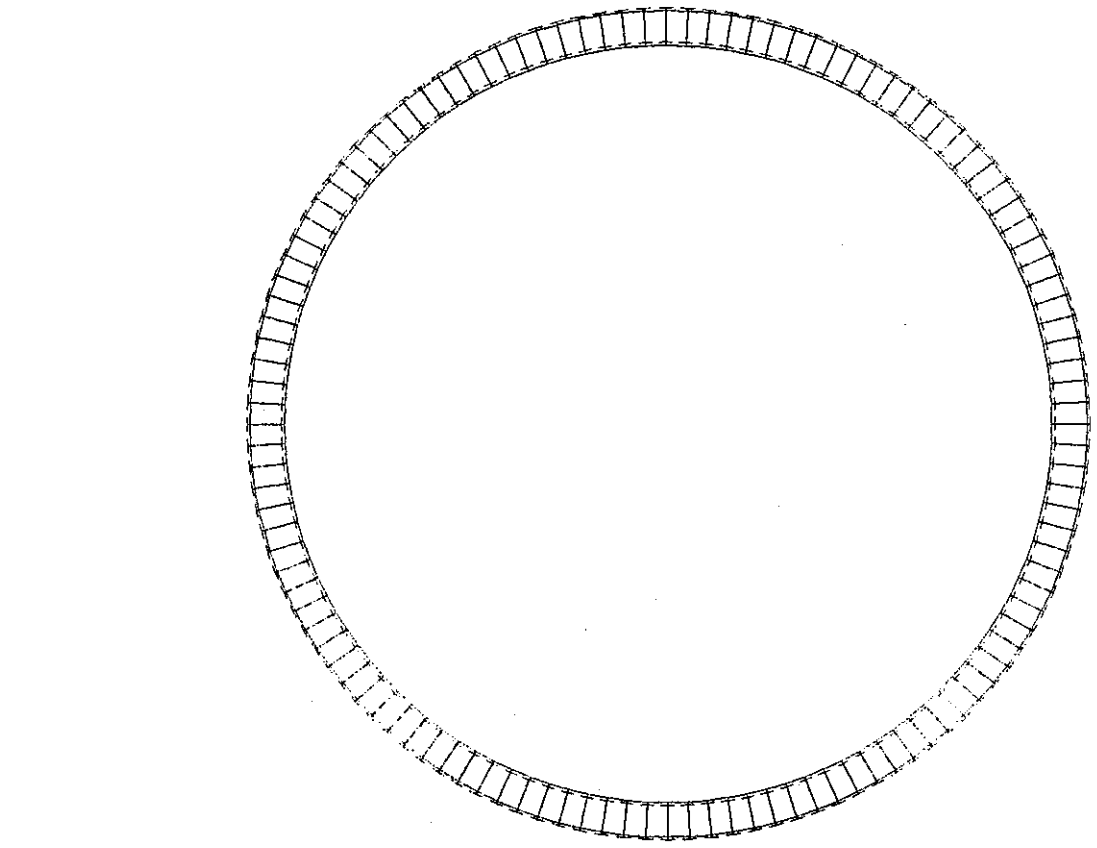

Fig. 4.4-5 Deformation at Critical Buckling Pressure (3 of 3 : plan)
(Elastic Large Deformation w/o Following Load)

agt9b\ch_4

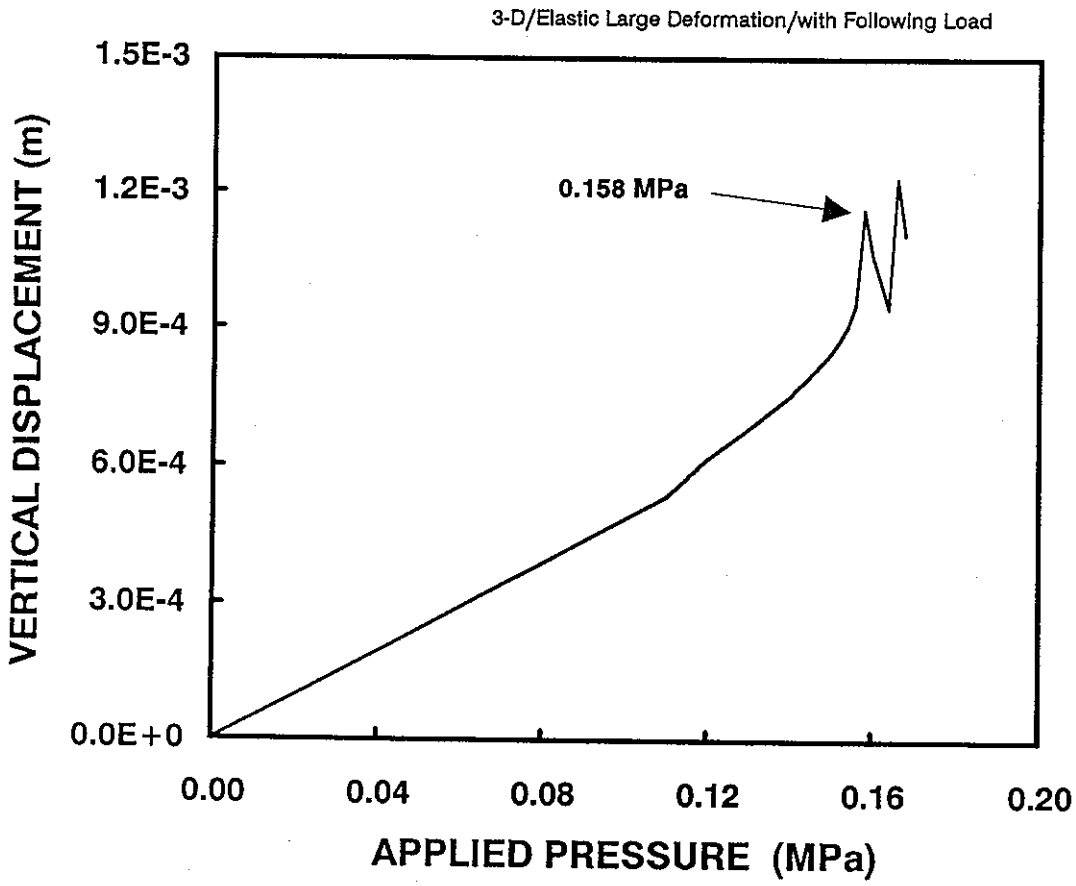

Fig. 4.4-6 Nodal Displacement vs. Applied Pressure (Elastic Large deformation with Following Load)

agt9b\ch_4

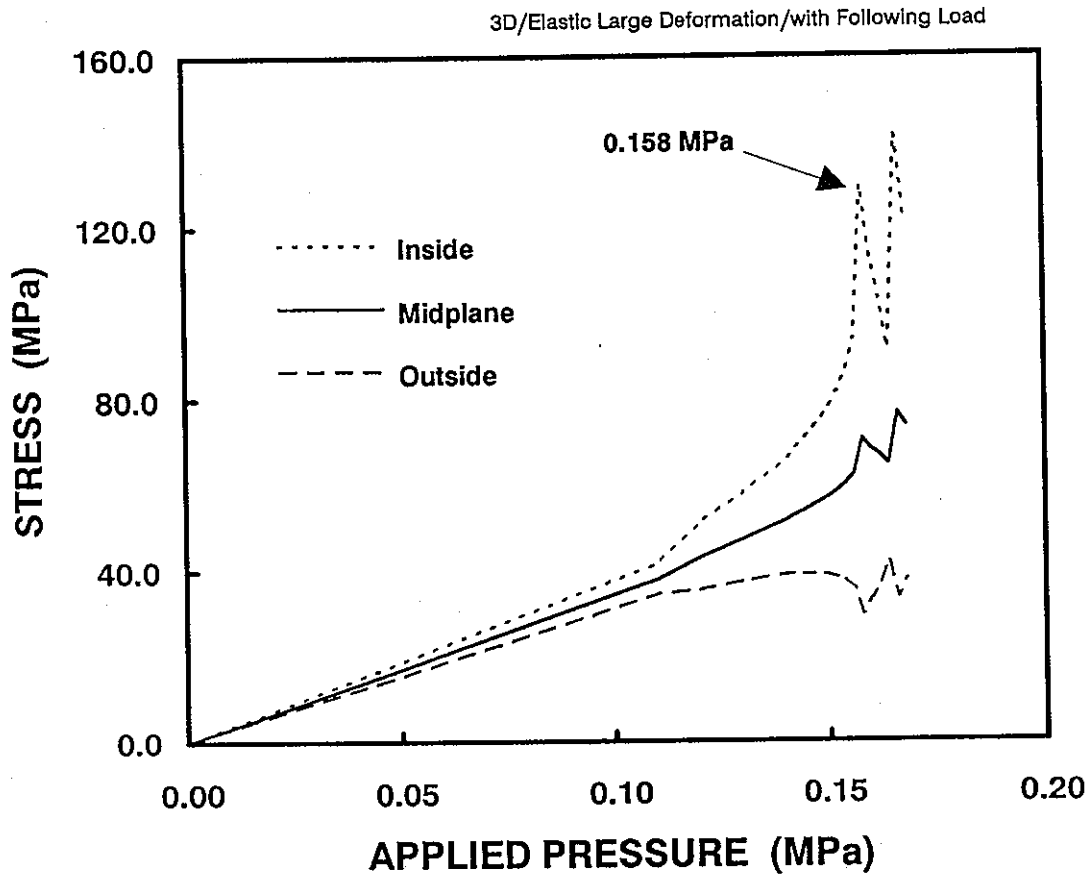

Fig. 4.4-7 Stress vs. Applied Pressure
(Elastic Large Deformation Analysis with Following Load)

agt9b\ch_4

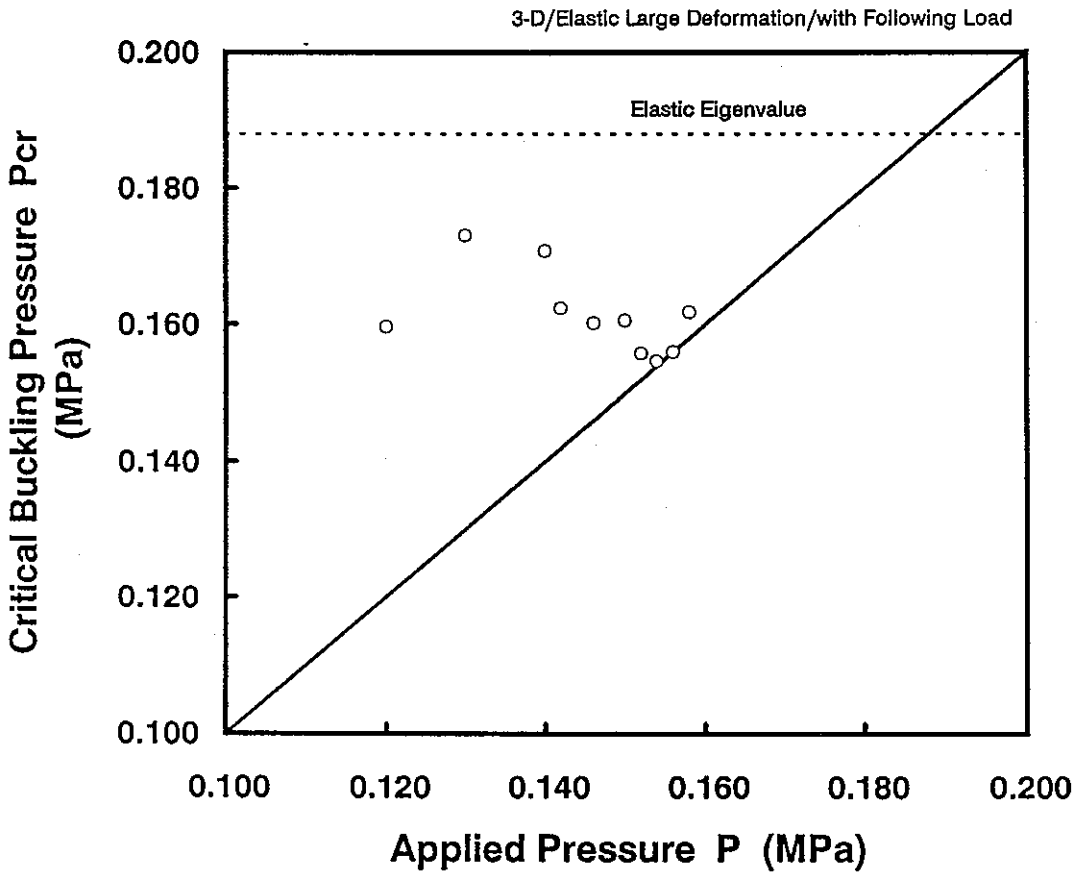

Fig. 4.4-8 Critical Buckling Pressure vs. Applied Pressure (Elastic Large Deformation Analysis with Following Load)

agt9b\ch_4

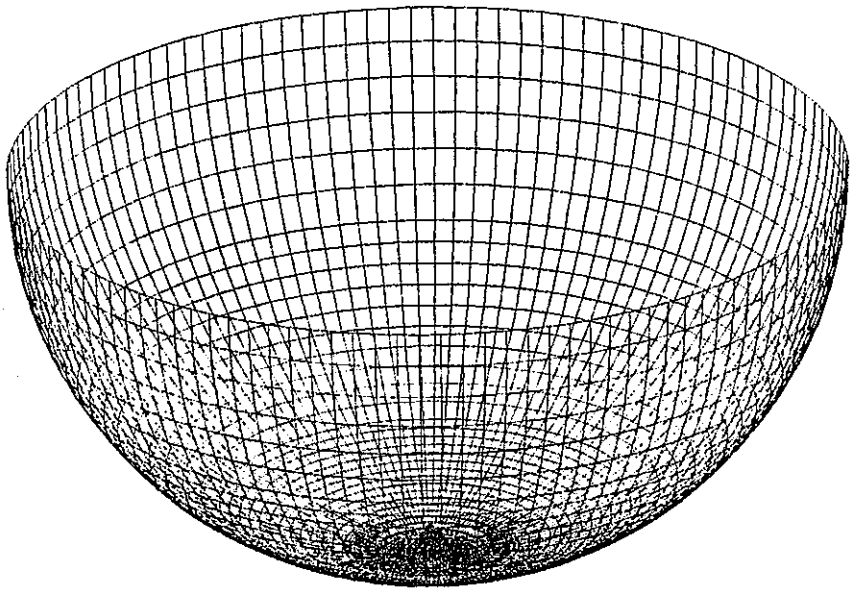

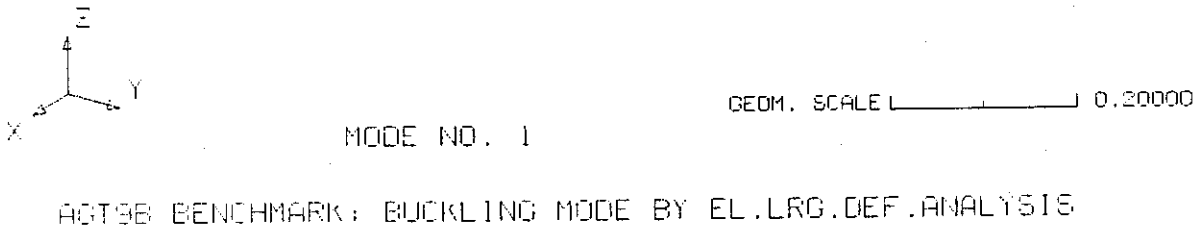

Fig. 4.4-9 Buckling Mode at Critical Pressure (1 of 3 : whole view)
(Elastic Large Deformation with Following Load)

agt9b\ch_4

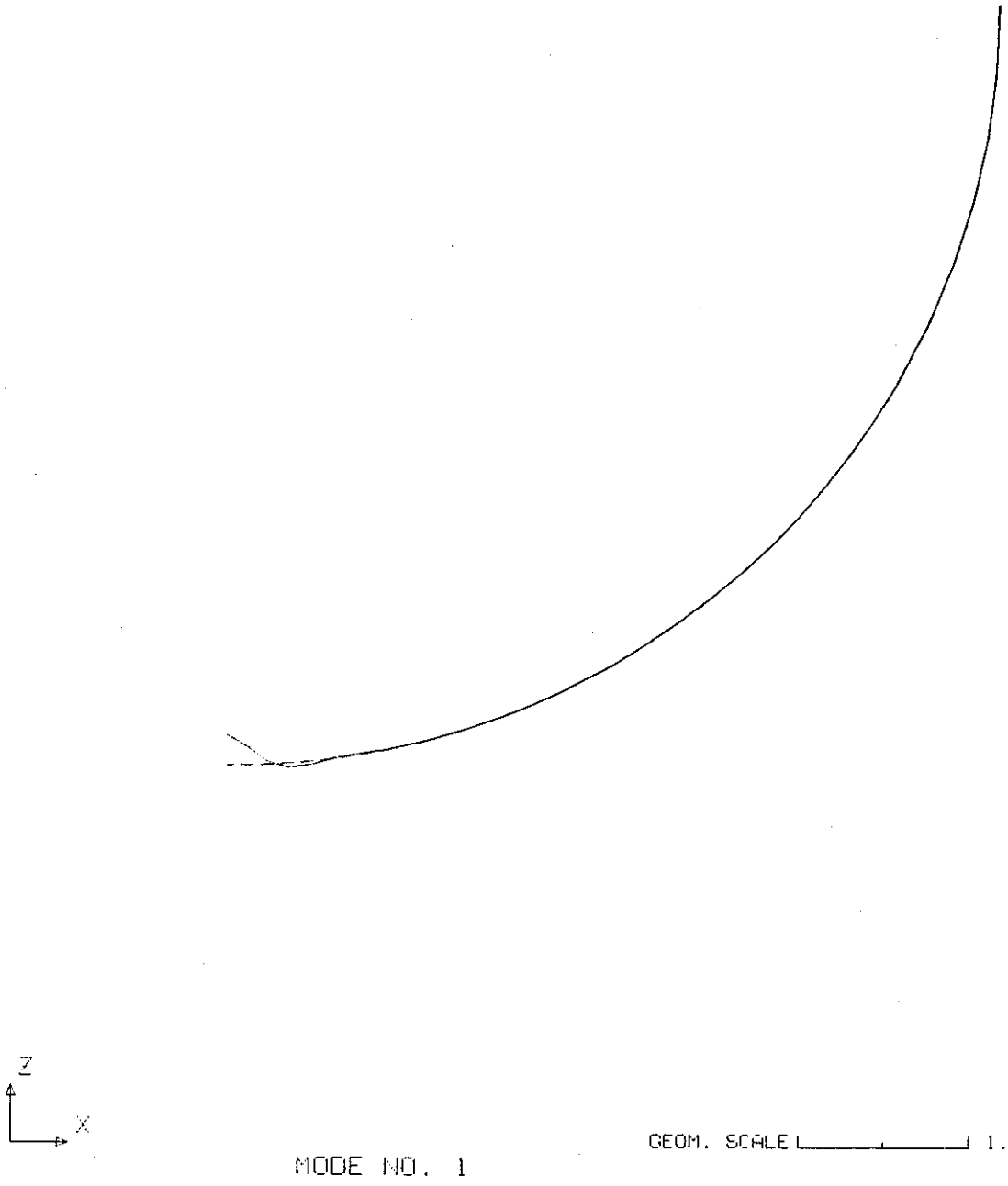

Fig. 4.4-9 Buckling Mode at Critical Pressure (2 of 3 : section)
(Elastic Large Deformation with Following Load)

agt9b\ch_4

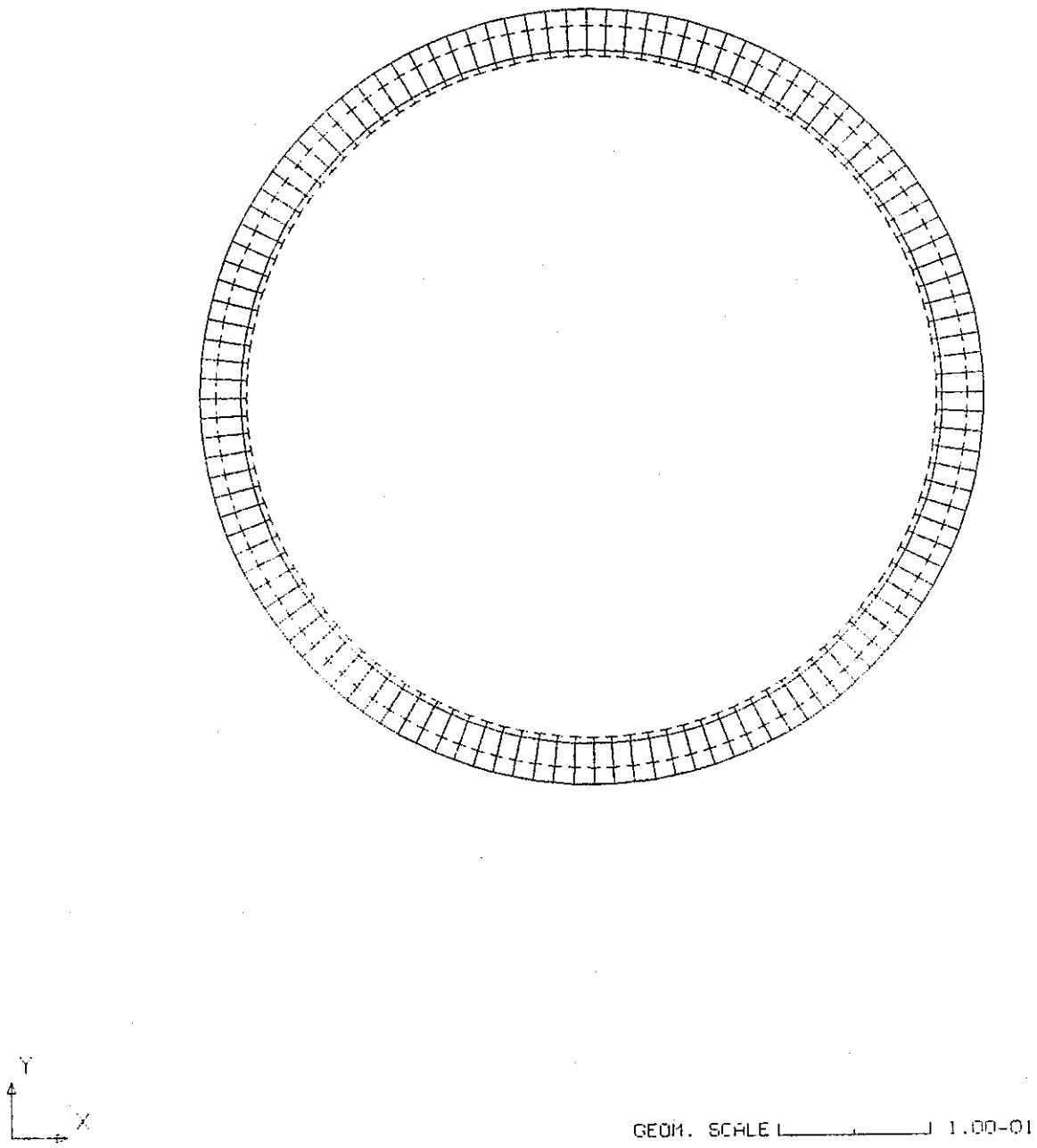

Fig. 4.4-9 Buckling Mode at Critical Pressure (3 of 3 : plan)
(Elastic Large Deformation with Following Load)

agt9b\ch_4

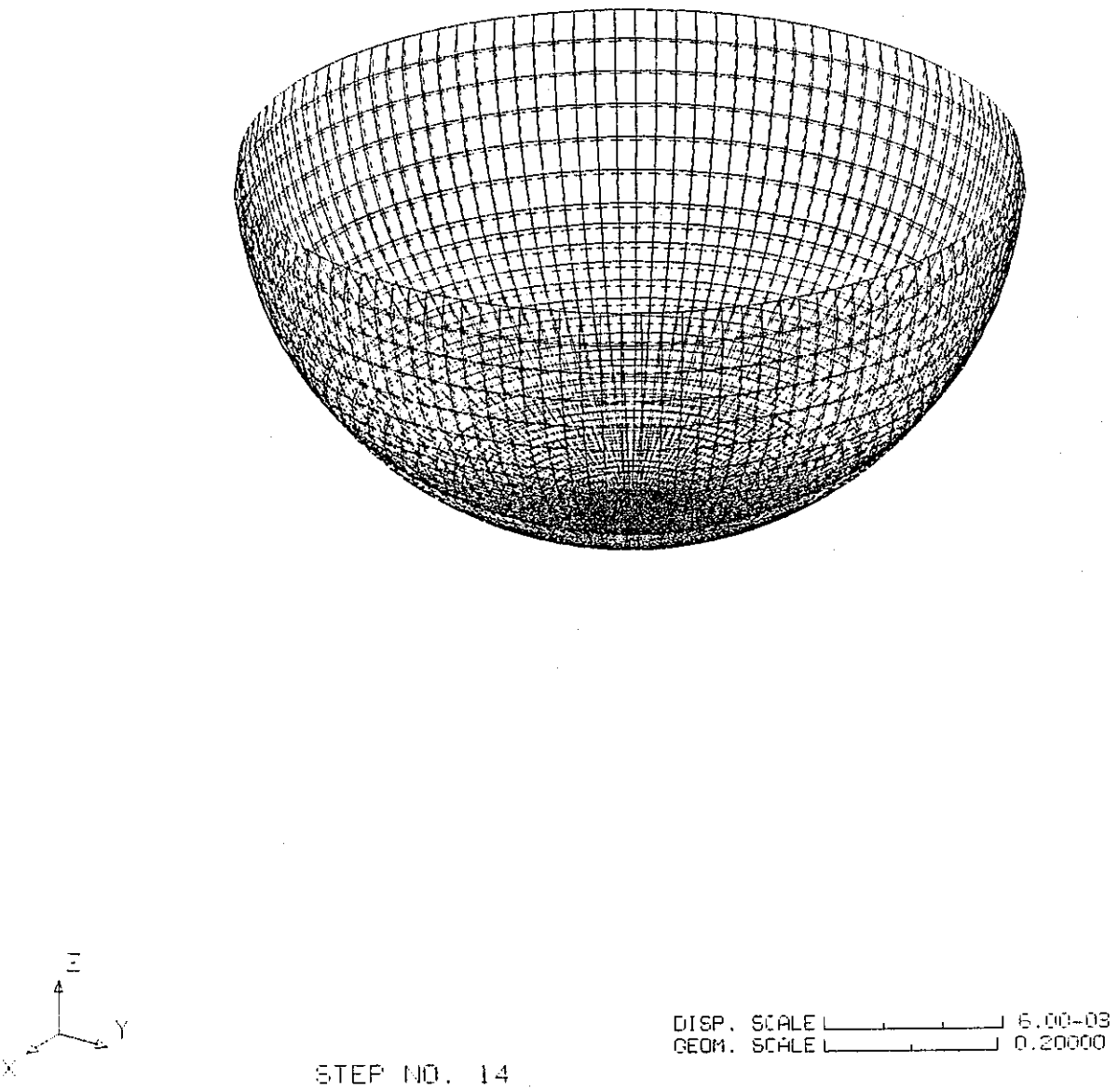

Fig. 4.4-10 Deformation at Critical Buckling Pressure (1 of 3 : whole view) (Elastic Large Deformation with Following Load)

agt9b\ch_4

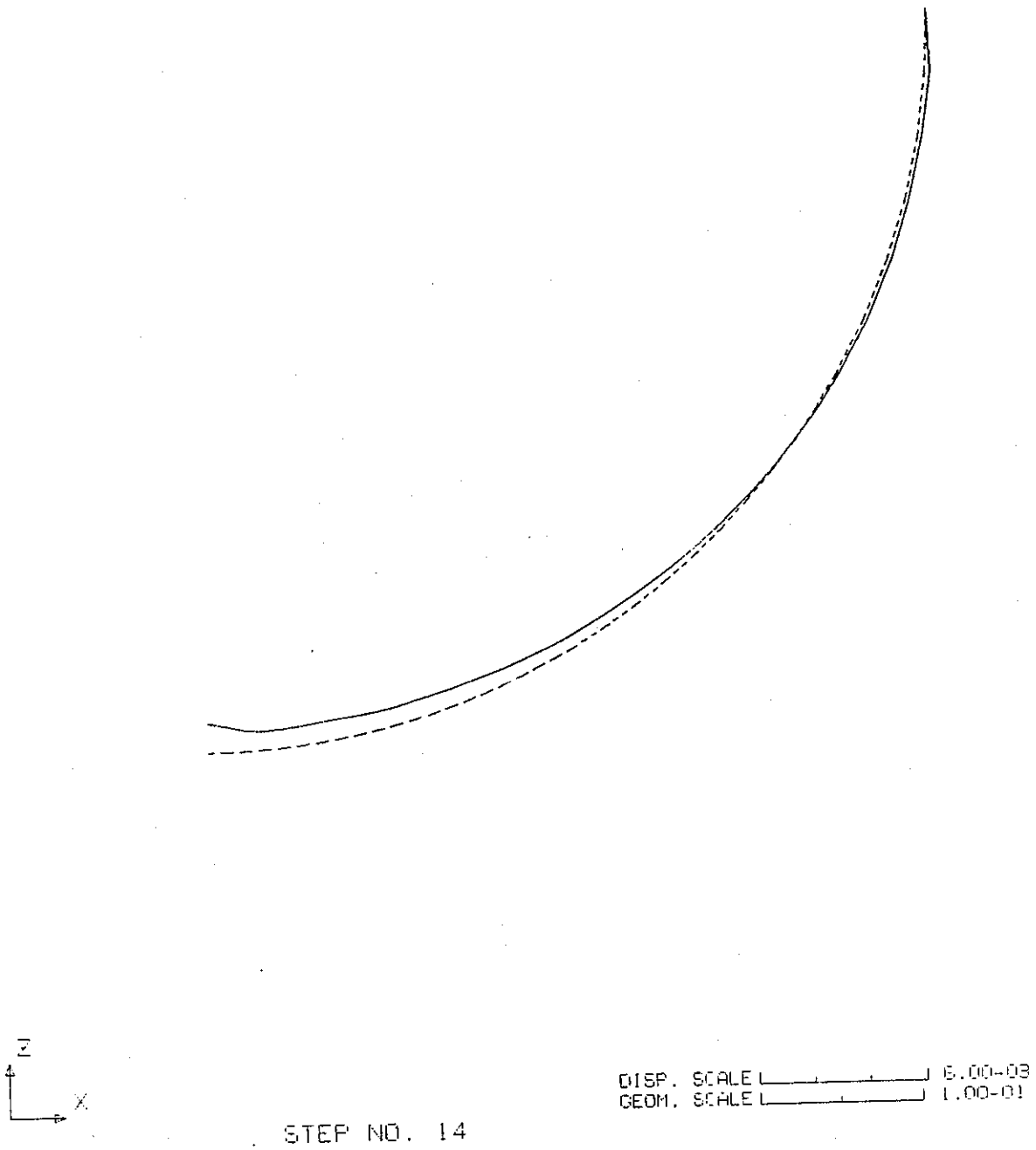

Fig. 4.4-10 Deformation at Critical Buckling Pressure (2 of 3 : section) (Elastic Large Deformation with Following Load)

agt9b\ch_4

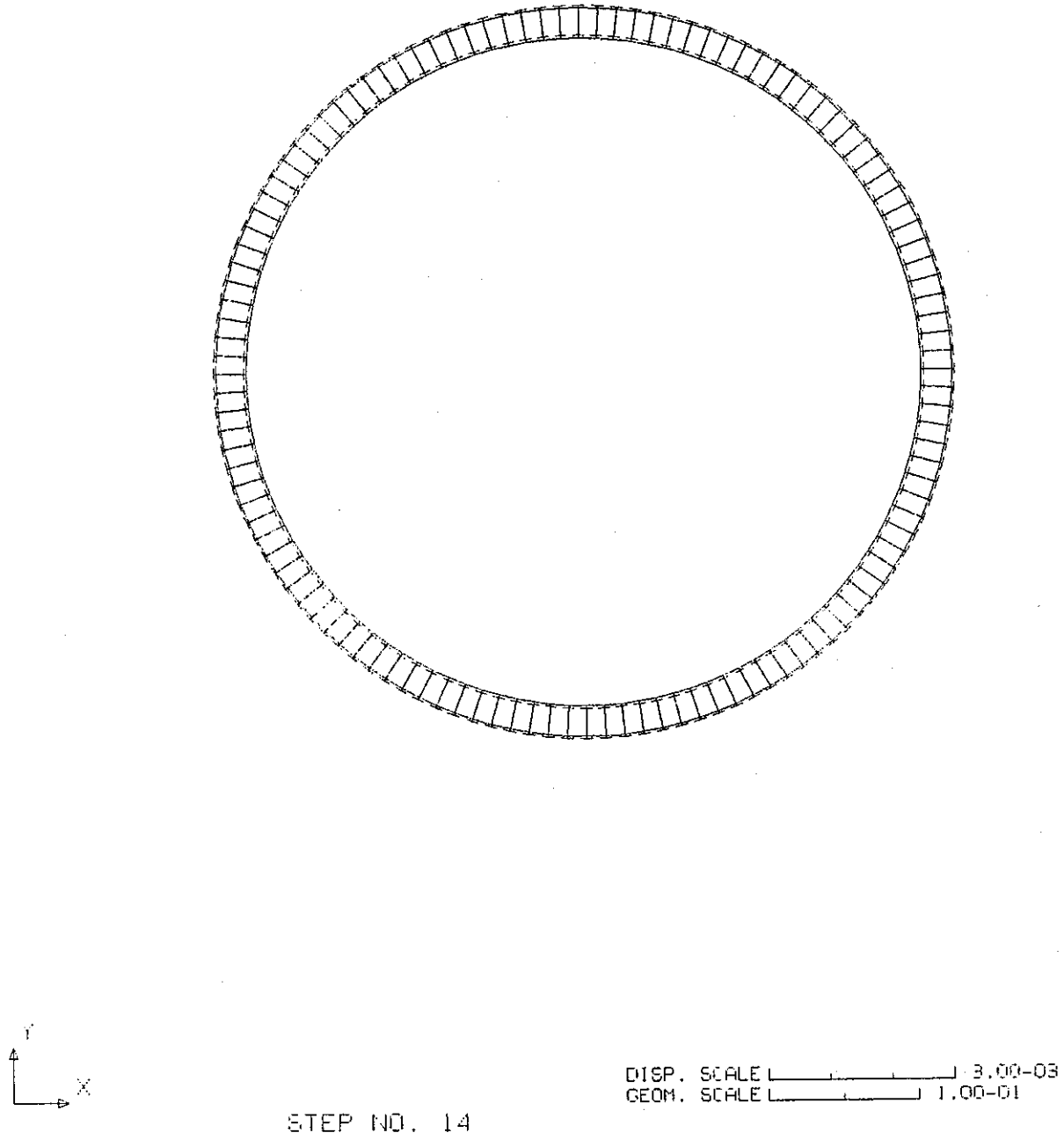

Fig. 4.4-10 Deformation at Critical Buckling Pressure (3 of 3 : plan)
(Elastic Large Deformation with Following Load)

agt9b\ch_4

5. CONCLUSION

As a benchmark study, a series of blind analyses was performed on the problem of dynamic buckling of a hemisphere by external fluid pressure. The result of the analyses can be summarized as follows;

- The frequency of the harmonic excitation applied, which is the fundamental frequency of the fluid-structure system concerned, is 27 Hz. The mode shape at this frequency is axi-symmetric. (see Fig. 3.2-3 and 3.2-10)

- The pressure profile is such that it takes its maximum at the bottom and gradually decreases to null along the meridiolal line towards the level of fluid surface. (see Fig. 3.2-22)

- The critical buckling pressure at the bottom of the sphere by 2-D elastic buckling eigenvalue analysis is 0.19 MPa, which well corresponds to a theoretical value.

- The critical buckling pressure by various analyses are:

0.170 MPa	by 2-D inelastic, w/o following load
0.163 MPa	by 2-D elastic, with following load
0.160 MPa	by 3-D elastic, w/o following load
0.158 MPa	by 3-D elastic, with following load

- The buckling modes are all axi-symmetric and the deformation is concentrated around the bottom point.

- From the above, it may be be inferred that the sphere buckles elastically at about 0.16 MPa, and the buckling mode is axi-symmetric.

ACKNOWLEDGEMENT

The analysis work was initiated by Mr. Kitamura of PNC H/Q.
The author is graceful to Dr. Iwata and Mr. Okada of PNC/OEC for their fruitful discussion.
Thanks are also given to Mr. O-oka of PNC/OEC for his assistance of post processing the analysis results.

APPENDIX A.

EXAMPLES OF FINAS INPUT DATA

Appendix A.1

FINSA INPUT DATA :
Dynamic Eigenvalue Analysis (2-D Axi-symmetric Model)

```
SYSTEM 0/0
FINAS
TITLE     AGT9B BENCHMARK :DYNAMIC BUCKLING OF SEMISPHERICAL HEAD
SUBTITLE                  DYNAMIC EIGENVALUE, AXISYM MODEL, N=0
NOPRINT   DESCR
DYNAMIC   M
$ATA CHECK
OPTIONS ISSPOPT=2
CONTROL
     EIGENVALUE        10   30    5.0E-2
     NONAXCASE      ANTI     0
$
MODEL
=OFF
COORDINATE SYSTEM
    1    3                0.0       0.0       0.0      10.0       0.0       0.0
                          0.0      10.0       0.0
NODE
$  NO CDSY  RPT  DLT      R(M)    THT(DEG)  PHI(DEG)          DIV PTCH DNOD NODE
$     FOR INNER SHELL
  100    1               0.455       0.0       0.0            6          1  106
  106    1               0.455     -30.0       0.0
  107    1               0.455     -31.0       0.0           59          1  166
  166    1               0.455     -90.0       0.0
$     FOR OUTER SHELL
  300    1               0.459       0.0       0.0            6          1  306
  306    1               0.459     -30.0       0.0
  307    1               0.459     -31.0       0.0           59          1  366
  366    1               0.459     -90.0       0.0
$     FOR FLUID REGION
  206    1               0.457     -30.0       0.0           60          1  266
  266    1               0.457     -90.0       0.0
$
ELEMENT TYPE
   11     NCONC2
   12     LNQAX4
   13     INLAX2
   14     SNLAX2
$
GEOMETRY
    1    1  0.80E-3
    2    1  10.0E-3
    3    1    9.806
$
MATERIAL
    1
          E         6.73E10
          NU        0.3
          RHO       2.700E3
    2
          E         1.96E11
          NU        0.3
          RHO       7.810E3
    3
          E         0.0
          NU        0.0
          RHO       1.000E3
$
CONNECTION
$  NO IETO IGEO IMAT    I    J    K    L    M    N    O    P  LP1  ND1  LP2  ND2
$       -   INNER SHELL  -
**ELOOP1     66   -1   -1   -1
```

agt9b\appndx

```
  166   11    1    1  165  166
**END1
$       -   OUTER SHELL  -
**ELOOP1     66   -1   -1   -1
  366   11    2    2  365  366
**END1
$       -   FLUID ELEMENTS   -
**ELOOP1     60   -1   -1   -1   -1   -1
 1166   12         3  166  266  165  265
 1266   12         3  266  366  265  365
**END1
$       -   FSI ELEMENTS -
**ELOOP1     60   -1   -1   -1
 2166   13           165  166
 2266   13           366  365
**END1
$       -     FREE SURFACE ELEMENTS    -
 3106   14    3    3  106  206
 3206   14    3    3  206  306
$
BOUNDARY
$  NO       NODS NODE DNOD      DOFS DOFE
    1
                100             1    1    3
                300             1    1    4
$               130             1    1    2
$               130             1    4
$               130             1    7
$               230             1    7
$               330             1    1    2
$               330             1    4
$               330             1    7
$
RESPONSE
     TIME
          BOUN      1
$         FAS       1
$
END MODEL
$
OUTPUT
PRINT SELECT
$SET2          1  100  166    1  300  366    1                              1
NSET2          1  105  166                                                  1
MODE           1
$ODE       ALL
$ODE       NONE
$RESS          1
POST TAPE
NSET2          9  105  166                                                  1
MODE           9
PRESS          9
STRUCTURE PLOT
FRAME      A4H
$  << MODE PLOT >>
PTITLE     AGT9B BENCHMARK PROBLEM; DYNAMIC BUCKLING OF SEMISPHERICAL HEAD
IPLOT
$  << MODE PLOT >>
ESET2         11  101  166                                                  1
ESET2         12  101  166    1  301  366    1 3106 3206    1              1
PTITLE     AGT9B BENCHMARK; VIBRATION MODE BY AXISYMMETRIC MODEL - N=0 -
VSCALE          0.25
MPLOT         11
$PLOT         12
AXES           X    Y    Z
VIEW             0.0       0.0       0.0
END OUTPUT
END FINAS
```

agt9b\appndx

Appendix A.2

FINSA INPUT DATA :
Dynamic Eigenvalue Analysis (3-D Model)

```
SYSTEM 0/0
FINAS
TITLE     AGT9B BENCHMARK :DYNAMIC BUCKLING OF SEMISPHERICAL HEAD
SUBTITLE                   DYNAMIC EIGENVALUE, 3-D MODEL
NOPRINT   DESCR
DYNAMIC   M
$ATA CHECK
$PTIONS ISSPOPT=2
CONTROL
     EIGENVALUE        24   30    1.0E-5
$
MODEL
$=OFF
COORDINATE SYSTEM
    1    3                0.0       0.0       0.0      10.0       0.0       0.0
                          0.0      10.0       0.0
NODE
$  NO CDSY  RPT  DLT      R(M)   THT(DEG)  PHI(DEG)          DIV PTCH DNOD NODE
$     FOR INNER SHELL
**NLOOP1      6  100     0.0         0.0      -5.0
    1    1               0.455       0.0       0.0            60          1   61
   61    1               0.455     180.0       0.0
**END1
**NLOOP1     21  100     0.0         0.0      -3.0
  601    1               0.455       0.0     -30.0            60          1  661
  661    1               0.455     180.0     -30.0
**END1
$     FOR FLUID REGION
**NLOOP1      6  100     0.0         0.0      -5.0
 3001    1               0.457       0.0       0.0            60          1 3061
 3061    1               0.457     180.0       0.0
**END1
**NLOOP1     21  100     0.0         0.0      -3.0
 3601    1               0.457       0.0     -30.0            60          1 3661
 3661    1               0.457     180.0     -30.0
**END1
$     FOR OUTER SHELL
**NLOOP1      6  100     0.0         0.0      -5.0
 6001    1               0.459       0.0       0.0            60          1 6061
 6061    1               0.459     180.0       0.0
**END1
**NLOOP1     21  100     0.0         0.0      -3.0
 6601    1               0.459       0.0     -30.0            60          1 6661
 6661    1               0.459     180.0     -30.0
**END1
$
ELEMENT TYPE
   11     QFLA4RT
   12     LHEX8
   13     IQFAC4
   14     SQFAC4
$
GEOMETRY
    1    1   0.80E-3
    2    1   10.0E-3
    3    1     9.806
$
MATERIAL
    1
          E         6.73E10
          NU        0.3
          RHO       2.700E3
```

agt9b\appndx

```
      2
            E         1.96E11
            NU        0.3
            RHO       7.810E3
      3
            E         0.0
            NU        0.0
            RHO       1.000E3
$
CONNECTION
$  NO IETO IGEO IMAT    I    J    K    L    M    N    O    P  LP1  ND1  LP2  ND2
$       -   INNER SHELL  -
**ELOOP1     26  100  100  100  100  100                                        4
    1   11    1    1    1    2  101  102                   60    1
**END1
$       -   OUTER SHELL  -
**ELOOP1     26  100  100  100  100  100                                        4
 3001   11    2    2 6001 6002 6101 6102                   60    1
**END1
$       -   FLUID ELEMENTS   -
**ELOOP1     26  100  100  100  100  100  100  100  100  100                   8
10001   12         3  101  102 3101 3102    1    2 3001 3002   60    1        8
13001   12         3 3101 3102 6101 6102 3001 3002 6001 6002   60    1        8
**END1
$       -   FSI ELEMENTS FOR INNER SHELL  -
**ELOOP1     26  100  100  100  100  100                                        4
20001   13              101  102    1    2                   60    1
**END1
$       -   FSI ELEMENTS FOR OUTER SHELL  -
**ELOOP1     26  100  100  100  100  100                                        4
23001   13             6102 6101 6002 6001                   60    1
**END1
$       -   FREE SURFACE ELEMENTS -
30001   14    3    3    2    1 3002 3001                   60    1
30101   14    3    3 3002 3001 6002 6001                   60    1
$
BOUNDARY
$  NO      NODS NODE DNOD CORD DOFS DOFE
    1
$  SUPORTING CONDITION
                1   61         1    1    4
                1   61         1    6
$  SYMMETRY
              101 2601  100    1    2    4
              101 2601  100    1    6
              161 2661  100    1    2    4
              161 2661  100    1    6
$  RIGID OUTER SPHERE
             6001 8661         1    1    6
$
FASTENING
    1
$          LOOP NOD1 DOF1 DND1 NOD2 DOF2 DND2 ICOR
     F1      60 2602    1    1 2601    1    0    1
     F1      60 2602    2    1 2601    2    0    1
     F1      60 2602    3    1 2601    3    0    1
     F1      60 2602    4    1 2601    4    0    1
     F1      60 2602    5    1 2601    5    0    1
     F1      60 2602    6    1 2601    6    0    1
     F1      60 5602    1    1 5601    1    0    1
     F1      60 5602    2    1 5601    2    0    1
     F1      60 5602    3    1 5601    3    0    1
     F1      60 5602    4    1 5601    4    0    1
     F1      60 5602    5    1 5601    5    0    1
     F1      60 5602    6    1 5601    6    0    1
$    F1      60 8602    1    1 8601    1    0    1
$    F1      60 8602    2    1 8601    2    0    1
$    F1      60 8602    3    1 8601    3    0    1
$    F1      60 8602    4    1 8601    4    0    1
```

```
132       $    F1       60 8602    5    1 8601    5    0    1
133       $    F1       60 8602    6    1 8601    6    0    1
134       $
135       RESPONSE
136            TIME
137                 BOUN      1
138                 FAS       1
139       $
140       END MODEL
141       $
142       OUTPUT
143       PRINT SELECT
144       $SET2          1  100  166    1                                          1
145       $ODE           1
146       MODE       NONE
147       $RESS          1
148       STRUCTURE PLOT
149       AXES          -Y    X    Z
150       $IEW               0.0       0.0       0.0
151       $  << MODEL PLOT >>
152       PTITLE     AGT9B BENCHMARK PROBLEM; DYNAMIC BUCKLING OF SEMISPHERICAL HEAD
153       ESET2         11    1 2560    1                                          1
154       ESET2         21 3001 5560    1                                          1
155       IPLOT
156       PTITLE     INNER SEMISPHERE
157       IPLOT         11
158       PTITLE     OUTER SEMISPHERE
159       IPLOT         21
160       $  << MODE PLOT >>
161       $SET2         11  101  166    1                                          1
162       $TITLE     AGT9B BENCHMARK; VIBRATION MODE BY 3-D MODEL                  D
163       $PLOT         11
164       $PLOT          1
165       END OUTPUT
166       END FINAS
167
```

Appendix A.3

FINSA INPUT DATA : Elastic Buckling Analysis (2-D Axi-symmetric Model)

```
SYSTEM 0/0
FINAS
$AVE
TITLE     AGT9B BENCHMARK :DYNAMIC BUCKLING OF SEMISPHERICAL HEAD
SUBTITLE                  ELASTIC BUCKLING ANALYSIS AXISYM MODE
$                         FOLLOWINF LOAD OPTION
$OPRINT   DESCR
STATIC    E
$ATA CHECK
$PTIONS ISSPOPT=2
CONTROL
$***5****0****5****0****5****0****5****0****5****0****5****0****5****0****5****0
     LARGE DISP    1
     BUCKLING          6
MODEL
$=OFF
COORDINATE SYSTEM
    1    3               0.0       0.0       0.0      10.0       0.0       0.0
                         0.0      10.0       0.0
NODE
$  NO CDSY  RPT  DLT      R(M)   THT(DEG)  PHI(DEG)          DIV PTCH DNOD NODE
$     FOR INNER SHELL
  100    1              0.455       0.0       0.0             6          1  106
  106    1              0.455     -30.0       0.0
  107    1              0.455     -31.0       0.0            59          1  166
  166    1              0.455     -90.0       0.0
$
ELEMENT TYPE
$***5****0****5****0****5****0****5****0****5****0****5****0****5****0****5****0
   11     NAXSHEL3
$
GEOMETRY
$   1    1   0.80E-3 /NOMINAL THICKNESS
   11    1    7.5E-4
   12    1    7.9E-4
   13    1    8.0E-4
   14    1    8.3E-4
   15    1    7.6E-4
   16    1    6.8E-4
   17    1    6.9E-4
   18    1    6.4E-4
   19    1    7.2E-4
   20    1    6.8E-4
$
MATERIAL
    1
$   1                   1    1    1
$                            MISES + ORTHOTROPIC HARDENING
          E           6.60E+10
          NU             0.3
$         SIGY        6.23E+07
$         HDASH     F6       7
$          0.000E+00 5.441E+10 9.924E-05 2.700E+10 2.178E-04 1.293E+10
$          4.962E-04 4.196E+09 1.044E-03 7.9412+08 1.926E-03 8.899E+08
$          2.937E-03 8.017E+05
$
CONNECTION
$  NO IETO IGEO IMAT    I    J    K    L    M    N    O    P  LP1  ND1  LP2  ND2
  101   11   11    1  100  101  102
  102   11   12    1  102  103  104
  103   11   13    1  104  105  106
**ELOOP1      3    1    2    2    2
```

agt9b\appndx

```
  104   11   14    1  106  107  108
**END1
**ELOOP1      4    1    2    2    2
  107   11   15    1  112  113  114
**END1
**ELOOP1      6    1    2    2    2
  111   11   16    1  120  121  122
**END1
**ELOOP1      4    1    2    2    2
  117   11   17    1  132  133  134
**END1
**ELOOP1      5    1    2    2    2
  121   11   18    1  140  141  142
**END1
**ELOOP1      6    1    2    2    2
  126   11   19    1  150  151  152
**END1
**ELOOP1      2    1    2    2    2
  132   11   20    1  162  163  164
**END1
$
BOUNDARY
$  NO       NODS NODE DNOD CORD DOFS DOFE
    1
              100                    1    2
$
FORCE
    1
$           NODS NODE DNOD CORD DOFS DOFE  DELTAP1
$***5****0****5****0****5****0****5****0****5****0****5****0****5****0****5****0
$                                                  PRESSURE IN PASCAL
          4  104                    1    3-7.909E+02 1.762E+04 3.658E+04
          4  105                    1    3 3.658E+04 5.607E+04 7.604E+04
          4  106                    1    3 7.604E+04 9.644E+04 1.172E+05
          4  107                    1    3 1.172E+05 1.384E+05 1.598E+05
          4  108                    1    3 1.598E+05 1.816E+05 2.036E+05
          4  109                    1    3 2.036E+05 2.259E+05 2.483E+05
          4  110                    1    3 2.483E+05 2.710E+05 2.937E+05
          4  111                    1    3 2.937E+05 3.166E+05 3.396E+05
          4  112                    1    3 3.396E+05 3.626E+05 3.857E+05
          4  113                    1    3 3.857E+05 4.087E+05 4.317E+05
          4  114                    1    3 4.317E+05 4.546E+05 4.774E+05
          4  115                    1    3 4.774E+05 5.001E+05 5.226E+05
          4  116                    1    3 5.226E+05 5.449E+05 5.670E+05
          4  117                    1    3 5.670E+05 5.888E+05 6.103E+05
          4  118                    1    3 6.103E+05 6.315E+05 6.524E+05
          4  119                    1    3 6.524E+05 6.729E+05 6.929E+05
          4  120                    1    3 6.929E+05 7.126E+05 7.318E+05
          4  121                    1    3 7.318E+05 7.505E+05 7.687E+05
          4  122                    1    3 7.687E+05 7.863E+05 8.034E+05
          4  123                    1    3 8.034E+05 8.199E+05 8.358E+05
          4  124                    1    3 8.358E+05 8.511E+05 8.657E+05
          4  125                    1    3 8.657E+05 8.797E+05 8.929E+05
          4  126                    1    3 8.929E+05 9.055E+05 9.173E+05
          4  127                    1    3 9.173E+05 9.284E+05 9.387E+05
          4  128                    1    3 9.387E+05 9.483E+05 9.571E+05
          4  129                    1    3 9.571E+05 9.651E+05 9.722E+05
          4  130                    1    3 9.722E+05 9.786E+05 9.841E+05
          4  131                    1    3 9.841E+05 9.889E+05 9.928E+05
          4  132                    1    3 9.928E+05 9.958E+05 9.980E+05
          4  133                    1    3 9.980E+05 9.994E+05 1.000E+06
$
HISTORY
$ ]]] FORCE (ELEMENT LOAD PRESSURE) IS WRITTEN IN MPA ]]]
INTERVAL
          BOUN     1
$***5****0****5****0****5****0****5
          FORC     1       1.0
BUCKLING
```

```
132       END MODEL
133       $
134       OUTPUT
135       PRINT SELECT
136       DISP      ALL
137       ELM       ALL
138       MODE      ALL
139       POST TAPE
140       DISP      ALL
141       ELM       ALL
142       STRUCTURE PLOT
143       $RAME     A4H
144       $  << MODEL PLOT >>
145       PTITLE    AGT9B BENCHMARK PROBLEM; DYNAMIC BUCKLING OF SEMISPHERICAL HEAD
146       $PLOT
147       $PLOT               NODES
148       $PLOT               ELEMENTS
149       PTITLE    AGT9B BENCHMARK; ELASTIC BUCKLING MODE WITH FOLLOWING LOAD
150       $***5****0****5****0****5****0****5
151       $SCALE          100.
152       MPLOT
153       END OUTPUT
154       END FINAS
155
```

Appendix A.4

FINSA INPUT DATA : Elastic Buckling Analysis (3-D Model)

```
SYSTEM 0/0
FINAS
TITLE     AGT9B BENCHMARK :DYNAMIC BUCKLING OF SEMISPHERICAL HEAD
SUBTITLE                  ELASTIC BUCKLING ANALYSIS, 3-D FULL MODEL
$                         WITH THICKNESS VARIATION
$                         ELASTIC LARGE-DISP ANALYSIS
$                         1.5 DEG PITCH BELOW 60DEG
NOPRINT   DESCR
$AVE
STATIC        E
$ATA CHECK
CONTROL
$***5****0****5****0****5****0****5****0****5****0****5****0****5****0****5****0
     LARGE DISP    1
$    BUCKLING           6
$
MODEL
=OFF
COORDINATE SYSTEM
    1    3                0.0       0.0       0.0      10.0       0.0       0.0
                          0.0      10.0       0.0
NODE
$  NO CDSY  RPT  DLT      R(M)   THT(DEG)  PHI(DEG)          DIV PTCH DNOD NODE
**NLOOP1      6  200      0.0        0.0      -5.0
     1    1               0.455      0.0       0.0            119          1  120
   120    1               0.455    357.0       0.0
**END1
**NLOOP1     10  200      0.0        0.0      -3.0
  1201    1               0.455      0.0     -30.0            119          1 1320
  1320    1               0.455    357.0     -30.0
**END1
**NLOOP1     21  200      0.0        0.0      -1.5
  3201    1               0.455      0.0     -60.0            119          1 3320
  3320    1               0.455    357.0     -60.0
**END1
$
ELEMENT TYPE
   11     QFLA4RT
$
GEOMETRY
$   1    1   0.80E-3 /NOMINAL THICKNESS
   11    1    7.1E-4
   12    1    8.1E-4
   13    1    7.7E-4
   14    1    8.3E-4
   15    1    7.6E-4
   16    1    6.8E-4
   17    1    6.9E-4
   18    1    6.4E-4
   19    1    7.2E-4
   20    1    6.8E-4
$
MATERIAL
    1
          E         6.60E10
          NU        0.3
$
CONNECTION
**ELOOP1      1  200  200  200  200  200                                      4
    1   11   11    1    1    2  201  202                    119    1
```

agt9b\appndx

Appendix A.4

```
      120   11   11    1  120    1  320  201                          1
**END1
**ELOOP1      2  200  200  200  200  200                                    4
  201   11   12    1  201  202  401  402                    119    1
  320   11   12    1  320  201  520  401                           1
**END1
**ELOOP1      2  200  200  200  200  200                                    4
  601   11   13    1  601  602  801  802                    119    1
  720   11   13    1  720  601  920  801                           1
**END1
**ELOOP1      3  200  200  200  200  200                                    4
 1001   11   14    1 1001 1002 1201 1202                    119    1
 1120   11   14    1 1120 1001 1320 1201                           1
**END1
**ELOOP1      3  200  200  200  200  200                                    4
 1601   11   15    1 1601 1602 1801 1802                    119    1
 1720   11   15    1 1720 1601 1920 1801                           1
**END1
**ELOOP1      4  200  200  200  200  200                                    4
 2201   11   16    1 2201 2202 2401 2402                    119    1
 2320   11   16    1 2320 2201 2520 2401                           1
**END1
**ELOOP1      4  200  200  200  200  200                                    4
 3001   11   17    1 3001 3002 3201 3202                    119    1
 3120   11   17    1 3120 3001 3320 3201                           1
**END1
**ELOOP1      6  200  200  200  200  200                                    4
 3801   11   18    1 3801 3802 4001 4002                    119    1
 3920   11   18    1 3920 3801 4120 4001                           1
**END1
**ELOOP1      9  200  200  200  200  200                                    4
 5001   11   19    1 5001 5002 5201 5202                    119    1
 5120   11   19    1 5120 5001 5320 5201                           1
**END1
**ELOOP1      2  200  200  200  200  200                                    4
 6801   11   20    1 6801 6802 7001 7002                    119    1
 6920   11   20    1 6920 6801 7120 7001                           1
**END1
$
BOUNDARY
$  SUPPORTING CONDITION
    1
$          NODS NODE DNOD CORD DOFS DOFE
              1  120          1    1    4
              1  120          1    6
$          5201               1    1    2
$          5201               1    4    6
$
FASTENING
    1
$          LOOP NOD1 DOF1 DND1 NOD2 DOF2 DND2 ICOR
     F1     119 7202    1    1 7201    1    0    1
     F1     119 7202    2    1 7201    2    0    1
     F1     119 7202    3    1 7201    3    0    1
     F1     119 7202    4    1 7201    4    0    1
     F1     119 7202    5    1 7201    5    0    1
     F1     119 7202    6    1 7201    6    0    1
$
FORCE
  100
$     TYPE ELMS ELME DELM PARA  IPS  IPE<   P1   ><   P2   ><   P3   ><   P4   >
         3 1201 1320    1          1     6.881E-04 6.881E-04-5.887E-02-5.887E-02
         3 1401 1520    1          1    -5.887E-02-5.887E-02-1.226E-01-1.226E-01
         3 1601 1720    1          1    -1.226E-01-1.226E-01-1.894E-01-1.894E-01
         3 1801 1920    1          1    -1.894E-01-1.894E-01-2.585E-01-2.585E-01
         3 2001 2120    1          1    -2.585E-01-2.585E-01-3.291E-01-3.291E-01
```

agt9b\appndx

```
127                3 2201 2320    1         1     -3.291E-01-3.291E-01-4.003E-01-4.003E-01
128                3 2401 2520    1         1     -4.003E-01-4.003E-01-4.711E-01-4.711E-01
129                3 2601 2720    1         1     -4.711E-01-4.711E-01-5.408E-01-5.408E-01
130                3 2801 2920    1         1     -5.408E-01-5.408E-01-6.084E-01-6.084E-01
131                3 3001 3120    1         1     -6.084E-01-6.084E-01-6.730E-01-6.730E-01
132                3 3201 3320    1         1     -6.407E-01-6.407E-01-7.035E-01-7.035E-01
133                3 3401 3520    1         1     -6.730E-01-6.730E-01-7.339E-01-7.339E-01
134                3 3601 3720    1         1     -7.035E-01-7.035E-01-7.621E-01-7.621E-01
135                3 3801 3920    1         1     -7.339E-01-7.339E-01-7.903E-01-7.903E-01
136                3 4001 4120    1         1     -7.621E-01-7.621E-01-8.159E-01-8.159E-01
137                3 4201 4320    1         1     -7.903E-01-7.903E-01-8.414E-01-8.414E-01
138                3 4401 4520    1         1     -8.159E-01-8.159E-01-8.639E-01-8.639E-01
139                3 4601 4720    1         1     -8.414E-01-8.414E-01-8.864E-01-8.864E-01
140                3 4801 4920    1         1     -8.639E-01-8.639E-01-9.057E-01-9.057E-01
141                3 5001 5120    1         1     -8.864E-01-8.864E-01-9.249E-01-9.249E-01
142                3 5201 5320    1         1     -9.057E-01-9.057E-01-9.405E-01-9.405E-01
143                3 5401 5520    1         1     -9.249E-01-9.249E-01-9.561E-01-9.561E-01
144                3 5601 5720    1         1     -9.405E-01-9.405E-01-9.678E-01-9.678E-01
145                3 5801 5920    1         1     -9.561E-01-9.561E-01-9.796E-01-9.796E-01
146                3 6001 6120    1         1     -9.678E-01-9.678E-01-9.871E-01-9.871E-01
147                3 6201 6320    1         1     -9.796E-01-9.796E-01-9.946E-01-9.946E-01
148                3 6401 6520    1         1     -9.871E-01-9.871E-01-9.973E-01-9.973E-01
149                3 6601 6720    1         1     -9.946E-01-9.946E-01-1.000E+00-1.000E+00
150                3 6801 6920    1         1     -9.973E-01-9.973E-01-9.958E-01-9.958E-01
151                3 7001 7120    1         1     -1.000E+00-1.000E+00-9.915E-01-9.915E-01
152        $                                    !!  ELEMENT FORCE IN PA   !!
153        $
154        HISTORY
155        INTERVAL      1
156                  BOUN     1
157                  FAS      1
158                  FORC   100   0.12E+6
159        INTERVAL      1
160                  BOUN     1
161                  FAS      1
162                  FORC   100   0.13E+6
163        INTERVAL      5
164                  BOUN     1
165                  FAS      1
166                  FORC   100   0.14E+6
167        INTERVAL      5
168                  BOUN     1
169                  FAS      1
170                  FORC   100   0.15E+6
171        $NTERVAL     10
172        $         BOUN     1
173        $         FAS      1
174        $         FORC   100   0.16E+6
175        $NTERVAL     10
176        $         BOUN     1
177        $         FAS      1
178        $         FORC   100   0.17E+6
179        $***5****0****5****0****5****0****5****0****5****0****5****0****5****0****5****0****5****0
180        $UCKLING
181        $
182        END MODEL
183        $
184        OUTPUT
185        $
186        PRINT SELECT
187        $***5****0****5****0****5****0****5****0****5****0****5****0****5****0****5****0****5****0
188        ESET2         1    1 7001  200                                                          1
189        NSET2         1    1 7201  200
190        DISP          1
191        ELM           1
192        $
193        STRUCTURE PLOT
194        $FRAME     A4H
195        $XES        -Y    X    Z
```

agt9b\appndx

```
196       $IEW            0.0       0.0       0.0
197       $  << MODEL PLOT >>
198       PTITLE    AGT9B BENCHMARK PROBLEM; DYNAMIC BUCKLING OF SPHERICAL HEAD
199       ESET2        11    1 7001    1                                          1
200       IPLOT
201       $  << MODE PLOT >>
202       ESET2        21    1 7001  200                                          1
203       ESET2        22 3001 3120    1
204       $SCALE         100.0
205       PTITLE    AGT9B BENCHMARK; ELASTIC LARGE DEFORMATION ANALYSIS
206       $         WHOLE VIEW
207       DPLOT
208       $         MERIDIONAL VIEW
209       AXES           Y    X    Z
210       VIEW             0.0       0.0       0.0
211       DPLOT        21
212       $         PLAN SECTION
213       AXES           Z    X    Y
214       VIEW             0.0       0.0       0.0
215       DPLOT        22
216       END OUTPUT
217       END FINAS
218
```

agt9b\appndx